Some Properties

of

Elementary Particles

or

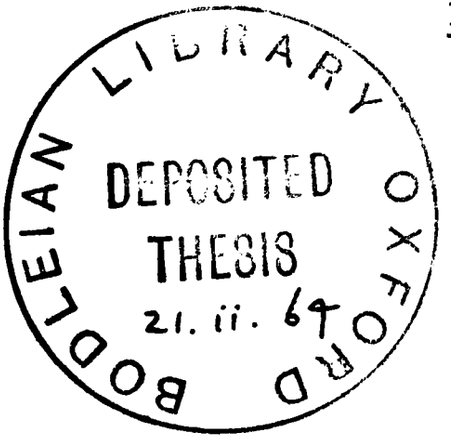
A Determination

of the

Lifetime

of the

Neutral π meson



being a dissertation submitted for
the degree of

Doctor of Philosophy in the University of Oxford

by

David Arthur Evans, of Balliol College.

November, MCMLXIII

" We are such stuff

As dreams are made on, and our little life

Is rounded with a sleep. "

The Tempest, IV, i.

Preface

This dissertation is a report of research done on a determination of the mean life of the neutral pion, at the Clarendon and Nuclear Physics Laboratories between October 1960 and November 1963, by the author under the supervision of Dr. J. H. Mulvey. Apart from the exposure and processing of the emulsion stack, all the work described is that of the author.

The author would like to express his thanks to his supervisor for his guidance and encouragement; to Dr. S. Lokanathan, Dr. Y. Prakash and the other members of the Oxford Emulsion Group for many helpful discussions. The essential and painstaking part played by the scanners of 9, Keble Road is greatly appreciated.

The successful construction and operation of the digitised micrometer eyepiece is due to a number of people to whom the author expresses his hearty thanks: Mr. S. Tolan who designed it; Mr. S. Stevens whose craftsmanship produced the finished model; Mr. D. Smith who was responsible for the design of the electronics; Dr. F. Foster who helped with the preliminary design; Mr. C. Band for the photographic reproduction of the gratings and cross-wires and Dr.McIlraith of the NPL for generously supplying the master grating negative.

The calculations could not have been performed without the aid of the Oxford Mercury and his operators. The diagrams are the careful work of Mrs. J. French and Miss. J. Walman.

Finally, the author thanks his wife for her continual encouragement which at times was essential.

Nov. 1963.

Abstract

Theoretical estimates of the lifetime of the neutral π meson have indicated a value of the order of 10^{-17}secs. In order to determine the lifetime by flight distance measurements a method employing very fine resolution is required. Nuclear emulsions provide a medium for resolution of distances of the order of a micron.

This experiment uses the same principle as that first tried by Harris et al.(1957). The decay at rest of the K^+ meson in the $K_{\pi 2}$ mode $(\pi^+\pi^o)$ provides a π^o of unique velocity and a direction directly opposite to that of the π^+; the latter being charged, leaves a track in the emulsion. The decay of the π^o is detected in emulsion if it takes place in the Dalitz mode:-

$$\pi^o \quad \gamma + e^+ + e^- \qquad \text{(br. ratio 1.2\%)}$$

Detection is possible because of the emission of charged particles.

A stack of Ilford L4 emulsions was exposed to a beam of stopping K^+ mesons. After processing, the stack was scanned for $K_{\pi 2}$ decays with the emission of a Dalitz pair. Other π^o producing decays of the K^+ ($K_{\mu 3}$, K_{e3}, τ') were at first indistinguishable from the desired $K_{\pi 2}$ decays.

In order to reduce this contamination, grain density measurements were made on the charged secondary from the K^+ decay. By rejecting events in which g^* was greater than 1.3 all τ' and 30% of the $K_{\mu 3}$ events were rejected. A correction

factor was calculated to account for the remaining decays.

The co-ordinates of the grains composing the events were measured relative to axes fixed in the field of view. A bifilar micrometer eyepiece was used which has the motions of the cross-wires digitised to enable rapid measurement. The co-ordinates were automatically punched out on to tape ready for input to the computer.

The tracks of the particles were obtained by fitting straight lines to the measured co-ordinates. The decay point of the π^o was defined as the intersection of the electron tracks with the line of flight of the π^+. The point of production was taken as the foot of the perpendicualr from the measured position of the K^+ on to the π^+ trajectory.

The effects of errors due to measurement, "grain noise" and grain size were thoroughly investigated. Use was made of co-ordinate measurements on τ decays of the K^+ ($\pi^+\pi^+\pi^-$) where it is known that the three tracks converge on the point of decay of the K^+.

An estimation of the lifetime was made using a likelihood calculation. It was discovered that the presence of events giving anomalous flight distances affected the estimate considerably. A suitable cutoff criterion was applied to reject these events.

The result after allowing for the effect of contamination events referred to earlier was:-

$$\tau_{\pi^o} = (1.56 \begin{smallmatrix} + 0.55 \\ - 0.45 \end{smallmatrix}) \times 10^{-16} \text{ secs.}$$

TABLE OF CONTENTS.

CHAPTER I.

A SHORT REVIEW OF THE ELEMENTARY PARTICLES.

1. I. Introduction. I.
2. 2. Interactions and Decays. 2.
1. 3. Classes of Particles and Conservation Laws. 5.
1. 4. Virtual States. 8.
1. 5. Electromognetically decaying particles. 9.

CHAPTER II.

THE NEUTRAL π MESON.

2. I. Existence and Mass. 12
2. 2. Decay Properties. 13
2. 3. Previous Lifetime Estimations. 14
2. 4. Experiment of Harris et al. 15.

CHAPTER III.

THE PRESENT EXPERIMENT.

3. I. Introduction. 18.
3. 2; Exposure and Processing. 19.
3. 3. Scanning. 20.
3. 4. Preliminary Measurement. 24.

CHAPTER IV.

THE METHOD OF CO-ORDINATE MEASUREMENT.

4. I. Introduction. 29.
4. 2. Preliminary Model. 29.
4. 3. Sources Of Error. 30.

CHAPTER V.

THE DIGITISED MICROMETER EYEPIECE.

5. I. Method of Digitising. 35.
5. 2. Requirements of Measuring System. 37.
5. 3. Discription of the Instrument. 39.
5. 31. Grating Production. 40.
5. 32. Mechanical Construction of Eyepiece. 41.
5. 33. Grating Optical System. 43.
5. 34. Cross Wires. 46.

TABLE OF CONTENTS CONT'D.

CHAPTER V. Cont'd.

5. 35. Electronics. 47.

5. 4. Calibration and Performance 50.

5.5 Setting accuracy 51.

5.6 Error due to digitising 53.

5.7 Limits to Accuracy Attainable 55.

5.8 Setting up procedure 57.

Addendum to Chapter V 60.

CHAPTER VI

Measurement of Events

6.1 Selection of events 61.

6.2 Optical technique 62.

6.3 Co-rdinate measurement 63.

6.4 Comparison with earlier eyepiece 65.

6.5 Difficulties of Measurement 65.

CHAPTER VII

Data reduction and Error calculations

7.1 Reconstruction of Event Geometry 67.

7.11 Discussion of "grain noise" 67.

7.12 Event Parameters 69.

7.2 Errors 70.

7.3 K^+ ending error 71.

7.4 Measurement of τ decays 722

7.41 Treatment of the results of τ measurements 74.

7.5 Error hypothesis 76.

7.6 Calculation of K^+ error 78.

Table of x and σ for 63 events used finally 81.

Chapter VIII

Estimation of Lifetime

8.1 Introduction 82.

8.2 Weighted Mean method 83.

8.3 Maximum likelihood method 83.

8.4 Investigation of Conflicting estimates 85.

8.5 Imitation results 85.

TABLE OF CONTENTS (CONT'D)

CHAPTER VIII (con't)

8.6 Presence of and effect of "wild" events 87.

8.8 Investigation of "wild" events 89.

8.9 Confidence Interval 91.

8.10 Correction for Contamination events 93.

CHAPTER IX

Discussion of Experiment

9.1 General Remarks 96.

9.2 Synopsis of the Experiment 96.

9.3 Miscellaneuos Errors 97.

9.4 Main Sources of Error 99.

9.5 Future Experiments 103.

9.6 Cause of "wild" events 103.

9.10 Other π^{o} lifetime determinations 105.

9.11 Theoretical aspects of the π^{o} lifetime 109.

9.12 Comparison of Emulsion experiments 110.

9.13 Summary of Existing Data on π^{o} lifetime 115.

List of references 116.

Appendix 118.

CHAPTER I

A SHORT REVIEW OF THE ELEMENTARY PARTICLES

1.1 Introduction

The definition of an "elementary" particle is dependent upon the present state of knowledge. Such a term could have been applied by contemporaries to Lucretius' atoms, Newton's luminous corpuscles or the atoms of Dalton. The problem in modern high energy physics has become more acute with an increasing number of apparently different particles. The following approach mentioned in [1] is useful. Consider as examples the deuteron and the π^+ meson.

The deuteron is a stable particle with well-defined mass, charge, spin and parity; the same remark applies equally to the π^+. However, the mass of the deuteron is very close to the sum of the masses of the proton and neutron while the spin and charge are those which might be expected from a "combination" of these two particles. The binding energy of the deuteron, if considered to be a composite particle, is a very small proportion of the masses of the constituent particles. In a crude way it may be said that the identities of these particles are not "swamped" by a large binding energy. Compare this with the model which regards the π^+ as a bound state of proton and neutron (in fact, anti-neutron) with a binding energy of about 1,700 MeV. In this case the

Table 1.1

Particle	Anti-particle	Mass (MeV)	Mean Life	Decay Modes
BARYONS				
Ξ^-	$\bar{\Xi}^+$	1320	1.4×10^{-10}	$\Lambda\pi^-$
Ξ°	$\bar{\Xi}^\circ$	1316	3.9×10^{-10}	$\Lambda\pi^\circ$
Σ^-	$\bar{\Sigma}^+$	1196	1.59×10^{-10}	$n\pi^-$
Σ°	$\bar{\Sigma}^\circ$	1191	$10^{-14} > \tau > 10^{-22}$	$\Lambda\gamma$
Σ^+	$\bar{\Sigma}^-$	1189	0.78×10^{-10}	$p\pi^\circ(0.51)$ $n\pi^+(0.49)$
Λ°	$\bar{\Lambda}^\circ$	1115	2.6×10^{-10}	$p\pi^-(0.66)$ $n\pi^\circ(0.34)$
n	$\bar{n}$	939	1013	$pe^-\bar{\nu}_e$
p	$\bar{p}$	938	∞	-
MESONS				
K^+	K^-	494	1.227×10^{-8}	$\mu^+\nu_\mu(0.57)$ $\pi^+\pi^\circ(0.26)$ $\mu^+\pi^\circ\nu_\mu(0.044)$ $e^+\pi^\circ\nu_e(0.045)$ $\pi^+\pi^+\pi^-(0.057)$ $\pi^+\pi^\circ\pi^\circ(0.021)$
K°	$\bar{K}^\circ$	498	K_1° 0.87×10^{-10}	$\pi^+\pi^-$ (0.69) $\pi^\circ\pi^\circ$ (0.31)
			K_2° 6.3×10^{-8}	$\pi^+\pi^-\pi^\circ(0.09)$ $3\pi^\circ$ (0.38) $\pi^-e^+\bar{\nu}_e$ (0.28) $\pi^+e^-\nu_e$ $\pi^-\mu^+\bar{\nu}_\mu$ (0.25) $\pi^+\mu^-\nu_\mu$
π^+	π^-	140	2.547×10^{-8}	$\mu^+\nu_\mu$
π°	π°	135	1.28×10^{-16}	2γ (0.988) γe^+e^- (0.012)
LEPTONS				
μ^-	μ^+	106	2.21×10^{-6}	$e^-\bar{\nu}_e\nu_\mu$
e^-	e^+	0.510976	∞	
μ	μ	2.5		
e	e	0.00025		
PHOTON				
γ	γ	0		

Note; Mean lives are in seconds; masses to nearest MeV; branching ratios in fractional form.

is of the same order as the masses of the constituents.

Using this criterion just described, one obtaines the normally accepted list of fundamental particles none of which can (at present) be profitably considered to be a composite particle. Fig 1.1 lists these particles together with masses, lifetimes and principal decay modes.

As the consideration of particle decays is of importance in this experiment, some mention of this subject is not out of place.

1.2 Interactions and Decays

Particle decays are special cases of the wider field of particle interactions. It is now well established that these interactions are of three main types of greatly differing strength.

The strength of an interaction is attributed by extending a concept of electrodynamics. The Hamiltonian density due to the interaction between a charge-current density $s_\mu(\underline{x})$ and an electromagnetic field $A_\mu(\underline{x})$ is given by:-

$$H_I(\underline{x}) = e s_\mu(\underline{x}) A_\mu(\underline{x})$$

Here, the "coupling constant" for the two fields is e, the electronic charge. In quantum field theory, where particles are represented by quantised fields, similar expressions can be written down to express the contribution to the total Hamiltonian due to the interaction between the particles. The constant which appears in the place of e in the above

is a measure of the strength of the interaction. For the purposes of comparison, a dimensionless measure of this strength is required. With the electromagnetic interaction, such a quantity is provided by the fine structure constant $\alpha = e^2/4\pi\hbar c = 1/137$ approx. An analogous quantity can be formed for the strong, or nuclear, interactions, namely $g^2/4\pi\hbar c = 15$. Here, g is the pion-nucleon coupling constant. The third class of interaction is the weak, or Fermi interaction; the best known example of this is β decay. The Fermi constant C which measures the strength of β decay is of the order of 10^{-49} erg.cm^3. This may only be written in dimensionless form if a length is specified. A convenient length is the pion Compton wavelength $\hbar/m_\pi c$. Since the probability of decay is proportional to C^2, this gives 10^{-14} as the dimensionless measure. It is clear that the somewhat arbitrary choice of length to obtain this constant does not affect the conclusion that the weak interactions are extremely weak compared with the other two types. Also, the consideration of any other weak process does not affect this general result - the similarity in strength between the various weak processes has given rise to the theory of the Universal Fermi interaction.

In addition to the differences in strength, the three interactions differ in the conservation laws which they obey. The following table summarizes these differences.

Interaction	Relative strength	i-spin	Conserves:- strangeness	parity
Strong	10^{1}	yes	yes	yes
Electromagnetic	10^{-2}	no	yes	yes
Weak	10^{-14}	no	no	no

A strong interaction implies a large production cross-section or a high decay probability, while a weak interaction implies a very small production cross-section or a low decay probability. It is possible to estimate the appropriate "time scales" for the different interactions; the unit for strong interactions may be taken as $\hbar/gm_{\pi}c^{2} = 10^{-23}$ sec.(g has been set equal to unity); similar quantites for the other two interactions are: electromagnetic, 10^{-19} secs.; weak, 10^{-9} secs. These figures are only to be regarded as the approximate order of magnitude of the lifetime of a particle decaying by the specified interaction. The matrix elements have not been calculated and these together with considerations of the available phase-space may change these basic figures by several orders of magnitude. (E.g. the neutron lifetime of order 10^{3} secs.)

With three exceptions, all the known particles (resonances excepted) decay through weak interactions. Strong decay is forbidden by at least one of the above conservation laws. Indeed, if strong decay were not forbidden, the extremely

short "lifetime" resulting from this would make the independent existence of the particle doubtful. However, some of the resonances may be termed "strongly-decaying" particles. Such a short lifetime results in the energy (mass) of such a particle to be ill-defined with a width inversely proportional to the lifetime (according to the Uncertainty Principle). The situation is completely analogous to that of "widths" of short lived energy levels in nuclei.

1.3 Classes of Particles and Conservation Laws

The elementary particles may be divided into three distinct groups:-

(a) Baryons,

(b) Mesons,

(c) Leptons.

(a) The baryons are all fermions (spin $\frac{1}{2}$) and are all "heavy", the lightest being the proton. They can all take part in any of the three fundamental interactions, e.g.:-

$$p + \pi \rightarrow p + \pi \qquad \text{(strong - high energy scattering)}$$

$$n \rightarrow p + e^- + \bar{\nu}_e \qquad \text{(weak - } \beta \text{ decay)}$$

$$p + p \rightarrow p + p \qquad \text{(Coulomb scattering)}$$

There are two sub-groups of baryons: the nucleons, comprising the proton and the neutron both of zero strangeness; and the hyperons which are all heavier than the nucleons and have non-zero strangeness.

(b) The mesons are bosons with zero spin and are lighter

than the baryons. Like the baryons, they can take part in all three types of interaction although they are not thought to take part directly in weak interactions. The apparent weak decay of the charged pion is assumed to take place through a nucleon-antinucleon pair.

There are two sub-groups; the π triplet of isotopic spin 1 and zero strangeness; and the K doublet of isotopic spin $\frac{1}{2}$ and unit strangeness.

(c) The leptons are fermions (spin $\frac{1}{2}$) and are all lighter than the mesons. In contrast to the other classes of particle, leptons do not take part in strong interactions and any weak interaction must involve two leptons (or more strictly, a lepton and an anti-lepton). There are no obvious sub-groups; strangeness is not a quantum number in weak interactions hence no value for this can be attributed to a lepton. Since also, isotopic spin is not conserved in weak processes, this quantum number is not meaningful. The four leptons are: μ^-, e^-, the neutretto (μ neutrino) and the neutrino (e neutrino).

In the above classes are also included the corresponding anti-particles obtained by reversing all the reversible quantum numbers. (Note; the antineutron is distinct from the neutron in having opposite relative orientations of spin and magnetic moment; also, the π triplet includes the anti-particles π^+ and π^- while the π^o is its own anti-particle.)

The numbers of baryons and leptons in any reaction are governed by two conservation laws:-

(a) the baryon number N is unaltered by <u>any</u> interaction,

(b) the lepton number ε is unaltered by <u>any</u> interaction.

The baryon (lepton) number is the number of baryons (leptons) minus the number of anti-baryons (anti-leptons).

The existence of law (a) ensures the stability of our universe since the lightest baryon (the proton) may not decay by any interaction to lighter particles - even a weak interaction with a minute cross-section would result in the inevitable disappearance of nuclei and atoms.

Since the establishment of the existence of two species of neutrino, law (b) is further strengthened by the condition that an electron is always accompanied by an electron neutrino, and likewise for the μ and neutretto. Thus the μ^+ decay:-

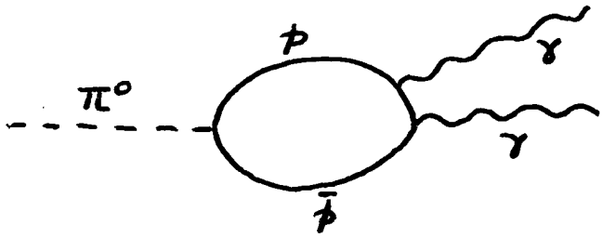
$$\mu^+ \rightarrow e^+ + \bar{\nu}_\mu + \nu_e$$

requires a ν_e for the e^+ and a $\bar{\nu}_\mu$ for the μ^+ on the other side of the reaction.

One other particle must be added to those included in the above three classes. Newton's luminous corpuscle reappears as the photon (γ) with zero rest mass and spin 1. It has only electromagnetic interactions with charged particles. Coulomb scattering is regarded as the exchange of photons between charged particles.

1.4 Virtual States

It may seem strange that although the photon is only coupled to charged particles, a neutral particle such as the π^o may undergo electromagnetic decay to 2γ. This is explained by the presence of "virtual states" forbidden by energy conservation but which may "exist" for a short enough time not to define the energy within the limits required for conservation. Thus the π^o "becomes" an $p\bar{p}$ pair, one of the charged particles emits a γ and then the two particles annihilate to produce a further γ. This process is pictorially depicted in a "Feynman graph":-



Here, the dotted line represents a meson, the full lines the baryons and the wavy lines the photons; each vertex represents an interaction between the particles converging there.

This situation where, in a sense, the π^o is regarded as a state of $(p\bar{p})$, is to be compared with the discussion earlier (section 1.1) concerning the nature of a Fundamental particle. Is the π^o truly fundamental? This question is as valid as the more familiar one "is the electron a wave or a particle?". The answer depends upon the problem under consideration. Using the criterion concerning binding

energy quoted earlier, the π^o cannot be regarded as a bound state of $(p\bar{p})$, or more strictly, of $(1/\sqrt{2})(p\bar{p}-n\bar{n})$. However, in some contexts such a model may be regarded as a rough qualitative description of the mathematics involved in the theory of the process. A single Feynman graph may be considered as representing one term in a perturbation expansion for the process. The one drawn above is the lowest order involving the least number of vertices. Many others can be drawn and, since the strength of the strong interaction (at the $\pi p\bar{p}$ vertex) is of the order of unity, the higher perturbation terms are not negligible. It is this non-convergence that reduces the value of such expansions in the treatment of strong interaction problems.

Little will be said here concerning the resonances; the existence of some is well established and their presence in the scheme of particles seems not inexplicable.

1.5 Electromagnetically decaying particles

It was stated above that only three particles decay by the electromagnetic interaction; these are the neutral π meson and the neutral Σ and $\bar{\Sigma}$ hyperons.

$$\pi^o \rightarrow 2\gamma \; ; \; \Sigma^o \rightarrow \Lambda^o + \gamma \; ; \; \bar{\Sigma}^o \rightarrow \bar{\Lambda}^o + \gamma$$

Most recent theoretical estimates of the lifetimes of these particles give:-

$$\tau_{\pi^o} \simeq 1.4 \times 10^{-16} \text{ secs.} \quad [2]$$

$$\tau_{\Sigma^o} < 10^{-19} \text{ secs.} \quad [3]$$

The following table illustrates the magnitudes of these lifetimes in comparison with those of the other particles.

Order of magnitude of lifetime. (secs)	Particle	Interaction
10^{3}	n	weak
10^{2} - 10^{-5}	-	weak
10^{-6}	μ^+, μ^-	weak
10^{-7}	-	weak
10^{-8}	$\pi^+, \pi^-, K^{\pm}, K_2^{\circ}$	weak
10^{-9}	-	weak
10^{-10}	$K_1^{\circ}, \Lambda, \Sigma^{\pm}, \Xi^{-}$	weak
10^{-11} - 10^{-15}	-	
10^{-16}	π°	electromagnetic
10^{-17}	-	electromagnetic
10^{-18}	-	electromagnetic
10^{-19} - 10^{-22}	Σ°	electromagnetic
10^{-23}	resonances	strong

(Note: the lifetimes of μ^-, π^- and K^- are not usually directly observable due to capture or interaction with a nucleus.)

Any determination of the lifetime of the electromagnetically decaying particles involves problems not encountered in those of the weak decaying particles. Any direct method depends, in essence upon knowledge, actual or implied, of the distance travelled x, and the speed βc, of the particle. From these, one has:-

$$x = \beta\gamma ct \qquad \text{where} \quad \gamma = (1 - \beta^2)^{-\frac{1}{2}}$$

and t is distributed according to the exponential law:-

$$p(t)dt = \tau^{-1} e^{-t/\tau} dt$$

where τ is the mean lifetime

We also have that the momentum of the particle is:-

$$p = m\beta\gamma \text{ MeV/c} \quad \text{where } m \text{ is the mass in MeV.}$$

thus $x = pct/m$

For the π^o, take $t = 10^{-16}$ sec. then if x is in cms.:-

$$p = \frac{mx}{3}. 10^6 \text{ MeV/c}$$

$m_{\pi}o = 135$ MeV so that the momentum required for 1 cm. flight distance is 4.5×10^4 GeV/c. Thus it can be seen that a detector with fine resolution is required to measure the flight distances of π^o's of energies normally encountered. Such a detector is provided by nuclear emulsions.

CHAPTER II

THE NEUTRAL π MESON

2.1 Existence and mass

The existence of a neutral meson decaying to photons was indicated in a study of high energy photons (up to 200 MeV) emitted in targets bombarded by protons with energies greater than 180 MeV. [4] The results were consistent with a neutral meson of mass around $300m_e$ and with a lifetime less than 10^{-11} secs. More definite evidence was provided by Steinberger et al. [5] who bombarded nuclei with X-rays (330 MeV) and observed the angular correlation between the emitted γ-rays. The results showed that the γ-rays were emitted in pairs and were the decay products of neutral mesons. The decay into 2γ indicates a spin of zero since such a decay is forbidden to particles of spin $\frac{1}{2}$ or 1. (Higher spins are excluded from consideration.)

The mass of the π^o was determined from experiments to deduce the mass difference $\delta = m_{\pi^-} - m_{\pi^o}$. The reactions:-

$$\pi^- + p \longrightarrow n + \pi^o \quad ; \quad \pi^o \longrightarrow 2\gamma$$

were used by observing π^- capture in a hydrogen target. The first experiment of this type [6] examined the spectrum of γ-rays. A broad group near 70 MeV was presumed to originate from the π^o decay. The result, assuming the π^- to be

captured at rest, was $\delta = (10.6 \pm 2.0)\ m_e$. A similar experiment [7]) using a liquid hydrogen target and observing the angular correlation of the γ-rays gave $\delta = (8.8 \pm 0.6)\ m_e$. It is of special interest to quote the experiment of Haddock et al. [8]) which also used the π^- capture reaction but which deduced the energy of the neutrons produced by time of flight measurements on them over distances of 12.44' and 17.50'. (The flight distances of the π^o measured in the present experiment are of the order of 0.1μ) The result was $\delta = (8.990 \pm 0.020)\ m_e$.

This very small mass difference between the π^o and the charged π mesons, its identical spin to these particles and the necessity to introduce a neutral pion to explain the p-p or n-n nuclear forces if the n-p force is considered due to the exchange of a charged π, place the π^o as the member of an isotopic spin triplet with $\tau = 1$ and $\tau_z = 0$. Since the charged pions are mutual anti-particles, the neutral pion is its own anti-particle, a property which it alone shares with the photon. The decay to 2γ indicates odd parity.

2.2 Decay properties

The π^o shares with only two other particles (Σ^o and $\bar{\Sigma}^o$) the property of decaying through the electromagnetic interaction; all other particles have decays dominated by the weak interaction. In consequence, the lifetime of the π^o is of a very different order from that of these particles, the

shortest-lived of which decay in about 10^{-10} secs. The coupling constant for electromagnetic interactions is very much larger than that for the weak, therefore a much more rapid decay is expected.

2.3 Previous lifetime estimations

Early experiments, [9-12] all using emulsion technique, set successively shorter upper limits on the lifetime, ranging from 3×10^{-13} secs. to 10^{-15} secs. Most of these methods depended upon the study of electron pairs produced in nuclei bombarded with high energy incident particles. (Such an event in emulsions is termed a "star" from the appearance.) Most of the electron pairs were produced in a rarer decay mode of the π^0 whose existence was pointed out by Dalitz [13] :-

$$\pi^0 \rightarrow \gamma + e^+ + e^-$$

This mode may be considered to be due to the internal conversion of one of the decay photons. The branching ratio of this mode is about 1.2%. The electron pair produced in this mode is termed a "Dalitz pair". This mode is of particular importance in emulsion work as it represents the only mehtod of detecting π^0's; the conversion length for a photon in emulsion is of the order of 1 cm. which makes correlation impossible for this mode.

The lifetime estimates depended upon measurement of the distance between the star centre (point of production of π^0) and the beginning of the Dalitz pair tracks. The final

attempt by this method was by Anand [14] who obtained a "most probable" lifetime of 5×10^{-15} secs. and also a value for the Dalitz branching ratio of $(1.3 \pm 0.4)\%$. As will be seen from the later and more refined experiments, this value is an order of magnitude too high. The probable explanation for this which has been given is that the ionizing power of an electron pair is much smaller than that for a single electron when the separation of the pair is very small, as it would be near the point of creation. Thus the apparent vertex of the pair would start some way along the actual trajectory and create a "gap" greater than that due to the flight of the π^0 alone.

2.4 Experiment of Harris et al.

The upper limit on the lifetime was reduced a further order of magnitude by Harris et al. [15] This experiment forms the basis of the method of the present determination and will be described in some detail.

A stack of Ilford G5 emulsions was exposed to a stopping beam of K^+ mesons at the Berkeley accelerator. The stack was scanned for events in which the K^+ decayed at rest in the $K_{\pi 2}$ mode and the resultant π^0 decaying in the Dalitz mode.

$$K_{\pi 2} \rightarrow \pi^+ + \pi^0 \quad ; \quad \pi^0 \rightarrow \gamma + e^+ + e^-$$

The $K_{\pi 2}$ being a two-body decay at rest, results in a unique energy for each of the decay products. The π^0 is produced with a velocity of 0.835c. Furthermore, the direction

of the π^o is known, it is directly opposite to that of the π^+ which, as it is charged, leaves a track in the emulsion. Thus, in principle, the point of production is located by the end of the K^+ track, and the point of decay is located by the intersection of the electron tracks with the π^+ line of flight produced backwards. These being known, the flight distance and, since the velocity is known, the lifetime are determined.

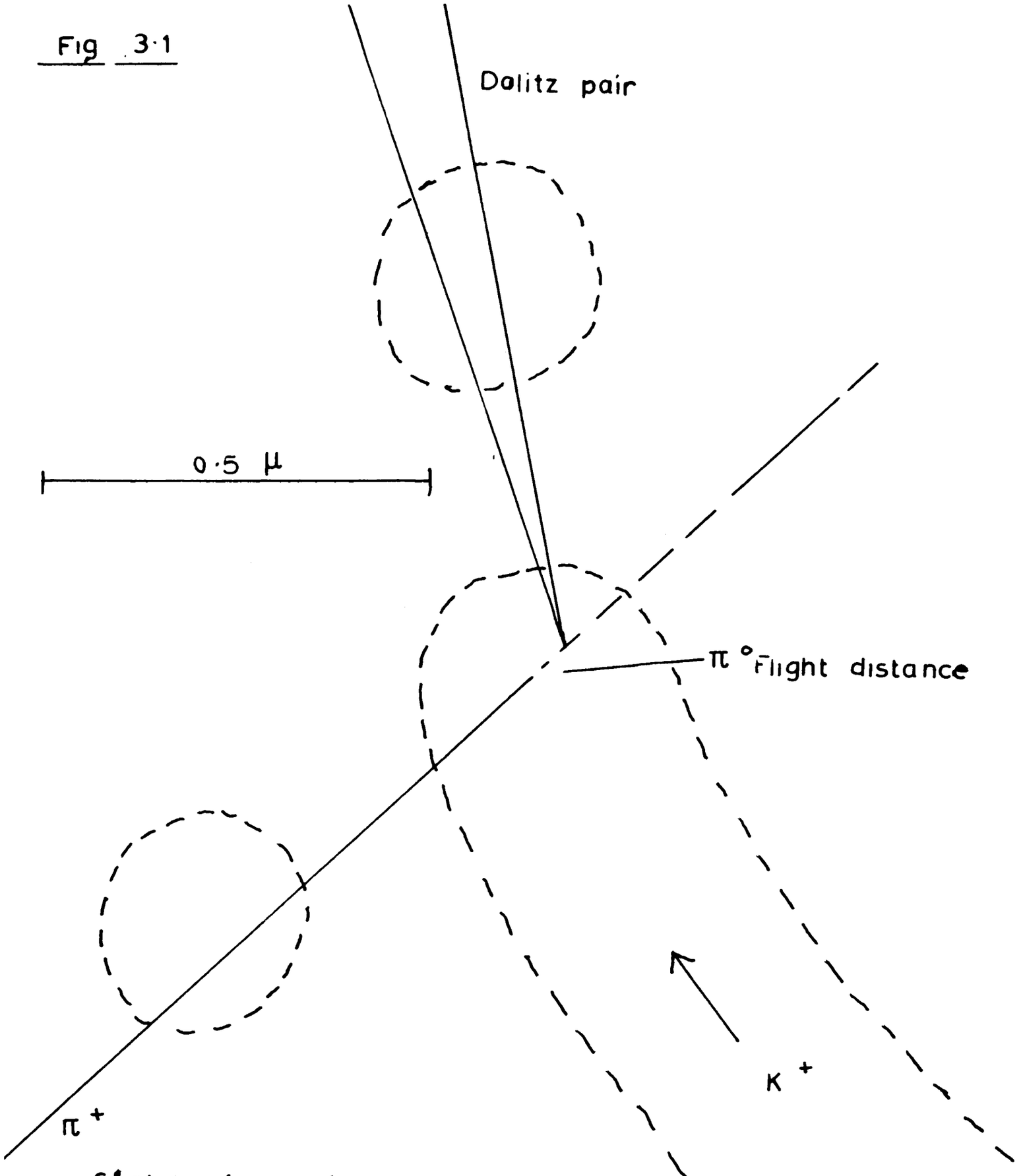
The actual execution of the experiment presents many difficulties which will be discussed in the introduction to the present experiment. Harris used a "camera lucida" to view the events and made tracings of the positions of the grains in each event. By fitting straight lines to the grains in the tracks it was possible, for each of the twelve events used, to obtain a "measured flight distance". The results were analysed by a maximum likelihood method and gave an upper limit of 4×10^{-16} secs. for the lifetime.

A number of other workers [16-18] have since performed similar experiments using this method but each has made the measurements in a different way. Another emulsion experiment [19] using a different approach, a counter experiment [20], and a method involving the reverse process (the photo-production of π^o's in the Coulomb field of a heavy nucleus)

[21]) have also been performed. These more recent and more accurate determinations will be described and discussed in a later chapter and compared with the present experiment.

The experiment to be described also employs the method of Harris, but the technique of measurement is different from that of other workers.

Fig 3·1



Sketch of event
showing relative grain site

CHAPTER III

THE PRESENT EXPERIMENT

3.1 Introduction

There are three main improvements which may be made in the basic method described in the preceding section:-

(i) Measure a greater number of events,

(ii) Improve the measurement technique,

(iii) Use a finer grained emulsion.

All three of these improvements have been made in the present experiment.

The basic method is illustrated in Fig. 3.1. For a lifetime of 10^{-16} secs., the flight distance is about 0.05μ. The dotted outlines in the figure indicate the typical appearance of the event in emulsion. Since the flight distance is so small, the point of decay of the π^{o} is located within the grain forming the end of the K^{+} track. No obvious "gap" due to the flight of a neutral particle will be visible in these decays, the appearance will be of three tracks emerging apparently from the same point.

It is clear that in view of the expected flight distance being small, errors due to the uncertain fitting of straight lines to the track grains and the consequent uncertainty in the intersection point will be important. The measurement

technique used involves the measurement of the co-ordinates of the grains forming the events by means of a bifilar microscope eyepiece. The trajectories are obtained by making straight line fits to the appropriate grains and calculating the flight distance using the ordinary formulae of analytical geometry.

The actual point of decay of the K^+ is not well defined due to the grain size of the emulsion, hence a reduction of this factor will increase the attainable accuracy.

It is anticipated that the errors in measuring the flight distance will be of the same order as that quantity itself. In addition to this, the actual time of existence is a distributed variable (the exponential law). Both these considerations make it essential to measure as large a sample of events as possible in order to obtain a meaningful result.

3.2 Exposure and Processing

A stack of 200 pellicles of Ilford L4 emulsion was exposed to a high intensity K^+ beam at the Berkeley Bevatron. The size of each pellicle was 8"x6"x 400μ. The initial momentum of the beam was about 700 MeV/c; this was degraded to about 400 MeV/c at which momentum the particles entered the stack. The stack was exposed for twelve hours, during which time 3-500,000 K^+ mesons stopped in it.

The stack was processed in Oxford. A previous test with

L4 emulsions had been carried out to determine the best development technique to give a small developed grain diameter consistent with a reasonable minimum ionization grain density and low background development and fogging. Full details of the processing are found in reference [22]. A mean diameter of 0.3μ was obtained for the grain size and a mean value of g_{min} = 19 grains/100μ for the grain density. The development of background grains was rather high. After processing, each pellicle was cut into three such that the centre section contained most of the K^+ decays. This was for ease of scanning so that it was only necessary to have a small plate on the microscope stage.

3.3 Scanning

An area scan was carried out in two stages. At first, a slow scan was made where the plates were examined under a scanning microscope with a total magnification of about 250x. All track endings were examined carefully and classified using the considerations outlined in the following paragraphs.

Each track ending may be due to one of the following particles: μ^+, π^+, K^+, p. Some of these are the decay products of the main beam, some due to contamination of the beam and some due to nuclear interactions produced by background radiation (cosmic rays etc.).

The μ^+ and π^+ were normally readily identified. The

μ^+ is a light particle, its track scatters considerably before coming to rest, moreover, this scattering occurs while the track is still "grey" (i.e. a high grain density but not yet a continuous track of touching silver grains). The π^+ decays into a μ^+ which is usually easily seen emerging from the end point of the π track, the μ^+ from this decay is monoenergetic an has a characteristic range in emulsion of about 600μ. (This π^+ decay is also another source of μ^+ contamination.) The proton is a heavy particle and suffers little obvious multiple scattering throughout the whole length of track. There is also no secondary decay product.

The appearance of a K^+ track lies somewhat between the two extremes of μ and p. Multiple scattering is not appreciable except where the particle is nearing the end of its range, by which time the track is "black" (i.e. continuous). In some cases the track end can greatly resemble that of a proton, suffering very little multiple scattering; in addition, the decay secondary may be minimum ionizing and therefore not easily visible under unfavourable conditions. Consequently and unambiguous identification of a K decay is not always possible. It was desirable that the scanners should become experienced in recognising K^+ track ends using the above qualitative considerations. This was the purpose of the preliminary slow scan.

The slow scan was conducted as follows. The search for track endings was carried out under a magnification of 250x in a small area of each plate which preliminary measurements had shown contained the densest concentration of K^+ decays. When a track ending was found, it was examined under a magnification of about 600x and, using the above criteria, assigned to one of the following categories: μ, π, K, p, K/p, the last class being for the ambiguous endings. In the early stages, two further ambiguous classes, π/K and μ/π were also used. If an ending was classified as a K, a secondary track was sought; if this was found, this was noted and then two further secondary tracks were looked for. If none were found within a short time, the ending was left.

The growing ability of the scanners to recognise K endings was judged by the decrease in the number of ambiguous cases noted and the increase in the number of K's with secondaries observed. When the efficiency of a scanner had been judged to have reached a high enough value, a fast scan was started. Only K endings with a visible secondary were noted, and if three secondaries were observed, the position of the event was noted by reference to a transparent grid stuck on to the bottom of the supporting glass plate.

It was important that a scanner should not spend too long searching for secondary tracks. The procedure adopted was

that an event was rejected if no secondary track was found at all after a specific time (this varied from about 15 to 60 secs. depending upon the personal experience of the scanner). A further 30 secs. were allotted for the search for additional secondaries; if none were found within this time, the event was abandoned. Once two secondaries had been located, a much longer time of several minutes was allowed for searching for the third track (which by charge conservation must be present). If a third track was found and all the tracks were near minimum ionizations, the event was recorded as a provisional $K_{\pi 2}$-Dalitz pair event (named for convenience as "KD" event). If only two secondaries could be found, the event was recorded as an "oddity" to be examined more thoroughly later. Such events were usually found to be crossovers or events where the third track dipped very steeply and was difficult to see. Three tracks are also present in the $K_{\pi 3}$ (or τ) decay mode of the K^+:-

$$K_{\pi 3} \rightarrow \pi^+ + \pi^- + \pi^+$$

However, in this decay, the least possible ionization for any of the tracks is about $1.4 g_{min}$ and the directions of the tracks "appear" to conserve momentum. The high density of the tracks meant that such decays were almost always seen without the need for the routine described above.

For KD's, oddities and τ's when found, the event was located with reference to the grid and a rough sketch of the

event was made noting the directions of the dips of the secondary tracks.

Use was made of the ease with which the τ decays were seen in checking the efficiency of the scanners in selecting K^+ endings for closer scrutiny. The branching ratio of the τ mode is about 6%. [23] If one assumes that the scanning efficiency for the τ's is very nearly 100%, the following conclusions may be drawn from branching ratios calculated from the scanning results. A low branching ratio (less than 4%) indicates that a number of endings examined were not K's and therefore, a wastage of time; a high branching ratio (greater than 8%) implies that too few K's were being examined and hence a danger of losing useful events.

The final results of the scanning were that about 70,000 K^+ decays were examined, yielding a total of 103 possible KD's and about 4,000 examples of τ decays.

3.4 Preliminary measurement

The events selected from the scanning contain not only the desired $K_{\pi 2}$ decays but also other K^+ decays in which a π^o is produced, subsequently decaying in the Dalitz mode. These contaminating decays are:-

	br. ratios [23]
$K_{\mu 3} \rightarrow \mu^+ + \nu_\mu + \pi^o$	4.4%
$K_{e3} \rightarrow e^+ + \nu_e + \pi^o$	4.5%
$K'_{\pi 3} \rightarrow \pi^+ + \pi^o + \pi^o$	2.1%

The branching ratio of the $K_{\pi 2}$ mode is 25.6 ± 1.5 so that, taking into account the double weighting of the τ' ($K'_{\pi 3}$) mode (there being two π^o's) the expected contamination is about 34%.

The contamination events are three body decays, hence the momentum of the π^o is not unique and neither can the direction of its trajectory be inferred from that of the charged secondary.

Some of these spurious events may be detected by measuring the grain density of the secondary track. The following table gives the range of energies, of β (=v/c) and of g^* (= g/g_{min}) for the charged secondary.

mode	KE (MeV)	β	g^*
$K_{\pi 2}$	109	0.83	1.1
τ'	0-53.3	0-0.69	>1.4
$K_{\mu 3}$	0-134	0-0.89	>0.95
K_{e3}	0-228	0-1	1.0

If secondaries with a grain density of more than $1.4 g_{min}$ are rejected, all the τ' decays will be eliminated together with about 30% of the $K_{\mu 3}$'s. (This fraction is estimated from the spectrum of the μ^+ calculated from phase-space.) By this means the contamination is reduced to about 23%.

All the events noted down as KD's and "oddities" were

examined under a magnification of about 2,000x. Measurements were made of the angles between the tracks (projected in the plane of the emulsion) and of the dips of the tracks, particularly that of the charged secondary. This is important because all the subsequent measurements are made on the projection of the event in the plane of the emulsion, consequently the measured flight distance of the π^o must be multiplied by sec α, where α is the dip angle of the supposed π^+.

As mentioned in a previous paragraph, a knowledge of the grain density of the charged secondary is useful in enabling the elimination of unwanted decay modes. Estimates of the required grain densities were made by grain counts performed upon the length of track available before leaving the plate. This frequently involved counting less than 100 grains, especially in steeply dipping tracks. This represents an error of at least 10% and this figure is further worsened by the dip factor sec α.

At this stage it was necessary to decide whether there was any advantage in performing a more accurate measurement of the grain densities by following the tracks through into adjacent plates in order to count a larger number of grains, taking into acoount the variation of the g_{min} from plate to plate and from top to bottom of the same plate.

It was decided not to proceed with such a measurement

but to reject the events with a measured g^* of more than 1.4 (calculated on the basis of a mean g_{min} of 19/100μ). Such a criterion ensured the elimination of nearly all the τ' decays even allowing for the error in the determination of g^*, while the probability of rejecting a true $K_{\pi 2}$ event was small. With this assumption together with the one that 30% of the $K_{\mu 3}$'s had been rejected, it was possible to calculate the effect of this contamination upon the final result. The rejection of events results in a reduction of the contamination to 23%. If one now assumes that these events if treated as $K_{\pi 2}$ events yield an average "flight distance of zero then the following relationship exists between the true lifetime and the measured lifetime with the spurious events:-

$$\tau_{true} = \frac{\tau_{exp}}{1 - 0.23} \cong 1.3\ \tau_{exp}$$

The effect of the contamination is seen to result in a simple correction factor applied to the final result. In fact, the situation is better than is assumed since the contamination events yield on the average a positive "lifetime" which is related to the true lifetime. This results in the correction factor being less than 1.3. A more accurate assessment of the correction factor will be given in a later chapter.

With some of the events it was not necessary to make a formal grain count as the track was quite clearly "grey".

Of the 103 original candidates, 19 were eliminated on the basis of grain counts. The contamination figure of 23% indicated an expected 24 spurious events. These figures are not inconsistent and indicate that the selection procedure was more likely to retain spurious events than to reject the desired $K_{\pi 2}$ decays.

CHAPTER IV

THE METHOD OF CO-ORDINATE MEASUREMENT

4.1 Introduction

In Harris' experiment, drawings of each event were made using a camera lucida and then straight line fits to the grains in the tracks were made by eye. The method of measurement of the events which is used in this experiment makes a considerable improvement upon this.

The event to be measured is placed in the field of view of a Koristka R4 microscope using a magnification of about 2,000x. The microscope is fitted with a bifilar micrometer eyepiece by means of which the (x, y) co-ordinates of the grains composing the event, may be measured relative to the fixed field of view. The filars of the eyepiece lie in the intermediate optical plane of the microscope, hence the co-ordinates measured are those of the considerably magnified image. This permits a high accuracy of measurement since the very small actual dimensions of the event are related to the necessarily coarser mechanical measuring device.

4.2 Preliminary model

The first bifilar eyepiece to be constructed had the normal type of micrometer scale with 0.01 mm. divisions. The instrument was calibrated against the fine 'X' stage

motion screw of the microscope. By using the vernier, this could be read to 1μ. By this means it was found that when using a Cooke 95x oil immersion objective, 1 mm. motion of the eyepiece filars corresponded to about 4μ in the object plane. A number of KD events and τ events were measured using this instrument and considerable experience was gained in developing the best measurement technique. The sets of co-ordinates were used in the development of the computer programme which fitted the straight lines and calculated the flight distance. This programme will be described fully later. Also, it was possible to assess approximately the sources of error and the order of accuracy to be expected.

4.3 Sources of error

The factors affecting the accuracy of the experiment may be divided into two classes, those which can be improved by modifying the instrument or the method of measuring, and those which are inherent in the emulsion itself. The main sources of error may be listed under these categories as follows:-

Instrument

(a) drift of the image in the field of view during measurement,

(b) measurement error in the positions of the grains due to difficulty in placing cross-wires over image of grain,

(c) optical distortion of the intermediate image,

(d) inclusion of spurious grains when measuring a steeply dipping track,

(e) difficulty in deciding which point of the K^+ track end to choose as the decay point,

Emulsion

(f) due to the finite grain size, the grain centres will not lie precisely on a straight line,

(g) also due to the finite grain size, the actual decay point of the K^+ may not be at the centre of the last grain of the track.

(a) Considerable drifting of the image in the field of view was experienced, the rate of drift being a few microns per hour. This amounted to about 0.5μ during the measurement of one event. The cause was eventually traced to the diurnal heating and cooling of the body of the microscope (the direction of the drift reversed at night). The changes in temperature were very small and were only detectable using a thermocouple and a microvoltmeter. The correlation between temperature and the drift in both X and Y directions was very high, indicating that the thermal effect was dominant.

The effect was combatted by enclosing the microscope in a box constructed of sheet aluminium and lined on the interior with $\frac{1}{2}$" thick expanded polystyrene sheeting. The focussing and stage motion controls were suitably extended outside the box and the whole of the eyepiece remained outside also. It

was fortunate that the design of the Koristka is such that the lamp is situated at the end of a long side arm so that it was not difficult to exclude this source of heat from the box. The box was in no way sealed from the outside air as it was found that the magnitude of the drift had been greatly reduced to negligible proportions without this further precaution. The effect of any residual drift was minimized by always measuring an event in a given order. This is described in a later chapter on the measurement of the events.

(b) The filars of the eyepiece were very fine (less than 5μ) lines etched on the glass slides. These were found to be unsatisfactory for two reasons. They were so fine that under certain illumination conditions, annoying diffraction fringes appeared about them and caused considerable confusion especially if the grain were a faint one. It was also difficult to judge when the line bisected a grain; this was due principally to the obscuration caused by the line itself.

(c) Calibrations were carried out in various parts of the field of view and no sensible optical distortion was detected.

(d) With steeply dipping tracks only one grain of the track is in focus at a time; it is then necessary to extrapolate the track direction by eye to detect the next grain in the track. As there are "background" grains present in addition to those of the tracks, there is a possibility of including

one of these if it happens to lie roughly in the line of flight. This problem was solved by incorporating in the line fitting routine of the computer programme a test for a grain lying considerably off the calculated line. Such a grain was rejected and a new fit made. This process was repeated until all spurious grains had been eliminated. (The full details of this routine are given in the section on data analysis and in the appendix.) A similar difficulty was encountered when measuring the tracks of an electron pair with a small opening angle. In this case it was often difficult to decide which track a grain belonged to. In the case of an error of judgement the wrong grain would be treated as spurious and rejected by the programme. The routine was tested by feeding in the co-ordinates of two pair tracks as a single track. All the grains from one track were rejected. (In this extreme case, the track rejected depended upon which grain was rejected first.)

(e) The problem of the correct location of the end of the K^+ track was recognised as one of the main sources of error in the method and is discussed in detail later.

Little can be done about sources of error inherent in the emulsion. By employing the finest grained emulsion available the errors are minimized. The effects of (f) and (g) are discussed in more detail in a later section.

Although considerable experience in measurement technique

had been acquired with the bifilar eyepiece described above, a greatly improved version was developed. In view of a proposed further experiment on the π^{o} lifetime which would involve similar co-ordinate measurements but in a much greater quantity, the new bifilar eyepiece built had each motion digitised so that the co-ordinates could be automatically and immediately punched out on to computer tape. A full description of the instrument is not out of place as its construction and development occupied some time and it incorporates certain novel features as a result of experience gained with the earlier model.

CHAPTER V

THE DIGITISED MICROMETER EYEPIECE

5.1 Method of Digitising

The motions of the cross-wires were digitised using moire fringe technique. Moire fringes are produced when two identical grating structures are superimposed with their grating lines at a slight angle. The effect is commonly seen with such things as folds in lace curtains, parallel fences, while an excellent example is seen in the wire meshing at the top of the Oxford City Church. The word "moire" is the name of fabric which is also described as being "watered" - such a fabric exhibits the fringes described above.

The explanation for the production of these fringes seems at first to be simply a mechanical effect heightened by optical illusion; the eye tends to "join up" the apparent intersections of the gratings to produce the ghostly fringes. However, this explanation becomes untenable when fringes can be demonstrated using two gratings with a pitch of only a few microns. The explanation of the effect is then quite complicated and depends upon an analysis of the effect of two diffraction gratings "in series". If the rulings of the two gratings are not exactly parallel, interference takes place between the diffracted beams, producing the fringes observed. The spacing and orientation of the fringes

is the same as is predicted by the "mechanical" theory. It is fortunate that the two effects can be predicted with the same formula as this implies that there is a smooth transition from one situation to the other. Thus, moire fringes may be obtained with any pitch of grating.

The application of moire fringes to metrology is due to the effect that relative movement of the grating systems perpendicular to the rulings, by one pitch length causes the moire fringe pattern also to move by one of its fringe spacings. The fringe spacing is a function of the angle between the rulings of the two gratings and can be made very much larger than the grating pitch. The fringes lie approximately perpendicular to the grating rulings and their separation is given approximately by the formula $l = d/\theta$, where l is the fringe spacing, d the grating pitch and θ the angle between the rulings (in radians).

The above effect results in a strictly linear magnification of displacements without the need for microscopy. For example, in the instrument to be described, the grating pitch was 1,000 lines/inch while the fringe spacing was about 0.5". Thus a displacement of 0.001" of one grating caused the fringe pattern to move by 0.5", i.e. a magnification of 500x.

The passage of the fringes can be detected with photocells and the resulting signals used to operate counter circuits.

5.2 Requirements of measuring system

The requirements for a moire fringe measuring system are as follows:-

(i) two identical pitch gratings, one moving (index) and one fixed (reference), the relative motion being perpendicular to the rulings;

(ii) an optical system passing collimated light through the two gratings and on to the photocells;

(iii) provision for rotating the fixed grating to adjust the angle between the rulings and hence the fringe spacing;

(iv) adjustment of the separation between the fixed and moving gratings;

(v) electronic equipment for interpreting the signals from the photocells.

The first requirement is easily met and needs no further discussion. Requirement (ii) depends upon the gratings used. If coarse gratings are employed (less than 250 lines/in.) the system may be simple, consisting of a lamp with a collimating lens to pass parallel light through the gratings. The photocells are simply placed on the other side so that the "shadow" of the fringes passes over them. However, when gratings with 6,250 lines/inch (i.e. a pitch of 4μ) are used, diffraction effects become important and spectra are produced at the photocell position. It is usual to have an optical

system similar to a normal spectroscope arranged in the "minimum deviation" position. The photocells are positioned so that they receive the colour to which they are most sensitive.

Requirements (iii) and (iv) may be met in the mechanical design of the instrument. The separation of the two gratings is of great importance when very fine gratings are being used. The contrast of the fringes is a sensitive function of this separation. For the 6,250 lines/inch gratings, an optimum figure of 0.002" is quoted, while a separation of only 0.010" gives extremely low contrast. The coarser gratings are not so sensitive to the separation, giving good contrast even when comparatively widely spaced.

The simplest form of detector (requirement (v)) would be a single photocell followed by a binary counter. By this means the number of fringes passing over the photocell can be counted and hence the displacement calculated. This method suffers from two great disadvantages; the counts are added irrespective of the direction of motion and the smallest possible movement detectable (one "digit") is one grating spacing.

The first difficulty can be overcome by using two photocells so placed that the signals from them are $\pi/2$ out of phase. This is accomplished by placing the photocells so that the fringe passes over them in succession and adjusting the fringe

spacing to be four times the distance between the photocells. If cell 1 is taken as the reference, the signals from cell 2 will lead in phase for one direction of motion and lag for the other. The electronics can be made to detect this relative phase and cause the signals to "add" or "Subtract" according to the direction of motion. In fact, four photocells are used, the other two having phases relative to cell 1 of π and $3\pi/2$. The "in phase" signal is obtained from the difference between cells 1 and 3 and the "quadrature" signal obtained similarly from cells 2 and 4. The purposed of this differencing is to minimize effects due to drift in the d.c. levels of the photocells or variations in the lamp brightness. It will also bee shown later that the effect of using these two phases of signal is to reduce the "digit" to 1/4 of a grating spacing.

5.3 Description of the instrument

It was decided to use gratings with a pitch of 1,000 lines/in. With these gratings the "digit" is 0.00025" or about 6μ (1/4 grating spacing). Comparing this with the calibration of the early eyepiece, a digit of 0.025μ in the objective plane of the microscope was anticipated. There would be no material advantage in using a finer pitch grating as the increased accuracy available would not be attainable due to the size of the setting errors. This point is illustrated later in the chapter.

5.31 Grating production

The gratings used were produced in the laboratory from a master given by the National Physical Laboratory. The master was a photographic negative and the replicas were produced from it by contact printing.

The master when examined under a microscope was seen to be formed by alternate lines of clear glass and black silver image, the lines being of equal width (0.0005"). The contrast was excellent. Although for our purposes the negative was a "master" it was itself a replica made from a true master at the NPL.

The copies were made on Kodak MR plates. The emulsion on these plates is claimed to have a resolution of 1,000 lines/mm or better. The emulsion layer is very thin in order to minimize "turbid spread" of the light. Turbid spread causes the apparent enlargement of the dark areas in the positive print which would alter the master's black/white ratio of 1:1. The prints produced were inspected under a microscope to judge the contrast and black/white ratio. Various combinations of exposure time and development time were tried; contrast is increased to some extent by extended development but there is also the danger of fogging; long exposure tends to enhance the effect of turbid spread. The finally accepted prints had contrast and black/white ratio which compared very favourably with the original.

An accurate glass-cutting machine is available in the laboratory and with the aid of this, it was possible to cut the pieces of grating to the size required and to ensure the rulings were perpendicular to the length of the grating. Both moving and fixed gratings were produced as described above.

5.32 Mechanical construction of eyepiece

The main details of the mechanical construction of the instrument may be seen in fig. 5.1. The body of the instrument has two guide channels which have accurately machined parallel sides. The two channels are perpendicular to each other. In each channel moves a brass slide which is an accurate sliding fit in the channel. On the slide is mounted one cross-wire and the moving moire-fringe grating. The motion of the slide is controlled by a screw thread which is rotated by the operating knob. The design of the slides is such that when in position in the body of the instrument, the two cross-wires have a separation of about 0.002". This is to ensure that both cross-wires are in focus simultaneously. The cross-wires and the intermediate image of the microscope are viewed by a standard 15x Kellner eyepiece.

The instrument was in use for a short while with the operating knobs on the body of the instrument. This was found to be disadvantageous for two reasons: touching the

instrument during measuring caused slight movements of the image; there was considerable fatigue and discomfort in holding the hands up in a position near the eyes.

To overcome these disadvantages, flexible drives were fitted to both motions. By this means, the control knobs were brought down to table level and the position of the eyepiece was not disturbed during measuring.

At this point it may be mentioned that any mechanical backlash present in either lead screw or flexible drive does not affect the measurement accuracy. This is because the cross-wire and the grating are rigidly connected together by both being mounted on the brass slide; hence the output of the photocell system relates only to movements made by the cross-wire, not those by the lead screw etc. This is an important feature of the instrument, namely that its accuracy does not depend upon an accurate and linear lead screw and that the read-out is completely free from backlash. This would not be the case, for example, with a similar instrument employing a rotary digitiser operating on the lead screw. (Such a design was among those considered for this instrument but was rejected for this reason and on account of the large bulk and weight involved.) In addition, such a design would depend upon <u>two</u> independent standards of measurement: the lead screw and the digitiser grating. The

present design depends for its measurement standard upon the accuracy of the grating rulings alone.

For convenience of use the backlash between the control knobs and the cross-wires was made as small as possible as a large amount of "lost motion" makes setting difficult.

The instrument was made to fit on the eyepiece slide of a Koristka R4 microscope. It was ensured that the length of the optical path to the cross-wires was the same as in the standard Koristka binocular eyepiece. When in use, the position of the eyepiece on the slide was standardized by arranging for the built-in fixed cross-wires of the microscope to be in focus; these cross-wires are situated at an intermediate image plane between the objective and the eyepiece.

No provision was made for rotating the eyepiece about the optic axis.

5.33 Grating Optical System

In the preceding general remarks concerning optical systems for moire-fringe digitisers, two main types were described for the coarse and for the very fine gratings. The 1,000 lines/inch gratings used lie between the two extremes and the optical system used has features from both.

The gratings are "mark/space" (or black/white) as opposed to the finer 6,250 lines/inch gratings which are plastic

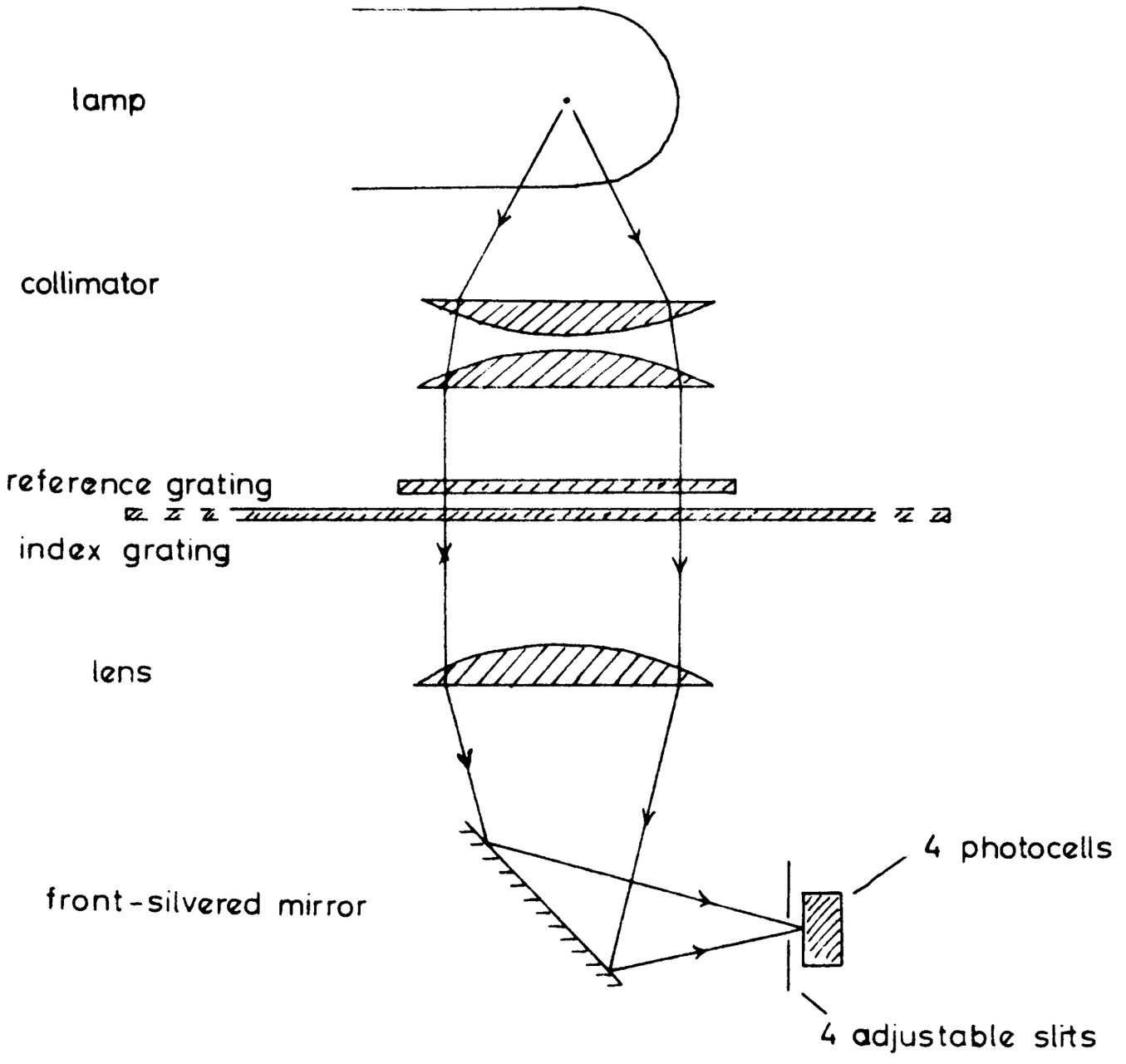


FIG 5.2 Moiré fringe optical system.

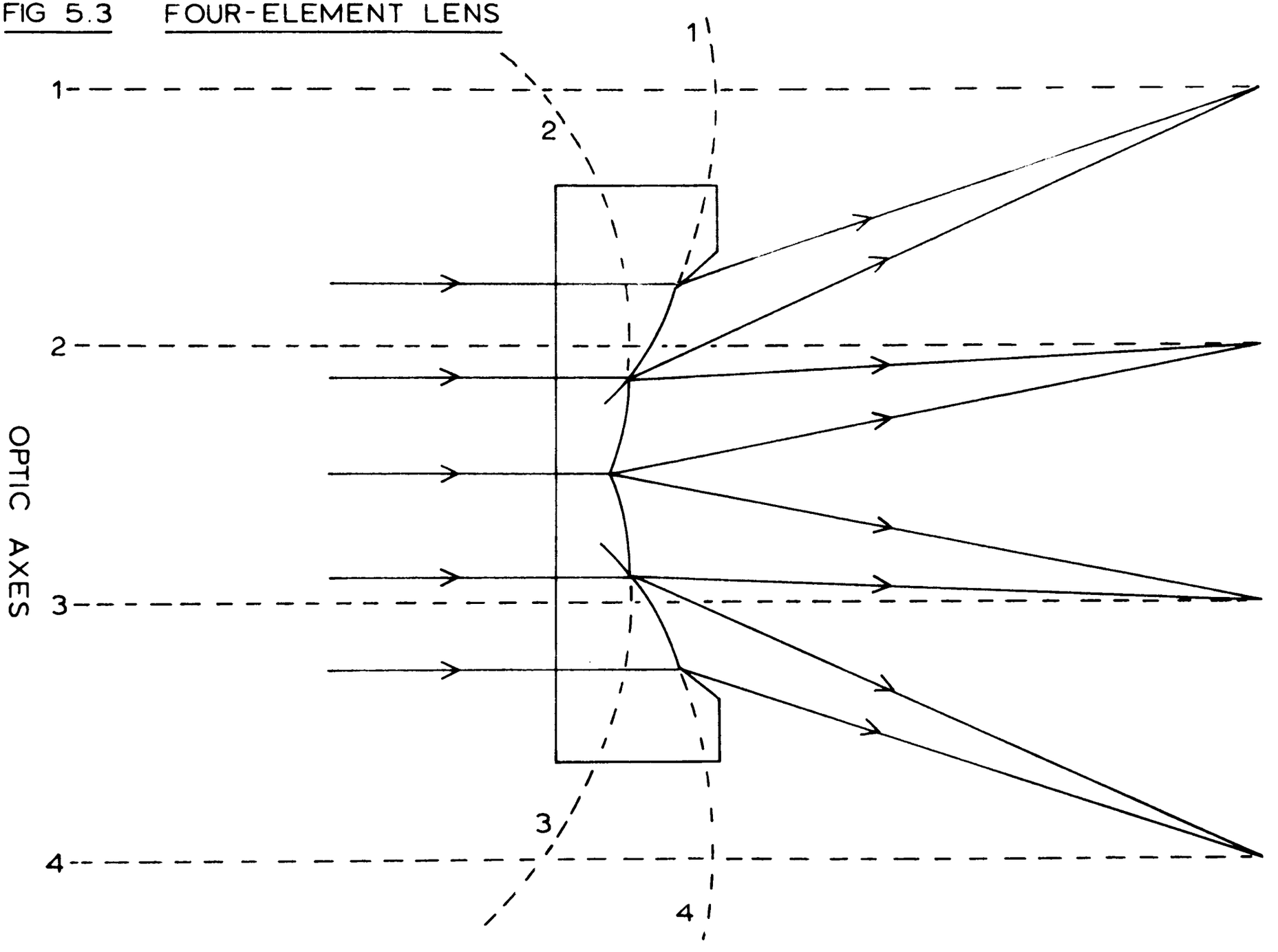
replicas with the "rulings" being prismatic in section. These prismatic gratings are said to be "blazed". The effect is to concentrate a large proportion of the energy into one of the first order spectra and the zero order is very much dimmer than with a straightforward grating. This in turn improves the contrast of the moire fringes; to make most use of it, the minimum deviation condition is used in the optical system.

The gratings used, as has been noted, are mark/space type and being coarser in pitch, fringes of good contrast may be obtained with very little trouble. For this reason a "straight through" light path is employed, the rays passing perpendicularly through the two gratings. A sketch of the system used is shown in fig. 5.2.

With the coarser gratings, the light emerging from the gratings falls straight on to four photocells. The photocells are placed near the gratings so that each receives light from a strip of the field of illumination, parallel to the fringe direction and 1/4 of a fringe spacing in width. The four strips are adjacent and together make up the whole field of illumination.

An improvement is made when using finer gratings by employing a "four-element lens" which has been developed by Ferranti Ltd. The operation of this lens is shown in fig 5.3.

FIG 5.3 FOUR-ELEMENT LENS



The final effect is that the light from each of the four strips described above is focussed on to the appropriate photocell. By this means it is possible to obtain a better output signal from the photocells.

The 45° plane mirror following the four-element lens was included merely for the compactness of the design to allow the photocell assembly to be mounted close to the body of the instrument.

The photocells employed were a photovoltaic type, Mullard MS1BE; their small dimensions make them very suitable for this application. Each photocell has in front of it a slit whose aperture may be adjusted by a small screw. The purpose of this is to allow for variations in the photocells and to maintain balanced outputs from the cells.

The connections to the photocells and to the exciting lamps are made by means of a 14-way sub-miniature plug and socket.

Provision is made for fine adjustment of the rotation of the fixed grating relative to the moving grating in order to obtain the correct fringe spacing (i.e. four times the spacing between adjacent photocells).

The separation between the fixed and moving gratings is not adjustable as the contrast of the fringes is not unduly sensitive to this figure for 1,000 lines/inch gratings. A figure of 0.002" was incorporated in the design.

5.34 Cross-wires

Mention was made while discussing the use of the earlier micrometer eyepiece of the difficulty in placing the cross-wires over the image of a grain. It was decided that the most efficient form of t cross-wire for the present application would be a pair of parallel lines instead of the single line used previously. With this system, the particular grain being measured is "nested" in the box formed by the intersections of the cross-wires. In this way, obscuration of the image is greatly reduced and the distracting diffraction effects caused by very fine hair lines are avoided.

The cross-wires themselves were produced photographically in the laboratory. Two lines were machined on a piece of translucent material to a scale ten times larger than that desired. The lines were filled with black paint. The material was illuminated from the rear and the lines photographed on to Kodak MR plates with a reduction of 10:1. The final positive prints were made by contact printing from this negative. Again, MR plates were used; their high resolution enabled a definite image, free from grainy appearance, to be obtained.

The separation of the lines was calculated to that under the magnification normally used for measurement, a silver grain of average diameter (0.3μ) appeared to fit between the

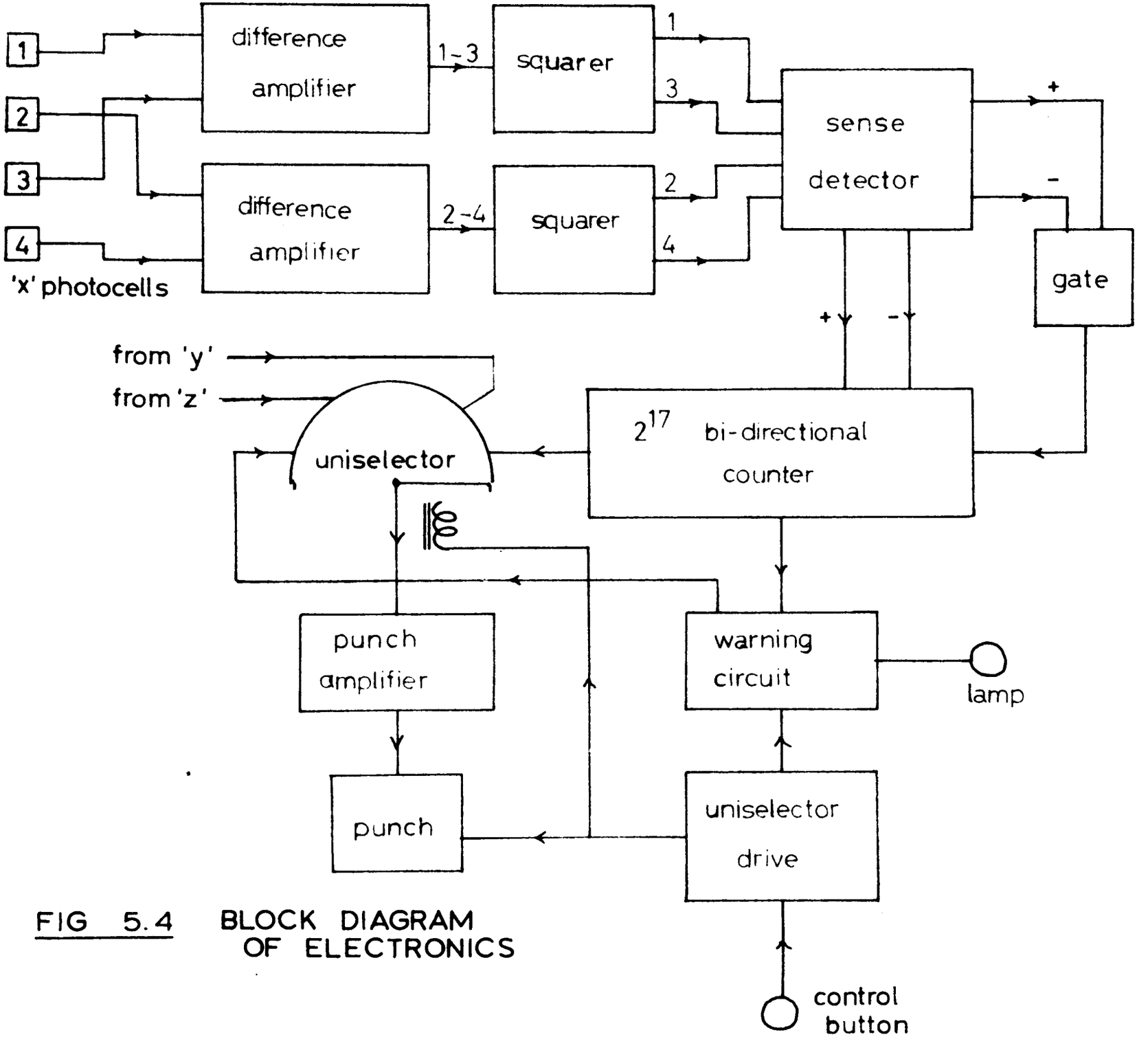


FIG 5.4 BLOCK DIAGRAM OF ELECTRONICS

lines. This gave a separation of 125μ. The thickness of the lines is of secondary importance, although if they are too thick, there is unnecessary obscuration of the immediate neighbourhood of the grain, while if too thin, the diffraction effects already noted appear. The final compromise decided upon was 10μ. This was found, when in use, to be a good choice giving bold yet unobtrusive lines.

The glass-cutting machine referred to previously was used to cut out the glass with the cross-wire on it to the size required for mounting on the slide. It was possible to check that the appropriate cuts were perpendicular to the cross-wire.

This new design of cross-wire was found to give greatly improved perfromance. The "nesting" of the grain in the box could be done quickly and accurately and, as the grain itself was not obscured, even faint grains could be measured.

5.35 Electronics

A block diagram of the electronic employed is shown in fig. 5.4. One channel only is shown feeding the uniselector. There are two other channels identical to the one shown. Three channels are provided as the equipment may be fed from other digitised systems giving (x, y, z) co-ordinates. In the present use, the 'Z' channel is not connected.

Each photocell gives a roughly sinusoidal output as the fringes pass over it. The relative phases of the cells 1,

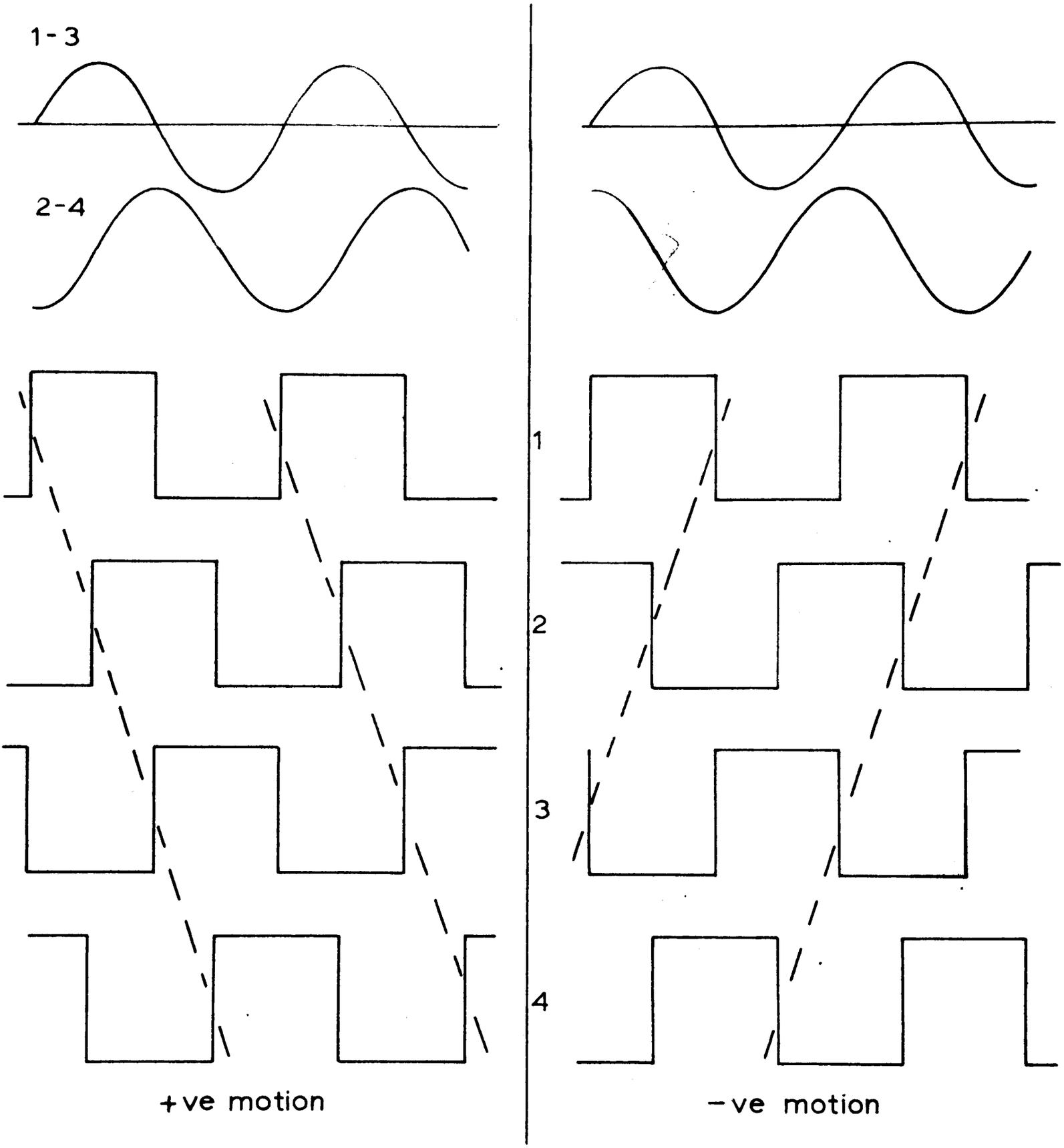


FIG 5.5 IDEAL WAVEFORMS

Counter pulses are obtained from the sharp sides of square waves.

Dotted lines indicate opposite senses of phase.

2, 3, 4 are respectively 0°, $\pm 90^{\circ}$, $\pm 180^{\circ}$, $\pm 270^{\circ}$, where the $\pm$ signs refer to the two directions of motion. The difference signal between cells 1 and 3 is amplified to give the "in phase" signal; cells 2 and 4 are treated similarly to give the "quadrature" signal. These two signal outputs are then applied to "squarers". These units ensure a sharp distinction between the "off" and "on" states. Each squarer gives two outputs in antiphase so that there are now four sets of square waves which correspond in phase to the original photocell signals.

The outputs are now fed to both a sense detector and to a bi-directional binary counter. The function of the sense detector is to determine the sign of the relative phases of the signals and accordingly to set the counter to either add or subtract the incoming pulses. The approximate forms of the signals are shown in fig. 5.5 where it can be seen that the passage of one fringe across the four photocells gives four pulses to the counter. Thus the "digit" of the system is 1/4 of a grating spacing. A 17 digit binary counter is employed, allowing a maximum count of 2^{16} fringes (2^{18} digits). The number contained in the counter is displayed by indicator tubes which represent the states of the bi-stable circuits composing the counter. The number is read in binary form (1 for tube alight, 0 for tube dark). The conventional zero

of the counter is taken to be 2^{17} (i.e. only the most significant light on), with this convention, subtraction may take place consistently and minus numbers have a representation. Without this convention, -1 would appear as "all lights on" i.e. $2^{18}-1$, while +1 appears as +1. With the convention, -1 is $2^{17}-1$ and +1 is $2^{17}+1$.

The final stage of the apparatus is that which transfers the contents of the three binary counters (one for each axis) on to standard five-hole computer tape. A uniselector samples the states of the bistable circuits in the counters in groups of five. A hole is punched for "1" and a blank left for "0". Hence one row of holes contains five digits and each complete co-ordinate occupies four rows; in order to bring the 17 digits up to the 20 required for four rows, the 3 least significant digits of the 20 are always blank. The sequence of the punching operation is as follows:-

1st. row	machine identification number
2nd. row	"(" character indicating that the following rows are co-ordinates
3rd. row	binary character for any number in range 0-15, set by knob on equipment
4th-7th	"X" co-ordinate
8th-11th	"Y" co-ordinate
12th-15th	"Z" co-ordinate
16th	")" character indicating close of co-ordinates

17th	may be totally or all five holes punched - see below
18th	blank

This sequence is followed each time a set of co-ordinates is punched out. The uniselector is set in motion by the operation of a push-switch and automatically stops at the end of the sequence. It is re-started when desired,- by the push-switch.

A typewriter modified by the addition of microswitches operated by the keys enables characters to be punched on the tape in addition to the co-ordinate sets.

A further refinement is a warning circuit which operates if the contents of the counters change while the uniselector is in sequence; the microscope lamp is switched off, a red light in the equipment is lit and row 17 of the co-ordinates set is punched as five holes instead of the normal blank (see above). A re-set button is provided which restores the circuit to normal. The 17th row of each set of co-ordinates is tested by the computer programme into which the data is fed and if five holes are found, the co-ordinate which has just been read in is ignored.

A zero re-set button is provided which returns all three counters to the conventional zero (2^{17}).

5.4 Calibration and performance

A calibration was carried out for the three objectives used

for measuring: Cooke, Troughton & Simms 95x and 80x, and Koristka 65x. The method employed was straightforward. A plate of emulsion was placed under the microscope, an easily recognised grain was selected and moved to one side of the field of view, the "X" stage micrometer was read and the counters set to zero. The grain was moved a known distance to the other side of the field of view by means of the stage micrometer screw. The "X" cross-wire was again placed on the grain and the contents of the "X" counter read from the indicator tubes. This was repeated several times with varying distances to obtain a mean value for the calibration factor. It had previously been checked that the stage motion and the motion of the eye-piece cross-wire were parallel.

The results for the three objectives were:-

Objective	Displacement for one fringe	Equivalent "digit" (1/4 fringe)
95x	0.15μ	0.038μ
80x	0.165μ	0.041μ
65x	0.25μ	0.063μ

5.5 Setting accuracy

A simple test was made to estimate the error introduced when measuring grain co-ordinates. A number of grains in the field of view were chosen (for convenience of identification they were all grains in the same track) and one of them was

taken as the origin of co-ordinates by operating the zero re-set when the cross-wires were set on that grain. The remaining grains were measured in turn and their co-ordinates recorded. This was repeated several times, always choosing the same grain as zero and always measuring in the same order. By this means the effect of any small thermal drift is minimized. Ten sets of readings were made on each of the ten grains (excluding the origin).

From the sets of co-ordinates for one grain (x_i, y_i) the mean co-ordinates were calculated:-

$$\bar{x} = (\sum_i x_i)/10 \quad ; \quad \bar{y} = (\sum_i y_i)/10$$

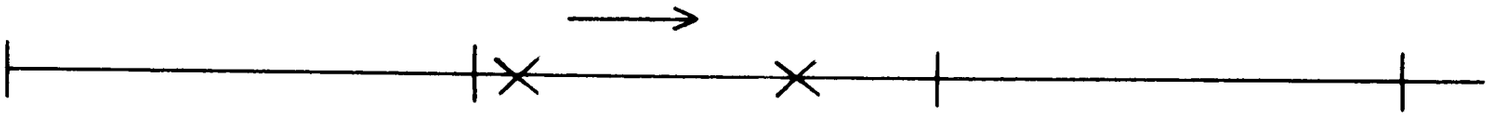
Assuming that the x_i's and y_i's are normally distributed about $\bar{x}$ and $\bar{y}$ with standard deviations σ_x and σ_y respectively, then the following estimates of σ_x and σ_y may be made:-

$$\sigma_x^2 = \frac{1}{9}\sum_i (\bar{x} - x_i)^2 \quad ; \quad \sigma_y^2 = \frac{1}{9}\sum_i (\bar{y} - y_i)^2$$

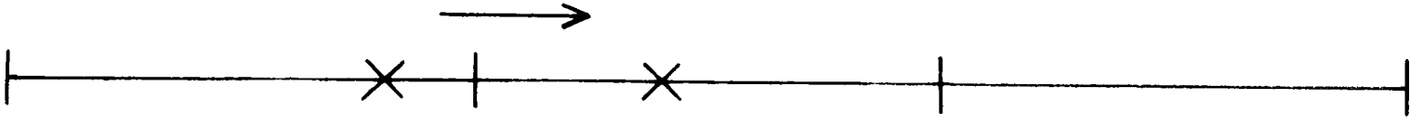
σ_x and σ_y were calculated for each of the grains measured. The results are given in the following table:-

σ_x	σ_y
0.035	0.031
0.037	0.047
0.045	0.057
0.043	0.057
0.037	0.050
0.052	0.053
0.056	0.055

FIG 5.6 ILLUSTRATION OF DIGITISING THEORY



NO COUNT



COUNT CHANGE BY 1

Key :-

| Trigger points for counter.

× Limits of displacement.

	0.061	0.052
	0.056	0.058
	0.069	0.047
Mean	0.049μ	0.051μ

It can be seen that it is reasonable to assume that $\sigma_x = \sigma_y = \sigma$ and $\sigma = 0.05\mu$.

It is of interest at this point to consider what error may be introduced due to the digitising. Any digitised system must introduce error on account of the "dropping" of fractions of the digit. A rough estimate of the effect was made.

5.6 Error due to digitising

Consider an attempt to measure a length x which is less than the basic digit. (The more general problem of any length reduces to this situation.) For convenience, call the digit the "unit length". Fig. 5.6 represents diagramatically the two possible situations; the count is unchanged, or it is changed by one unit. The lines represent the points at which a change in count is recorded; the crosses represent the start and finish of the displacement x. If a vertical line lies between the crosses, the count increases by one. The starting point will be randomly distributed in one digit interval so that the following probabilities are obtained:-

No count change $p(0) = 1 - x$

Change by 1 $p(1) = x$

If the measurements are performed N times, where N is very large, then there will be aprroximately (1 - x)N zeros and Nx units. Then mean is therefore x. This indicates that digitisation does not introduce any bias. The variance of the distribution can be calculated:-

$$\sigma^2 = (Nx^2(1 - x) + N(1 - x)^2x)/N$$

$$= x(1 - x)$$

In most applications the value of x varies randomly between 0 and 1, hence a value for the mean variance in a measurement is obtained by integrating σ^2 with respect to x between the limits 0 and 1. This gives:-

$$\overline{\sigma^2} = \frac{1}{6} \quad ; \quad \text{i.e.} \quad \bar{\sigma} = 0.4 \text{ digits.}$$

(The distinction between the r.m.s. value of σ and $\bar{\sigma}$ is ignored, the notation $\bar{\sigma}$ above is intended to represent the r.m.s. value.)

Applying this rough result to the figures obtained in section 5.5, the basic digit was 0.038μ (the 95x objective was used) so that $\sigma_{dig} = 0.4 \times 0.038\mu = 0.015\mu$. Assume that the total error (σ_{tot}) is composed of the setting error (σ_{set}) and the digitising error (σ_{dig}) by the relation:-

$$\sigma_{tot}^2 = \sigma_{set}^2 + \sigma_{dig}^2$$

We have obtained a figure for the total accuracy $\sigma_{tot} = 0.05\mu$, and using this figure with the calculated value of σ_{dig} we obtain $\sigma_{set} = 0.048\mu$. This is not significantly different from the total error and therefore it may be concluded that

digitising has not introduced an error which is comparable with the setting error. Moreover, it indicates that a grating of 1,000 lines/inch was a good choice. There would have been no advantage in using a finer grating since, as has been demonstrated, the setting error is dominant, while the finer grating would require a more complicated optical system etc. However, a coarser grating would soon bring σ_{dig} to a magnitude comparable with σ_{set}, a 250 lines/inch grating would give $\sigma_{dig} = 0.06\mu$.

The achievement of the accuracy in setting of 0.05μ (1/6 of a grain diameter) is largely due to the improved cross-wire design. Whether this accuracy can be improved is a point worthy of discussion.

5.7 Limits to the accuracy attainable

It was demonstrated in the previous section that the main contribution to the error in measuring the co-ordinates of a grain is that due to the uncertainty in positioning the cross-wires on (or rather, with the present design, about) the grain. This error can be affected by various causes:-

(a) the magnification between the object and the image at the cross-wires,

(b) the grain size,

(c) the definition of the image as the cross-wires,

(d) the design of the cross-wires.

The first three of these factors are interrelated. The wavelength of the green light used in the microscope illumination is about 5,000 Å, i.e. about 0.5μ; the diameter of a grain is 0.3μ. Thus there is a limit to the definition which may be attained, and one may expect that every effort is made in the design of the microscope used, to obtain the maximum possible definition. The image of a grain, under these conditions, does not have "sharp" edges clearly defining the shape, but rather has a less abrupt change from opacity to transparency. In using the cross-wires described above, the best technique is to set the lines so that they pass either side of the grain and pass through regions of approximately equal opacity. This adjustment is necessarily subjective although it would not be impossible to achieve a more objective measurement photometrically. Such an apparatus would be far more complicated than the present arrangement and it is doubtful whether any improved accuracy would be useful.

A reduction in grain size would not greatly affect the measurement error because, as has been pointed out, the grain size is already less than the wavelength of the light. However, grain size has a very great effect on the main source of error in the experiment and will be discussed later.

A further increase in magnification would not be useful as the reduction of the size of the field of view would not allow sufficient grains to be measured in each track. The

From these comments it may be seen that very little may be dome to improve the accuracy of the bifilar eyepiece. It will be appreciated later, in the discussions of the errors present in the whole experiment, that the measurements introduced an error small compared with those from other sources.

5.8 Setting up procedure

Before the instrument may be used for any measurements, certain adjustments are necessary. These may be listed under the following headings:-

(a)adjustment of grating separation,

(b) adjustment of skew angle of gratings to give correct fringe spacing and phase relations,

(c) balancing of the signals from the photocells to ensure correct operation of the electronic equipment.

The first of these is fixed in the design of the instrument as the fringe contrast is not exceptionally sensitive to this adjustment with the gratings used.

In the description of the electronic equipment, it was stated that the signals from each of the four photocells must be separated in phase by successive increments of 90°. The adjustment of phase is achieved by altering the fringe spacing. Monitor points are provided in the electronics at the output of the photocell amplifier. There are two outputs which are approximately sinusoidal and, when correctly adjusted, in quadrature. These two outputs are fed to the X and Y plates

of an oscilloscope. As the index grating was moved the spot on the screen described some form of Lissajou figure. For a phase difference of 90^{o} the figure becomes a circle or, if the signals to the X and Y plates are unequal in amplitude, an ellipse with axes coinciding with the X and Y directions of the oscilloscope. For other phases, an ellipse is obtained whose axes are "tilted" with respect to those of the oscilloscope.

Slight deviations from quadrature do not affect the correct operation of the electronics, consequently an appraisal of the Lissajou figures by eye is sufficiently accurate.

The out puts from the four photocells could be balanced by means of the adjustable slits varying the amount of light falling on each cell. A state of unbalance was revealed in the Lissajou figures obtained above; when one side appeared to "flatten" indicating overloading of one photocell amplifier. The position of the figure on the screen was also affected by unbalance of the cells, correct balance being when the figure was centrally placed.

Considerable trauble was encountered due to transients caused by the operation of the uniselector and the punch. Both these components involve the rapid switching of currents of a few amperes which, in turn, give rise to spurious "spikes" in the waveforms in other circuits. The early stages of

the equipment operate at very low signal levels and the presence of these powerful transients upsets the correct working. The problem was most noticeable when a co-ordinate set was punched and one of the counters was just on the verge of registering another count. The transients caused the digits in the counter to alter in a completely random manner. Such a fault was very serious as it rendered any measurements of co-ordinates made just previously, completely useless. When the fault occurred the warming circuit operated so that measurements could be halted.

The source of the transients was extremely elusive. The usual measures were taken such as suppressing sparking at contacts, shunting coils with diodes and screening the leads carrying the heavy currents. Despite this some transients still remained and continued to cause the fault. It was often difficult to decide whether the fault had been rectified as its occurrence was inherently intermittent. This resulted in many useless readings being made.

The solution finally adopted was of the "brute force" type. A condenser and resistor were connected in series from each output of the photocell amplifiers to earth. This resulted in the transients being shorted to ground at this point. The signal level here is about 1 volt peak-to-peak; using the oscilloscope and a quick eye, the transients could be seen with an amplitude greatly in excess of this. When the

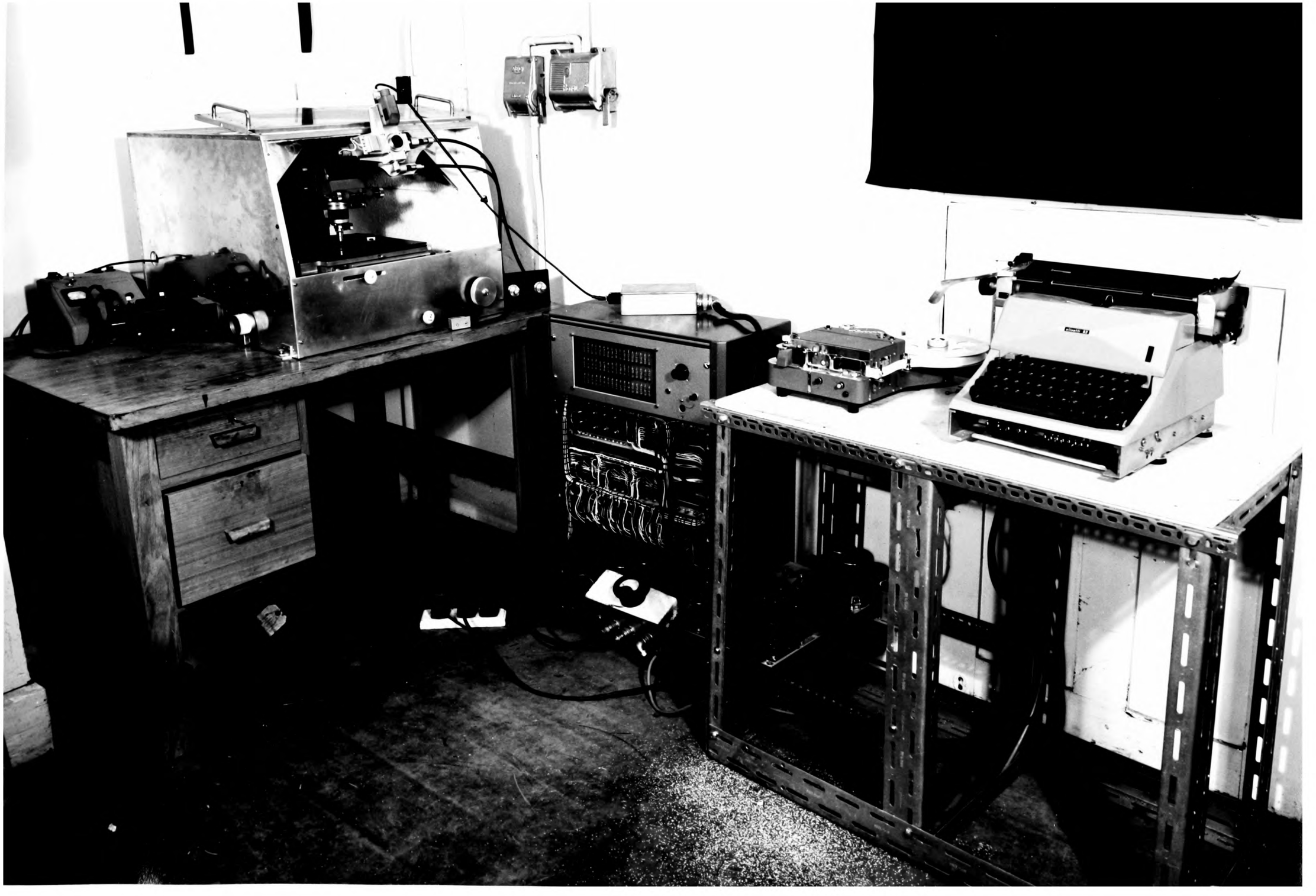
condensers and resistors were inserted no transients were seen. It was necessary to adjust the time constant of the C-R combination so that it did not appreciably attenuate the wanted signals even at the highest frequency (i.e. greatest speed of travel of the grating) encountered. It should be pointed out that all the circuits of the equipment were d.c. coupled as the signals from the photocells even when in a steady state with the index grating at rest indicate the position of the fringe pattern.

The solution described was found to be very effective and did not affect the correct operation of the circuits. The worst that was found to happen was that operation of the uniselector sometimes altered one counter by one unit and operated the warning circuit. However, this was not serious of the co-ordinate could easily be re-punched, the redundant co-ordinate was ignored by the subsequent data analysis and the previous co-ordinates measured were not rendered useless.

Considerable space has been devoted to this fault as its rectification was essential to the continuation of the experiment and a considerable time was spent dealing with it.

ADDENDUM TO CHAPTER V

It should have been noted in the description of the electronics that the whole system employs transistors. Consequently it was possible to contain the whole equipment in a small space and problems of heat dissipation and power supply were not encountered.



CHAPTER VI

MEASUREMENT OF EVENTS

6.1 Selection of events

As a result of the preliminary measurements described in section 3.4, a total of 84 possible KD events were selected. In some of these, one or more tracks were very steeply dipping in the emulsion; such tracks are very difficult to follow grain by grain and to obtain a reasonable projected length of track, the true track must be followed for a greater distance. This introduces the possibility of multiple scattering and the consequent deviation of the track from a straight line. For a flat track, a length of about 20μ was normally used. The effect of multiple scattering on such a length is negligible. However, for a track of dip angle α with sec $\alpha = 4$, an actual track length of 80μ must be employed; multiple scattering may now be important. In addition to these considerations, if the π^+ track dips steeply, the error in the flight distance of the π^o is increase by a factor sec α.

A further selection of events was made on the basis of the dips of the tracks in the event - if the dip of any track was more than 50μ/100μ (in the shrunk emulsion) the event was not measured. A total of 67 events were finally selected for measurement.

6.2 Optical technique

During the scanning, each event of interest was gridded so that re-location was simple. The event was located under low power magnification (10x objective) and then one of the higher power objectives was inserted. In general the 95x objective was tried first. If an insufficient number of grains in each track could be included in the field of view, the next lower objective was tried (80x) while in very difficult cases the 65x lens was necessary. The following table gives the number of events measured with each objective:-

Objective	No. of events
95x	48
80x	16
65x	3

All the objectives used were of the oil immersion type and an oil immersion condenser was used. The image of the field stop of the illumination system of the microscope was focussed in the plane of the objective and the stop closed down to illuminate only the field of view. The condenser stop was also closed down so that the objective accepts the correct cone of light. These precautions ensured maximum contrast of the image and consequently facilitate measurement.

The bifilar eyepiece permitted monocular vision only and it was found most comfortable to wear an eyeshade for the eye not being used.

6.3 Co-ordinate measurement

The event was positioned in the field of view so that as many grains as possible were visible in each track. The stage motion controls were used for this. The apparatus was then allowed to "settle down" for a few minutes to allow any mechanical strains to ease. During this time the identification number of the event was punched on to tape (using the typewriter described in section 5.35) together with the date and a number indicating the objective used.

The co-ordinates to be measured fall into four groups:-

(a) those of the π^+ track,

(b) of one electron track,

(c) of the second electron track,

(d) the estimated end of the K^+ track.

In order to distinguish these groups, use is made of the facility noted in section 5.35 which enables a pre-determined binary number to be punched with each set of co-ordinates. The number is set by a knob on the panel of the electronics. Each group was allotted a code number: '0' for the π^+; '1' for one electron; '2' for the other and '3' for the K ending. These code numbers are read in the computer programme which analyses the co-ordinate data and allows sorting of the co-ordinates into tracks. This facility enables the grains of an event to be measured in any order. However, the following order was

usually observed:-

(i) π^+ track, working in from the edge of field of view,

(ii) K^+ ending,

(iii) one electron track, working outwards from K ending,

(iv) the other electron track, working in from edge of field of view.

This sequence minimizes the effect of any small thermal drift and there is also little useless movement of the cross-wires (the only being between (iii) and (iv)). The end of the measurement of an event was designated by punching a "dummy" co-ordinate with code number '4'.

In some events, both electron tracks were not suitable for measurement. This was due either to one electron having a very low energy and scattering considerably or to the chance effect of there not being many grains in the first part of the track. In such cases as the latter, if the other two tracks had sufficient grains it was decided not to use a less powerful objective. Occasionally the angle between the electron tracks was not large enough to allow an easy decision to be made in allotting the grains to their correct tracks. In these cases all the grains were considered to belong to a single track. When only one electron track was measured, no co-ordinates were punched with the code '2'. This was detected in the programme analysis and the necessary modifications to the calculation were made. (See the appendix for details.)

Four separate measurements of each event were made. The use of the digitised eyepiece greatly speeded up the measuring. The total time required, including setting up the event under the microscope, was about half an hour.

6.4 Comparison with earlier eyepiece

Some of the events had previously been measured with the non-digitised eyepiece. Such measurements were both tedious and fatiguing. For each grain, the two micrometer scales were read and the co-ordinates noted down. In addition to this the very fine cross-wires was difficult to use. The continual focussing and re-focussing of the eyes was found to be very tiring resulting in inaccurate settings. The time required for three measurements of an event (excluding the setting up time) was rarely less than 3/4 hour and often more than an hour. Furthermore, it was then necessary to teleprint the measured co-ordinates on to computer tape; this was another time-consuming operation and source of error. The speeding up of the measuring also meant that any residual thermal drift would have a smaller effect than with the more lengthy process.

6.5 Difficulties of measurement

The main difficulties encountered during measurement were due to steeply dipping tracks, very close electron pairs and the accurate location of the stopping point of the K^+.

Steep tracks in which only one grain at a time was in focus presented a source of error by the chance of including spurious grains, or even by the possibility of transferring to a spurious track. The difficulty could have been resolved by providing the eyepiece with an additional rotatable hairline. However, the complications involved would have been considerable and out of proportion to the benefits derived.

Close electron pairs were mentioned in section 6.3 where the resolution of the difficulties involved were described. This problem was encountered with most events with the grains close to the K^+ ending where the separation of the electron pair tracks is small.

The problem of accurately locating the decay point of the K^+ represents a very great, if not the greatest, source of error in the experiment. Two factors are involved: (i) the measurement error in locating the centre of the last grain in the track; (ii) the "intrinsic" error due to the actual decay point not corresponding with the centre of the last grain. A detailed discussion of the magnitude and effect of these errors will be given in a later chapter.

CHAPTER VII

DATA REDUCTION and ERROR CALCULATIONS

7.1 Reconstruction of event geometry

The data from the measurements is in the form of the co-ordinates of the grains forming an event. The first stage of the analysis is the geometrical reconstruction of the event from these co-ordinates and from this, a computation of the apparent distance travelled by the π^{o}.

The straight lines representing the tracks of the particles are obtained by minimizing the sum of the squares of the perpendiculars on to the line from the measured co-ordinates. This procedure differs from the usual type of "least squares fit" which assumes the x co-ordinate measurement is exact. This latter routine presents difficulties when the line is nearly perpendicular to the x axis. With the "minimum perpendiculars fit" both axes are treated identically and this problem does not arise. Also, this type of fit is the more logical when the process of track formation is considered. Details of the theory of the fitting process are given in the appendix.

7.11 Discussion of "grain noise"

Some measure of the deviation of the grains of a track from a true straight line was required. A useful quantity is the r.m.s. perpendicular from the grains on to the calculated track. The distributions of these quantities

FIG 7.1(b) DISTRIBUTIONS OF δ_{rms}

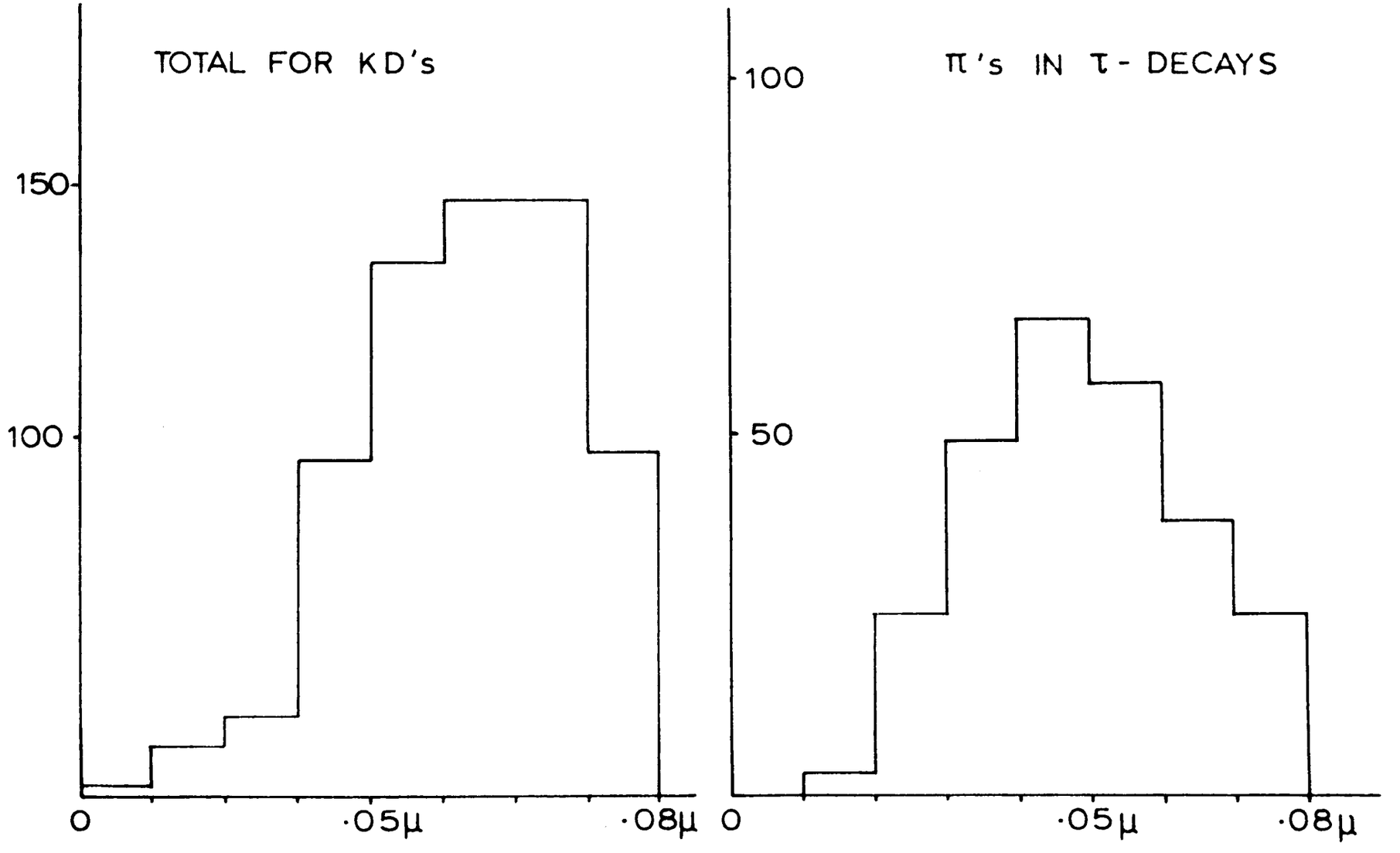
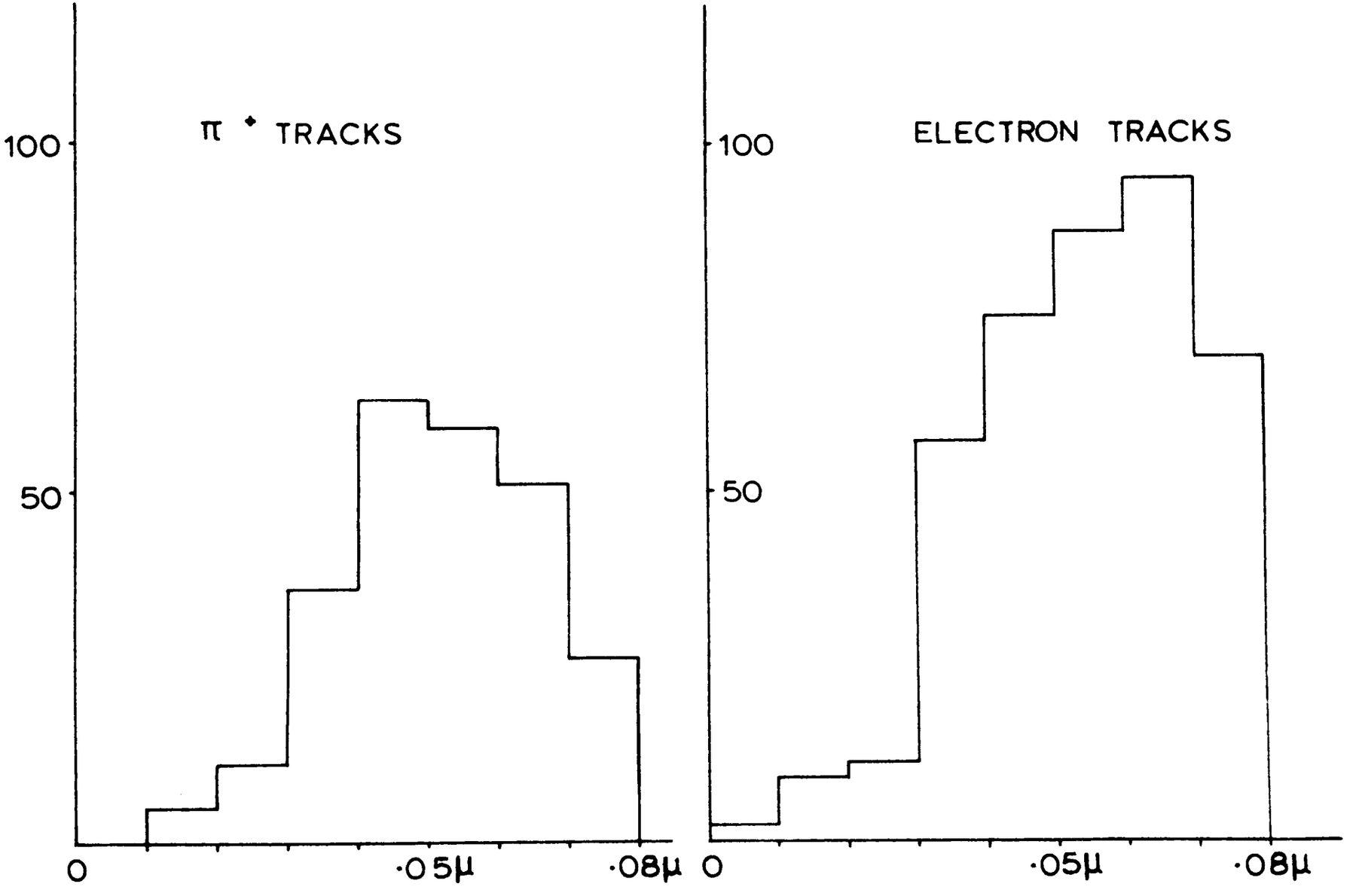


FIG 7.1 (a) DISTRIBUTIONS OF δ_{rms}



for the tracks in the events measured are shown in fig. 7.1. It is seen that the distribution for the electron tracks peaks at a larger value of δ_{rms} than does that for the π^+. This is attributed to the effect of the increased multiple scattering for the light particle.

It is seen that no track has a value of δ_{rms} greater than 0.08μ; this is due to a cutoff procedure applied. It was found during preliminary measurements that the large majority of tracks had δ_{rms} less than about 0.08μ. It has been noted in earlier sections that there is a chance of including spurious grains when measuring a track. Such grains would give rise to a large δ_{rms}, a slightly faulty track and a large calculated error in the flight distance. A cutoff routine was tried which, if the δ_{rms} was greater than a specified parameter, rejected the grain which lay furthest from the calculated track. The new straight line fit was made and the test re-applied; if necessary a further grain was rejected and the process repeated until δ_{rms} was less than the specified value. Several trials of cutoff parameter were made to check the sensitivity of the test to the inclusion of spurious grains. A final choice of 0.08μ was made. It is seen from the distributions of δ_{rms} that a number of normal tracks would be expected to have δ_{rms} greater than 0.08μ. However, the reduction in "grain noise" for these tracks

gives a more certain fit and hence better error. The routine also detected useless co-ordinates due to faulty operation of the electronic equipment or the punch. Reference was made to this type of fault in a previous chapter. The effect was to shift the origin of co-ordinates in an unknown manner during the measurement of a track; such a fault if undetected during measurement would be indicated by the rejection of a large number of grains from a track together with a clearly meaningless set of results.

Measurement was made easier and quicker by the presence of this cutoff as, in cases of doubt whether to include a grain in a track or not, it was incorder to include it and leave the selection to the calculations. The difficulty encountered with close electron pairs was mentioned previously.

7.12 Event parameters

The equation of each track was calculated in the form "y=mx+c", m and c being the characteristic parameters for each track. From these equations the following quantities were calculated:-

(i) the apparent flight distance of the π^o in microns,

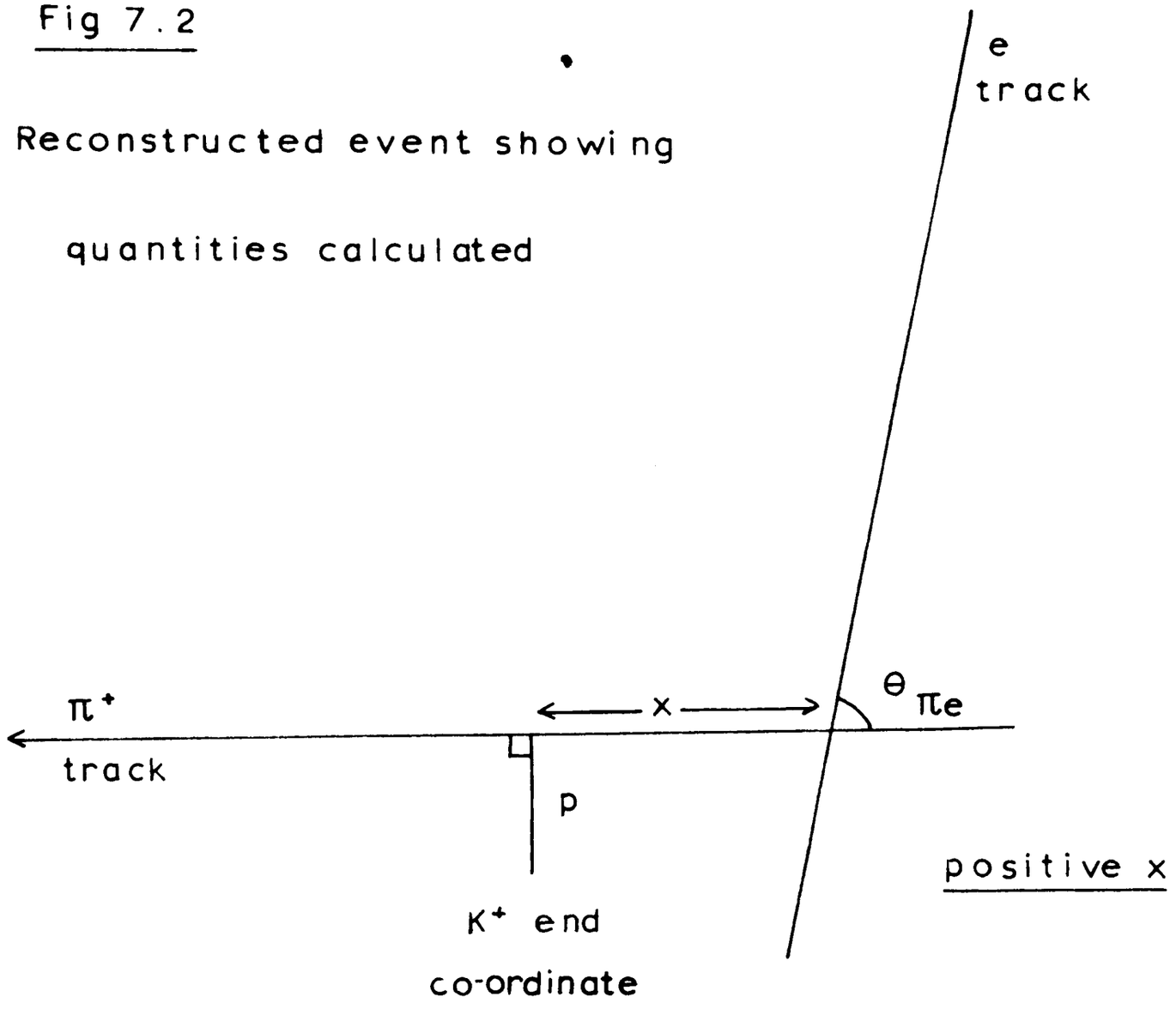
(ii) $\text{cosec}^2\theta_{\pi e}$, where $\theta_{\pi e}$ is the angle between the π^+ and the electron trajectories,

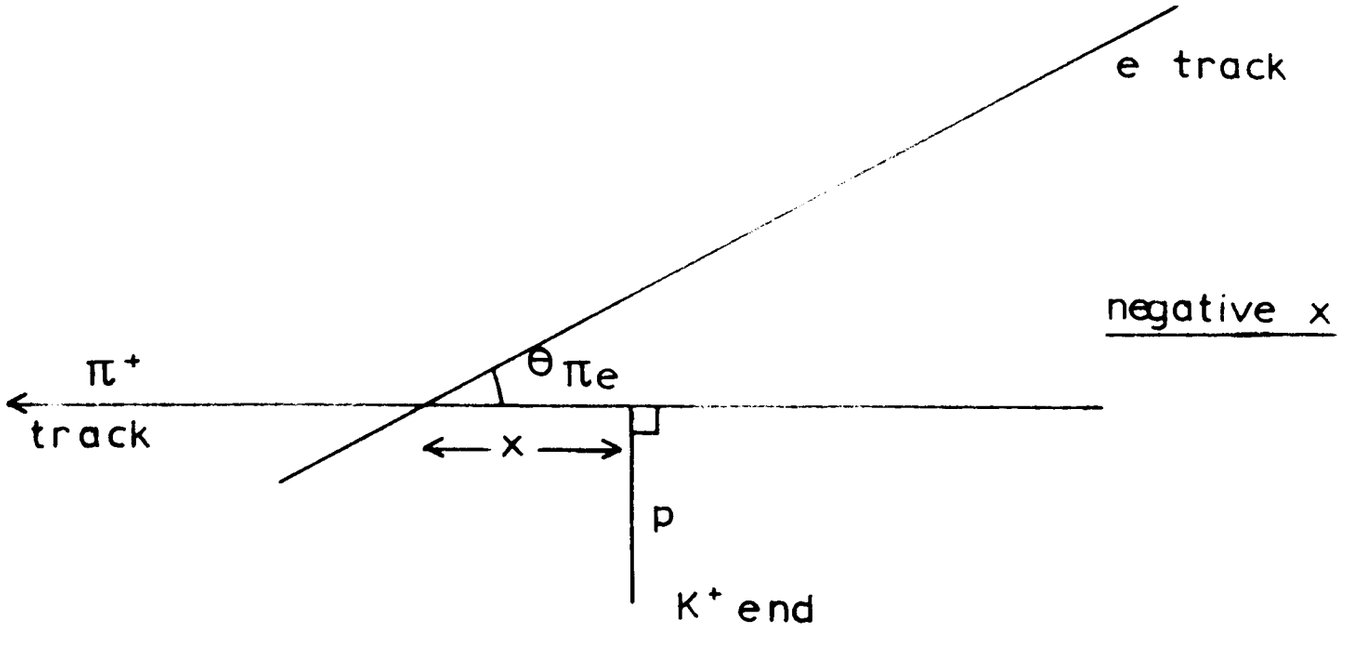
(iii) p, the length of the perpendicular from the measured K^+ ending on to the π^+ track.

Fig 7.2

Reconstructed event showing

quantities calculated





In general, two sets of these quantities were obtained by taking the π^+ with each electron in turn.

In addition to the above quantities calculated from the geometry, the following were obtained:-

(iv) σ, the error in x due to the uncertainty in the line fitting, this depended upon $\theta_{\pi e}$ and upon δ_{rms} (the theory of the error calculation is given in the appendix),

(v) δ_{rms} for each track (after rejection of spurious grains),

(vi) the initial number of grains in each track and identifying numbers of those rejected.

For identification purposes, the code number of the event, the date of measurement and the code number of the objective used were printed out with the results; of these three only the objective code number was used in the calculations to apply the correct calibration factor to the co-ordinates.

Fuller details of the calculations and of the computer programme are given in the appendix.

7.2 Errors

The σ mentioned in (v) above represents only part of the error present in the apparent flight distance x. It represents the error in locating the decay point of the π^o. This point is located from the information contained in the positions of the 10-20 grains composing the two intersecting

tracks. Thus for good geometry events ($\theta_{\pi e}$ not near 180° or 0°) it is to be expected that the location of this point is better than the location of a point by a single measurement of a co-ordinate. The point of production of the π° is located by such a single measurement. Estimation of the size and investigation of the nature of this error was considered to be of great importance and a major feature of the whole experiment. Consequently it will be discussed in some detail.

7.3 K^{+} ending error

The difficulties experienced in the measurement of the end of the K^{+} track were indicated in section 6.5. It was stated there that the source of error was two-fold:-

(i) measurement error due to the subjective choice of the "centre" of the last grain of the track,

(ii) "intrinsic" error due to the decay point of the K^{+} not coinciding with the centre of the last grain of the track.

For convenience, these two errors will be denoted by σ_{k1} and σ_{k2} respectively, and the error from the intersection of the tracks will be denoted by $\sigma_{\pi e}$.

σ_{k1} may be expected to be of the same order as the error in a single measurement on a grain noted in section 5.5, namely 0.05μ. σ_{k2} is a consequence of the mechanism of track formation and the grain structure of the emulsion.

The theory of track formation is not well understood particularly for the end of the range of a particle. An experimental estimation of σ_{k1} and σ_{k2} was made.

It has been stated that the intersection of two tracks locates a point better than the single measurement of a grain, providing that the angle between the tracks is not too acute or obtuse. Thus, if the position of the decay of a K^+ may be located by this means and compared with the location by the measurement on the end of the track, some information about the errors may be obtained. The three charged body decay of the K^+, the τ mode provides an excellent opportunity for such a set of measurements. It was noted in section 3.3 that the location of these events was noted during the scanning, the branching ratio is favourable (about 6%) and about 4,000 such decays were noted.

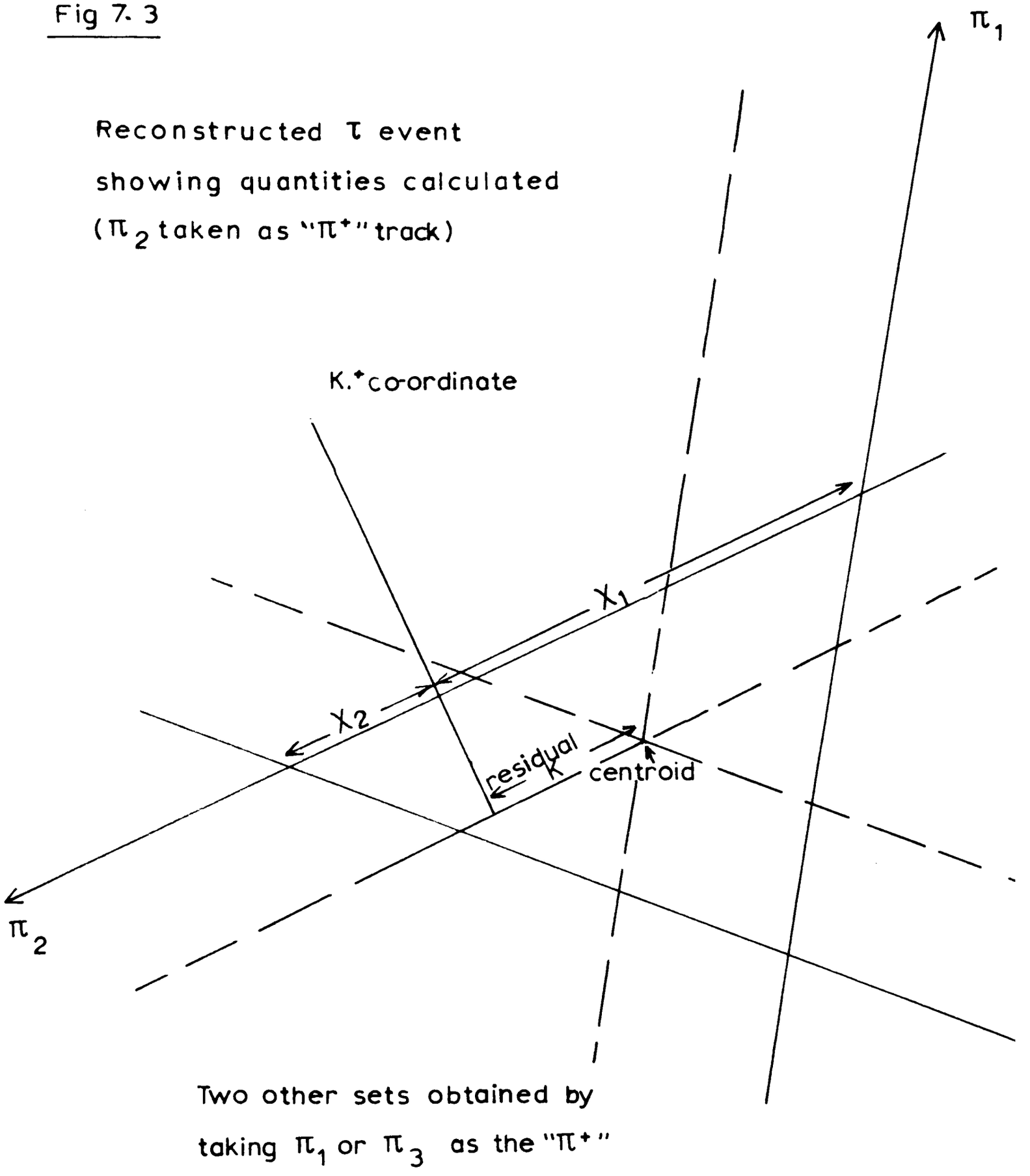
7.4 Measurement of τ-decays

30 examples of τ-decay were chosen for measurement. Events were chosen in which the angles between the tracks lay in the range 40° - 140° and in which the tracks were not steeply dipping. This gave the best possible location of the decay point. No bias could be introduced by this selection of events since the location of the decay point must be independent of the configuration of the decay particles.

Each event was measured in a similar manner to the main set of KD events as described in chapter VI, except that

Fig 7. 3

Reconstructed τ event
showing quantities calculated
(π_2 taken as "π^+" track)



Two other sets obtained by
taking π_1 or π_3 as the "π^+"

when a heavily ionizing track was being measured, not all the grains were included, in particular, large and mis-shapen grains were ignored. Each event was measured independently three times.

The co-ordinates were analysed in a similar programme to that used for the KD events. The track fitting procedure was identical and the 0.08μ cutoff for spurious grains was included. The distribution of δ_{rms} for all the π tracks measured is shown in fig. 7.1; it is seen that the agreement with the distribution for the π tracks from the KD events is satisfactory.

The quantities calculated are indicated in fig. 7.3. The tracks do not intersect in a point due to measurement error and grain noise. The distances labelled x_1 and x_2 in the figure are obtained by taking π_2 as the "π^+" and π_1 and π_3 as the "electron pair" in a pseudo-KD event and calculating the "flight distance" of the supposed "π^o". x_1 and x_2 are these flight distances; four other similar quantities are obtained by taking each of the other π tracks in turn as the "π^+".

The distances and parameters calculated for each event may be listed as follows:-

(i) "x" defined above (6 values for each event),

(ii) "σ" corresponding to each x, calculated as for the KD events,

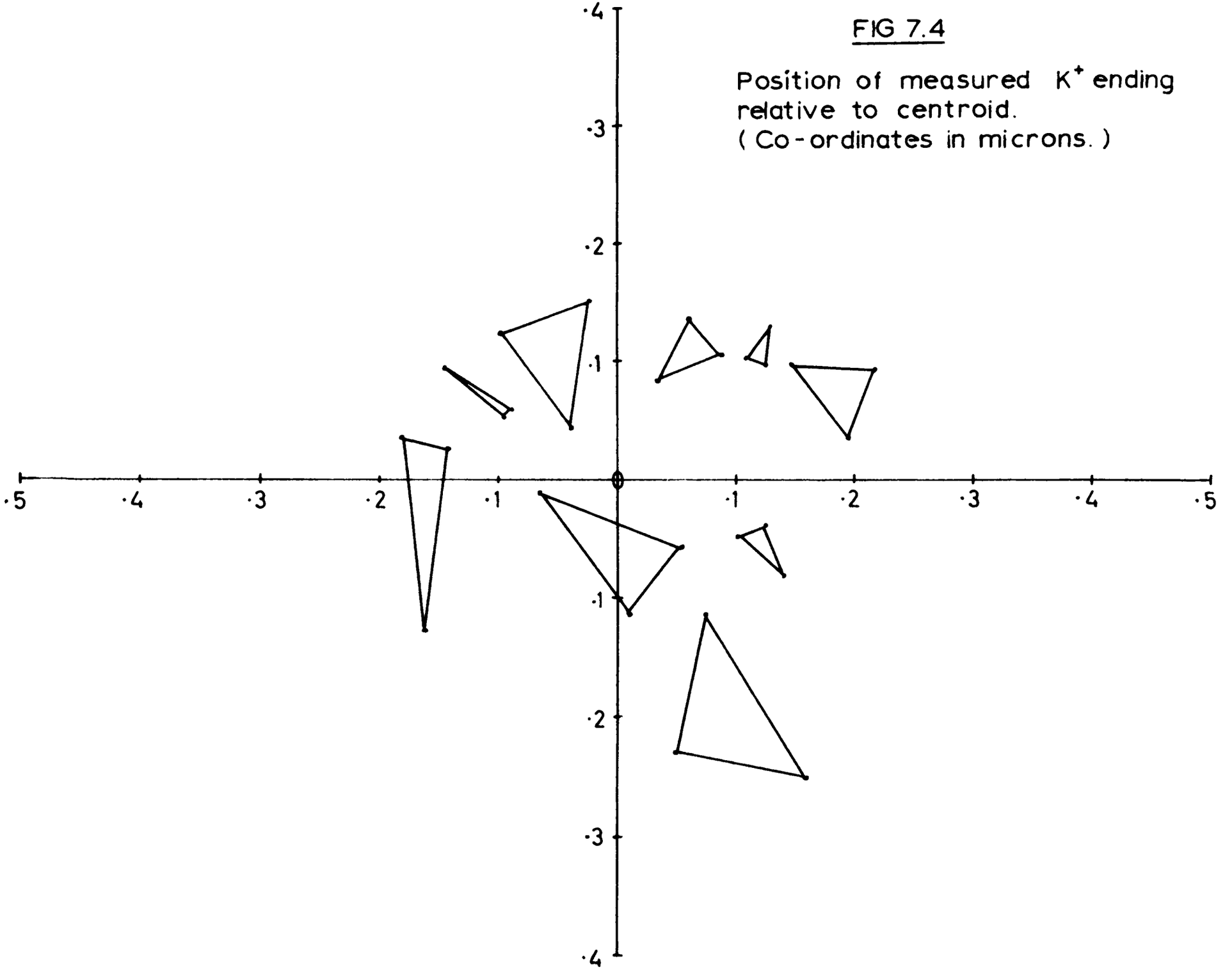


FIG 7.4

Position of measured K^+ ending relative to centroid.
(Co-ordinates in microns.)

(iii) $\text{cosec}^2\theta$ for each combination of tracks,

(iv) the co-ordinates of the vertices of the "triangle of confusion", taking the centroid of the triangle as the origin,

(v) the cartesian and polar co-ordinates of the K^+ ending measured co-ordinate relative to the same origin as (iv),

(vi) the lengths of the perpendiculars from the K^+ ending on to the three tracks,

(vii) the lengths of the perpendiculars from the centroid of the triangle on to the three tracks,

(viii) δ_{rms} for all three tracks,

(ix) a length "r", the radius of a circle having the same area as the triangle of confusion.

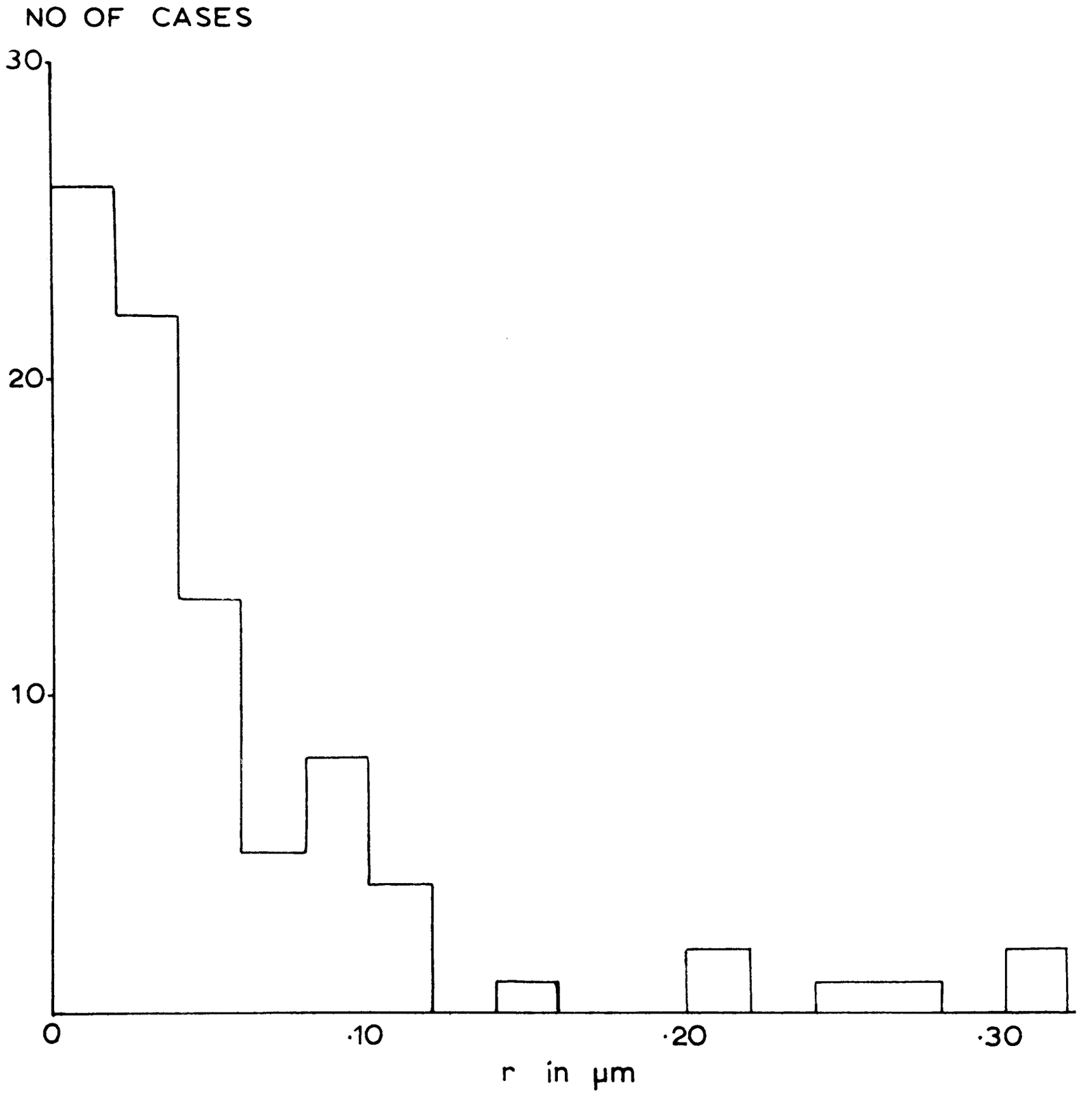
7.41 Treatment of the results of σ measurements

The "true decay point" of the K^+ was assumed to be at the centroid of the triangle of confusion. A more rigorous definition would have been the centre of the inscribed circle such that the lengths of the perpendiculars were equal. However, these two points do not differ greatly except for triangles with one very acute angle and as these had been excluded by the selection of the events, the centroid was chosen as being an easier point to calculate.

A plot was made of the positions of the measured K decay point relative to the "true decay point". Fig. 7.4 illustrates

FIG 7·5

DISTRIBUTION OF r



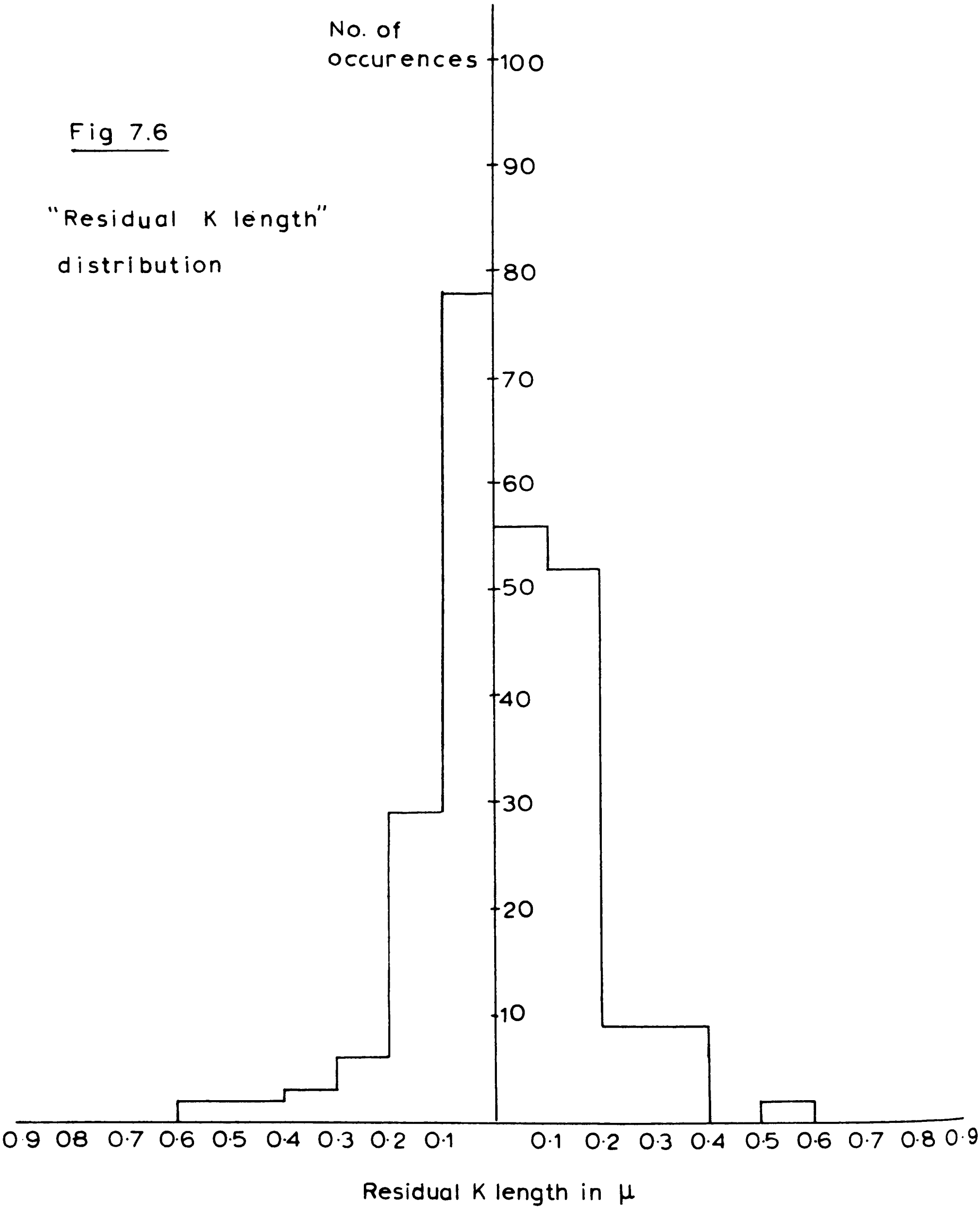
the general trend observed. Only a few events are plotted as the diagram becomes very congested if all the events are included. The events plotted have been selected to show clearly that measurement error alone is not responsible for the difference between the measured and true decay points. Not all events displayed this effect so clearly. Points in the figure, linked by lines indicate different measurements of the same event.

The distribution of r is shown in fig. 7.5. This is of interest qualitatively as it demonstrates the accuracy obtained using the intersection of tracks (a kind of microscopic surveying). It should be pointed out that the total length of track used in each case is about 20μ, the three tracks intersect in a "circle of confusion" of about 0.05μ radius.

If it is assumed that the true decay point of the K^+ is at the centroid, it is possible to calculate the contribution to x due only to the error in locating the decay point. Three lines are drawn parallel to the track directions and all passing through the centroid (dotted lines in fig. 7.3). These may then be assumed to be the true tracks of the secondary particles. Perpendiculars are dropped from the measured K^+ ending on to each of the three new tracks. The distance from the foot of the perpendicular to the centroid is the contribution due to the displacement of the measured point of the K decay.

Fig 7.6

"Residual K length" distribution



This length is labelled "residual K" in fig. 7.3. The distribution of this quantity is shown in fig. 7.6. The mean and standard deviation was calculated, the mean was 0.009μ and standard deviation 0.154μ. This confirmed the indication that the effect did not cause a systematic error as the small mean shows; the standard deviation is a measured of the random error to be expected from this source. The figure of 0.154μ is of a reasonable order being comparable with the radius of a grain.

The analysis just described does not take explicit account of the two independent errors defined previously as σ_{k1} and σ_{k2} and it is not clear which of these, or in what combination gives the figure just quoted. A more refined analysis was developed using guidance from a qualitative assessment of the nature of the error obtained by studying the distributions mentioned above.

7.5 Error hypothesis

The following assumptions were made:-

(a) that the error due to the measurement of the last grain in the K^+ track (σ_{k1}) is <u>random</u> between independent measurements of the <u>same</u> event,

(b) that the error due to the <u>actual</u> displacement of the decay point from the measureable decay point (σ_{k2}) is <u>systematic</u> for independent measurements of the <u>same</u> event, but is <u>random</u> between different events.

These assumptions are reasonable and are derived from the study of the τ decays described above. It is also assumed that the error due to the intersection of the tracks ($\sigma_{\pi e}$) is correctly estimated.

Consider the error present in x the flight distance in either a true event (KD) or pseudo-event (τ). The <u>random</u> error in a single measurement, x_i, is that due to $\sigma_{\pi e}$ and σ_{kl}:-

$$\sigma_i^2 = \sigma_{kl}^2 + \sigma_{\pi e}^2 \quad ; \quad \text{where } \sigma_i \text{ is the error in } x_i$$

The weighted mean of x for the three measurements of the same event is:-

$$\bar{x} = \frac{\sum_i x_i/\sigma_i^2}{\sum_i 1/\sigma_i^2}$$

with a corresponding error of:-

$$\overline{\sigma^2} = (\sum_i 1/\sigma_i^2)^{-1}$$

The <u>total</u> error for the event is then:-

$$\sigma_{tot}^2 = (\sigma_{k2}^2 + \overline{\sigma^2})$$

(If two electrons are measured, the sums are taken over the six pairs of x_i, σ_i.)

With the τ events the true value of x is known to be zero. If N events were measured, the calculations above give a set of N values of $\bar{x}$ and σ_{tot}; for convenience these will be written as x_j and σ_j. The probability of obtaining a value of x in the range x_j to x_j+dx_j, given σ_j, is:-

Fig 7·7c

Contours of $L(\sigma_{k1}, \sigma_{k2})$ at intervals of 2 units.

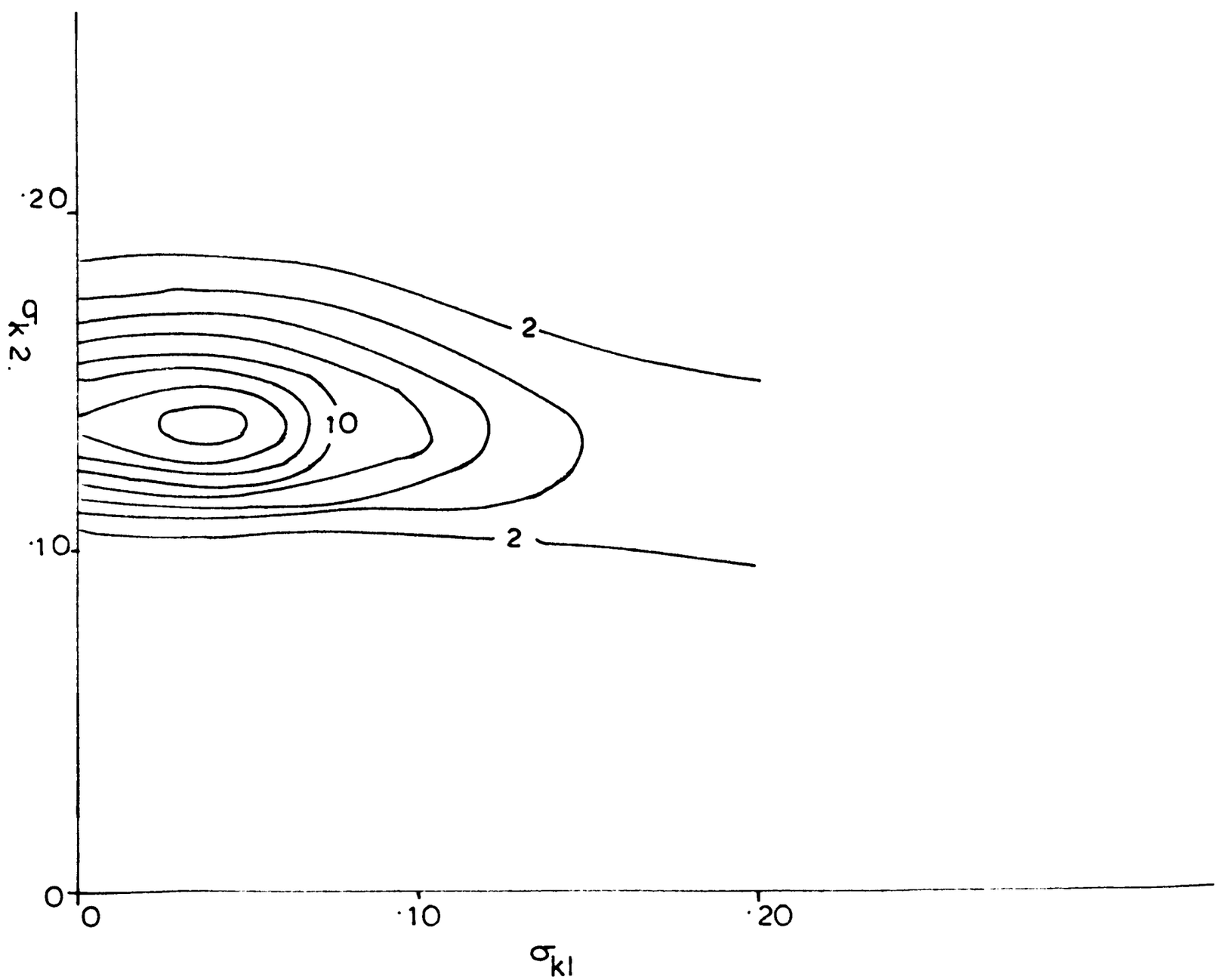


Fig 7·7b

Curves of $\mathcal{L}(\sigma_{k1}, \sigma_{k2})$ vs. σ_{k1} for constant σ_{k2}

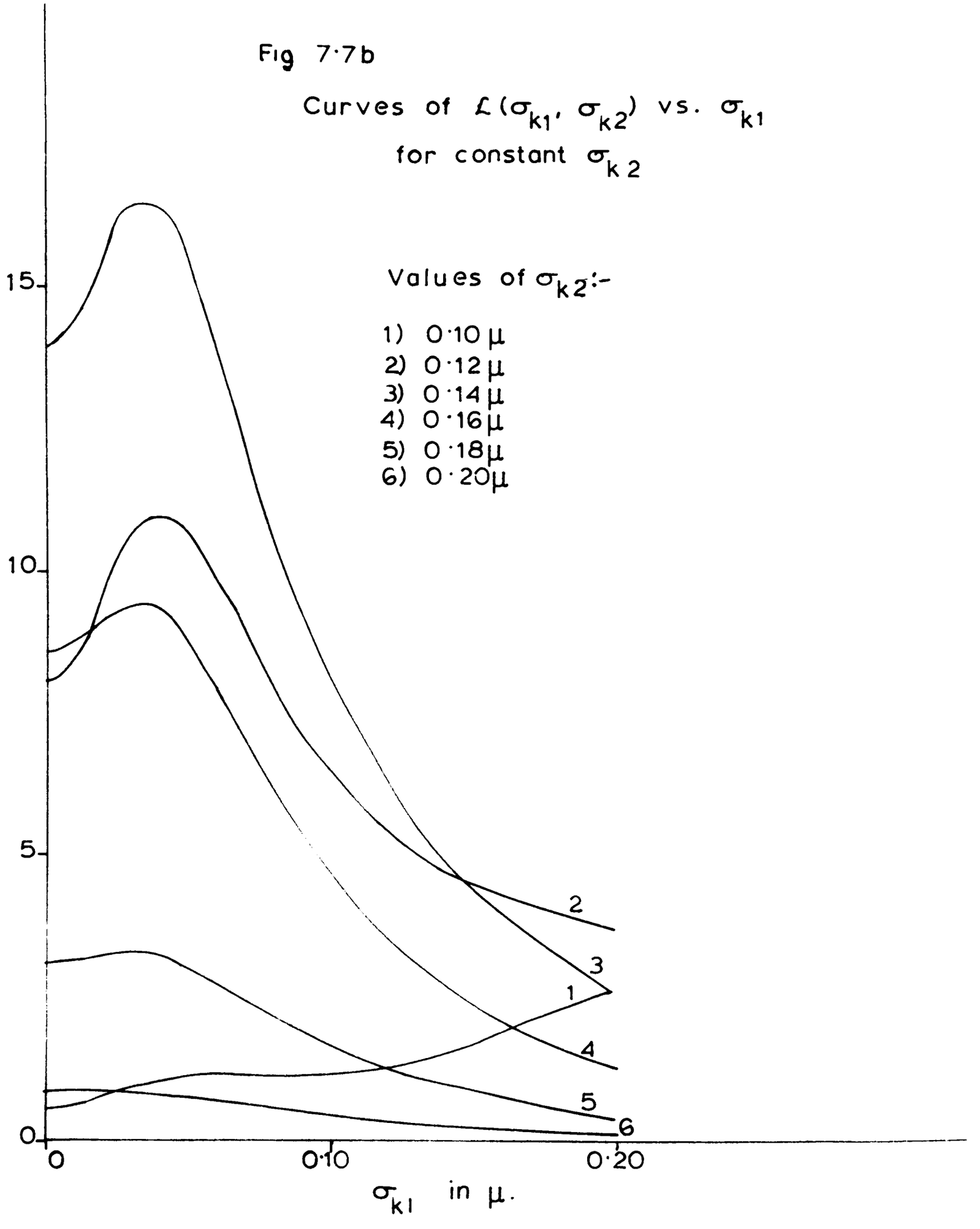
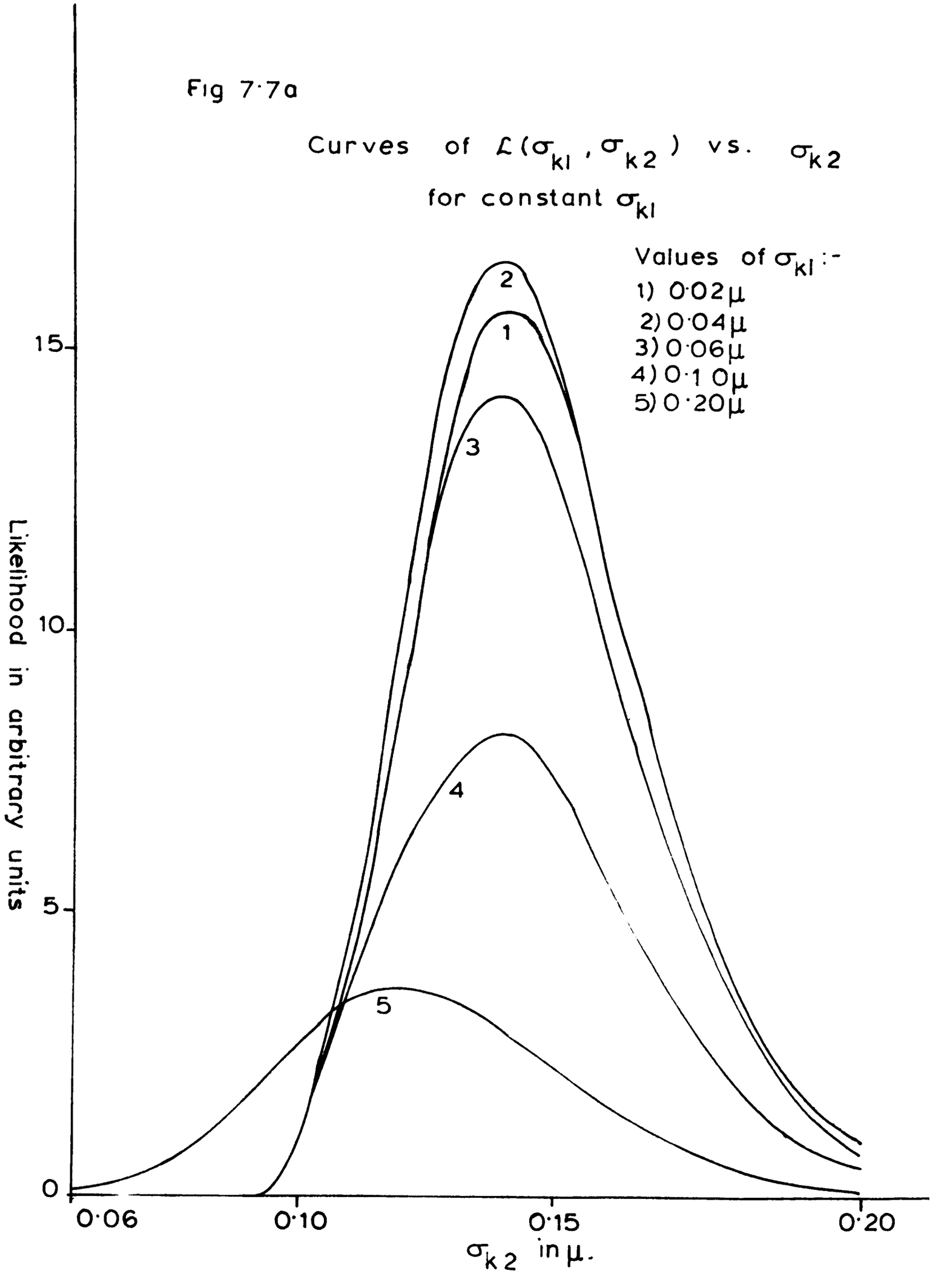


Fig 7·7a

Curves of $\mathcal{L}(\sigma_{k1}, \sigma_{k2})$ vs. σ_{k2} for constant σ_{k1}



$$p(x_j)dx_j = \frac{1}{\sigma_j\sqrt{2\pi}}\, e^{-x_j^2/2\sigma_j^2}\, dx_j$$

where it is assumed that x is distributed normally.

The likelihood function for the set of N events is then:-

$$L(\sigma_{k1}, \sigma_{k2}) = \prod_j^N p(x_j)$$

L is a function of σ_{k1} and σ_{k2} since the σ_j's are functions of these quantities.

The maximum likelihood estimates of these two parameters are those values which simultaneously maximize L, i.e. are the solutions of:-

$$\frac{\partial L}{\partial \sigma_{k1}} = \frac{\partial L}{\partial \sigma_{k2}} = 0$$

These equations are not soluble analytically. However, by calculating L as a function of the two parameters the position of the peak may be found.

7.6 Calculation of K^+ error

For each of the τ decays measured, one track was chosen at random (using a table of random numbers) to represent the π^+ in a pseudo-KD event while the other two tracks were taken as electrons. The appropriate values of x_i and σ_i had been previously calculated in the main τ analysis programme. A further programme was written to calculate L as a function of σ_{k1} and σ_{k2}, given as data the set of x_i and $(\sigma_{\pi e})_i$. The results are presented in figs. 7.7a,b,c.

It is seen that σ_{k2} is quite well defined by a sharp peak

whereas σ_{k1} has a much broader peak. This is to be expected as the former is based on thirty events while the latter is only based on the three measurements of each event. It was not considered worthwhile to attempt a better determination of σ_{k1}. A simple calculation shows that the total error of an event is insensitive to small variations in this parameter. The relative magnitudes of the two parameters is of interest. They indicate that the "intrinsic" source of error dominates so that further attempts to locate the centre of the last grain more accurately would have contributed little to the overall accuracy of the experiment.

The estimates chosen from the likelihood curve were:-

$$\sigma_{k1} = 0.04\mu$$

$$\sigma_{k2} = 0.137\mu$$

The values are satisfactorily near the expected magnitudes. σ_{k1} is not significantly different from the figure of 0.05μ quoted earlier for the measurement error on a single grain; σ_{k2} is of the order of the radius of a grain and compares favourably with the former cruder estimate of the error.

With the aid of these two parameters, the mean measured flight distance and its error were calculated for each of the π^o events measured. These values must also be corrected for the dip of the π^o path which is identical to the dip of the π^+ track. Both flight distance and error are multiplied

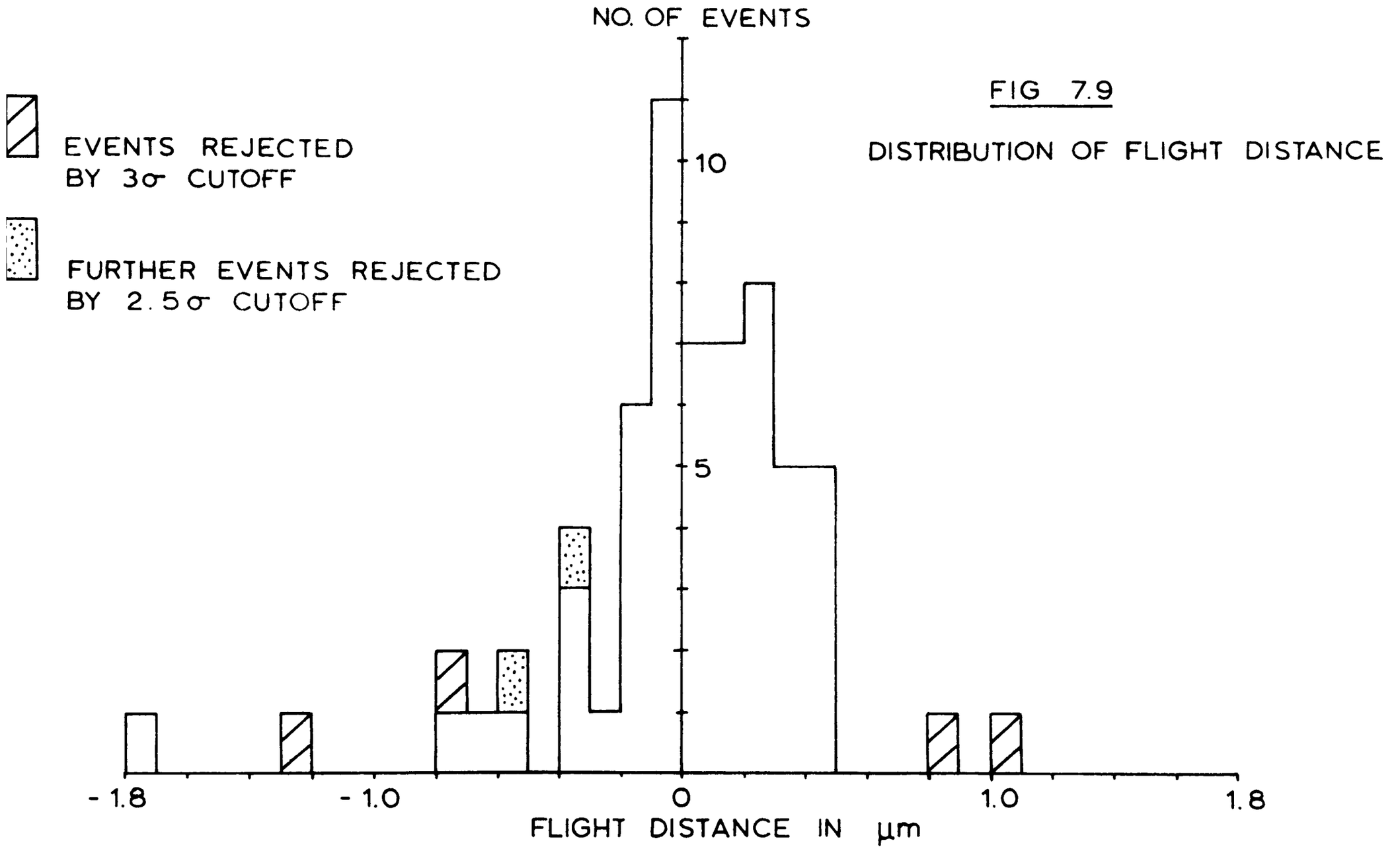


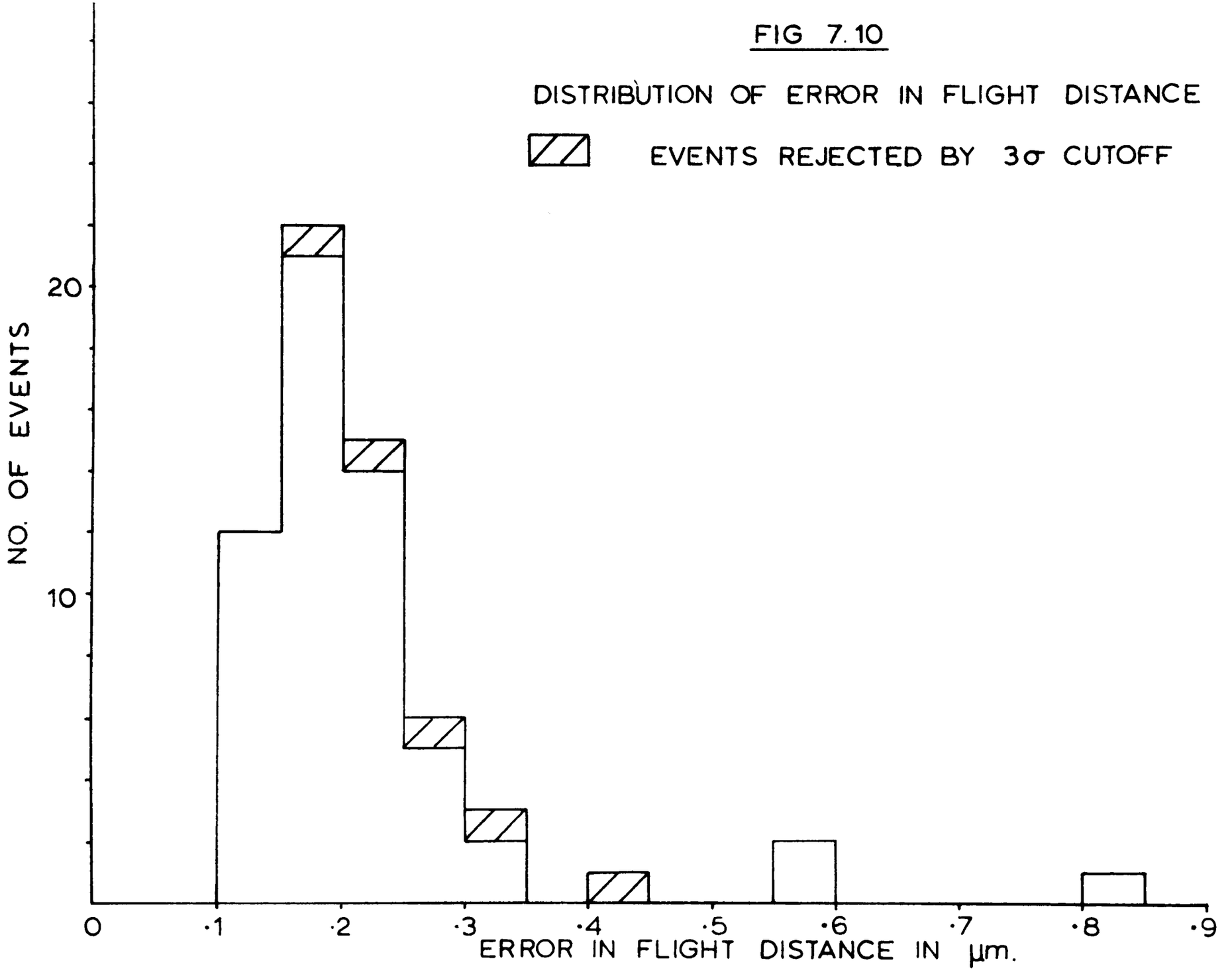
FIG 7.9

DISTRIBUTION OF FLIGHT DISTANCE

FIG 7.10

DISTRIBUTION OF ERROR IN FLIGHT DISTANCE

EVENTS REJECTED BY 3σ CUTOFF



by sec α, where α is the dip angle. The measured dip has to be corrected for the shrinkage which takes place in the thickness of the emulsion during processing. It was assumed that the shrinkage was by a factor of two (the 400μ pellicles becoming approximately 200μ thick). It will be shown later that a more accurate estimation of this factor was not necessary. A table of the values of X and σ finally used is given at the end of this chapter. The distributions of x and σ are shown in figs. 7.9 and 7.10. It is noticed that there is a sharp cutoff for the smaller errors; this is due to the effect of σ_{k2} since the error attributed to any event can never be less than this figure. The presence of the larger errors is due to the effects of the geometry of the event ($\sigma_{\pi e}$ large) and dip factor (sec α large).

The calculation of x and σ for each event is done in the manner described in section 7.5.

Table of x and σ for 63 events used finally

x	σ	x	σ
0.37	0.81	-0.07	0.22
-0.32	0.16	0.30	0.57
-0.34	0.17	0.44	0.22
0.13	0.14	-1.80	2.30
-0.65	0.33	-0.72	0.56
0.20	0.15	-0.21	0.40
-0.03	0.26	0.41	0.20
0.22	0.15	-0.05	0.16
-0.17	0.21	-0.00	0.20
-0.51	0.34	-0.11	0.24
0.21	0.25	1.10	0.24
0.21	0.19	0.21	0.19
0.09	0.16	0.30	0.16
0.21	0.15	-0.17	0.21
0.18	0.15	-0.15	0.27
0.13	0.18	-0.16	0.15
-0.08	0.18	-0.09	0.16
0.12	0.15	-0.09	0.14
0.48	0.23	0.20	0.26
0.05	0.15	0.32	0.16
0.07	0.19	0.45	0.18
0.08	0.16	0.09	0.14
0.08	0.15	-0.03	0.14
-0.06	0.14	-0.17	0.17
0.33	0.16	0.11	0.16
-0.02	0.24	0.05	0.27
-0.75	0.17	0.20	0.21
-1.28	0.33	-0.34	0.24
-0.10	0.21	0.14	0.21
0.39	0.14	0.84	0.25
0.08	0.14	-0.57	0.25
-0.39	0.17		

The events rejected by 3σ cutoff are underlined.

CHAPTER VIII

ESTIMATION OF LIFETIME

8.1 Introduction

Of the 67 events which were measured, 7 did not at first pass through the programme described in section 7.1; this was subsequently found to be due to faulty punching of the data tape. Two further events were excluded as they gave results which were clearly spurious, i.e. flight distances of the order of $\pm$ several microns. When these events were investigated it was found that in one case the electron pair was steeper than the selection criterion had demanded, a large number of the grains in both electron tracks had been rejected; in the other case the π^+ track was difficult to follow and it was found that the track followed was spurious, in each measurement the grain nearest to the K^+ ending had been rejected and it was reasonable to assume that this was the only grain of the true π^+ track which was included.

As a result of the data failure and the other spurious events a total of 58 events was obtained. The following description of the estimation of the lifetime contains the intermediate results obtained and indicates the reasons for introducing a cutoff factor. The final result however, includes the seven events which did not initially pass the flight distance calculation.

8.2 Weighted mean method

In all the error calculations described in section 7.5 it was assumed that the flight distances were normally distributed with a standard deviation given by the calculated error. In such a situation, given a set of x_i with errors σ_i the simplest estimate of x is the weighted mean $\bar{x}$, where:-

$$\bar{x} = \frac{\sum_i x_i/\sigma_i^2}{\sum_i 1/\sigma_i^2} \quad ; \quad \text{the error in } \bar{x} \text{ is given by:-} \quad \overline{\sigma^2} = (\sum_i 1/\sigma_i^2)^{-1}$$

To obtain the corresponding mean lifetime the relationship:-

$$\bar{x} = \beta\gamma c\tau$$

is used with $\beta = 0.835$; $\gamma = (1-\beta^2)^{-\frac{1}{2}}$ and $c = 3 \times 10^{10}$ cm/sec. The result for the 58 events was:-

$$\underline{\tau = (0.58 \pm 0.55) \times 10^{-16} \text{ secs.}}$$

8.3 Maximum likelihood estimation

The method of calculation described above is open to criticism; the main disadvantage appears to be that it does not explicitly take into account the exponential decay distribution. It is true that the parameter defined as the "mean" lifetime could be derived from the mean of the flight distances <u>if they could be measured with infinite accuracy (i.e. all $\sigma_i = 0$).</u> This follows since the mean of the exponential distribution:-

$$p(t)dt = \tau^{-1} e^{-t/\tau} dt$$

is τ. However, it is not clear whether the same is true when the σ_i are of the same order as the x_i.

The distribution function of the x_i's may be calculated as follows. The distribution function for the time of existence of the particle has just been quoted. It is convenient to work in terms of distance instead of time using the relation quoted in section 8.2. The distribution of x, the <u>actual</u> distance travelled is then:-

$$p(x)dx = x_o^{-1}\, e^{-x/x_o}\, dx, \text{ where } x_o = \beta\gamma c\tau$$

Let x' be the actual distance travelled by the π^o in an event where the <u>measured</u> flight distance is x_i and the calculated error σ_i. We then have:-

$$p(x_i)dx_i = (\sigma_i \sqrt{2\pi})^{-1}.e^{-(x'-x_i)^2/2\sigma_i^2}.\ dx_i$$

but since x' is also distributed according to the exponential law, we must multiply the two distributions and integrate over all possible values of x',(i.e. zero to infinity) to obtain the true distribution function:-

$$p(x_i)dx_i = (x_o\sigma_i \sqrt{2\pi})^{-1} \int_0^{\infty} \exp\left(\frac{x'}{x_o} - \frac{(x'-x_i)^2}{2\sigma_i^2}\right) dx'.\ dx_i$$

This function depends upon two parameters: x_o (and hence τ) and σ_i the error in x_i.

Using this compound distribution function we immediately obtain the likelihood function for a set of events with given x_i and σ_i; this function is then only dependent upon τ:-

$$L(\tau) = \prod_{i}^{N} p(x_i)$$

The value of τ which maximizes $L(\tau)$ is taken to be the maximum likelihood estimate.

The details of the calculation of $L(\tau)$ from the experimental values of x_i and σ_i are given in the appendix. The maximum was found to be at $\tau = 2.3 \times 10^{-16}$ secs. and a rough estimate of the error from the width of the curve indicated a value similar to the error in the weighted mean.

8.4 Investigation of conflicting estimates

The two estimates obtained were:-

Weighted mean: $\tau_{wm} = 0.58 \times 10^{-16}$ secs.

Max. likelihood: $\tau_{ml} = 2.30 \times 10^{-16}$ secs.

Error in both is of the order of 0.55×10^{-16} secs.

The inconsistency of these two estimates was surprising, identical estimates were not anticipated but the above estimates differ by more than three standard deviations. Considerable attention was paid to the causes of the discrepancy and a description of the course of the investigation is not out of place.

For reasons explained in the appendix, the method of calculating $L(\tau)$ was suspected. However, this was found not to be so, although close examination of the computations yielded a less time-consuming method of calculation.

8.5 Imitation results

It was considered desirable to check whether any great

disparity between the two methods of calculation was to be expected. For convenience, a lifetime of 1.5×10^{-16} secs. was assumed. Using a technique similar to that employed in "Monte Carlo" calculations, a number of samples of ideal x_i were concocted with the same set of σ_i as the experimental values, and consistent with the assumed lifetime. Fuller details of the method are given in the appendix. Ten samples of this type were made up, each consisting of 58 sets of "x_i" and σ_i. These samples were then treated by the weighted mean and the maximum likelihood programmes. The results are presented in the following table where the third column represents the difference $(\tau_{wm} - \tau_{ml})$ in units of σ_{wm}. Since the values of σ_i used were the experimental ones, the value of σ_{wm} was unchanged, i.e. $\sigma_{wm} = 0.55 \times 10^{-16}$ secs.

	τ_{ml}	τ_{wm}	diff/σ_{wm}
	0.54	0.68	0.25
	1.63	1.68	0.09
	1.81	1.77	-0.07
	1.27	1.30	0.05
	0.80	1.17	0.67
	1.49	1.63	0.25
	0.55	0.52	-0.05
	1.14	1.23	0.16
	0.55	0.62	0.13
	2.09	1.55	-0.98
mean	1.19	1.22	

It is clear from this table that a large difference between the two estimates is not to be expected. In the samples tested the difference was never greater than one standard deviation. It is noted however, that there are indications that there is a bias whereby τ_{wm} is greater than τ_{ml}; there is also a sign that there is an overall bias since the means of the computed values are not the same as the assumed lifetime.

8.6 Presence of and effect of "wild" events

An examination of the experimental values of x_i and σ_i discovered some events which were seemingly inconsistent with the main set of results; such events had large flight distances both positive and negative in separate cases and yet were attributed with a σ_i which could not account for the large distance. Examples of such values are:-

x(in μ)	σ (in μ)
-1.21	0.33
-1.26	0.22
1.10	0.24
-1.23	0.27
0.62	0.14

Such events as these will be termed "wild".

A simple argument shows that these "wild" events have different effects upon the two methods of calculation. With the weighted mean, both positive and negative values are

admitted with equal weight. Examination of the possible "wild' events indicated that there were more with a negative flight distance than with a positive, hence the effect would be to reduce the weighted mean. The maximum likelihood method however, does not admit negative lifetimes; a "wild" event with a large negative flight distance merely tends to reduce the likelihood less for the near zero values of τ; a positive "wild" event is interpreted as being due to an event which truly can have that large lifetime and so the position of the maximum of $L(\tau)$ is shifted to a more positive value. A simple analytical illustration of this effect is not possible, but the above qualitative remarks indicate that the positive "wild" events are weighted much more than the negative ones. Hence it may be expected that the value of τ_{ml} which has been obtained is higher than it should be.

In order to exclude the effect of the "wild" events a cutoff procedure was included in both the programmes which calculate the estimates. When the estimate had been found from all the events, each value of x_i was tested to determine whether it differed by more than a given multiple of σ_i from the calculated estimate. If the difference was too great, that event was excluded from a re-calculation of the estimate. The test was applied again for the new estimate, all the events were tested including those previously rejected. The process was continued until identical samples of events were presented

for successive iterations. Three values of cutoff parameter were used: 3σ, 2.5σ and 2σ. The results of the final iterations are presented in the following table:-

Cutoff	τ_{ml}	no. of events	no. of iter'ns	τ_{wm}	no. of events	no. of iter'ns
none	2.30	58	-	0.58	58	-
3 σ	1.07	49	1	0.48	51	1
2.5σ	1.25	47	2	1.17	47	1
2 σ	1.32	43	2	1.56	43	2

(the lifetimes are in units of 10^{-16} secs.)

It is seen that the exclusion of the "wild" events regains agreement between the two methods of estimation.

8.8 Investigation of "wild" events

The eleven events excluded by the 2.5σ cutoff were examined and it was found that they could be classed as follows:-

(i) events where the four measurements gave consistent results, which had both electrons measured but one of them gave an apparently "wrong" flight distance,

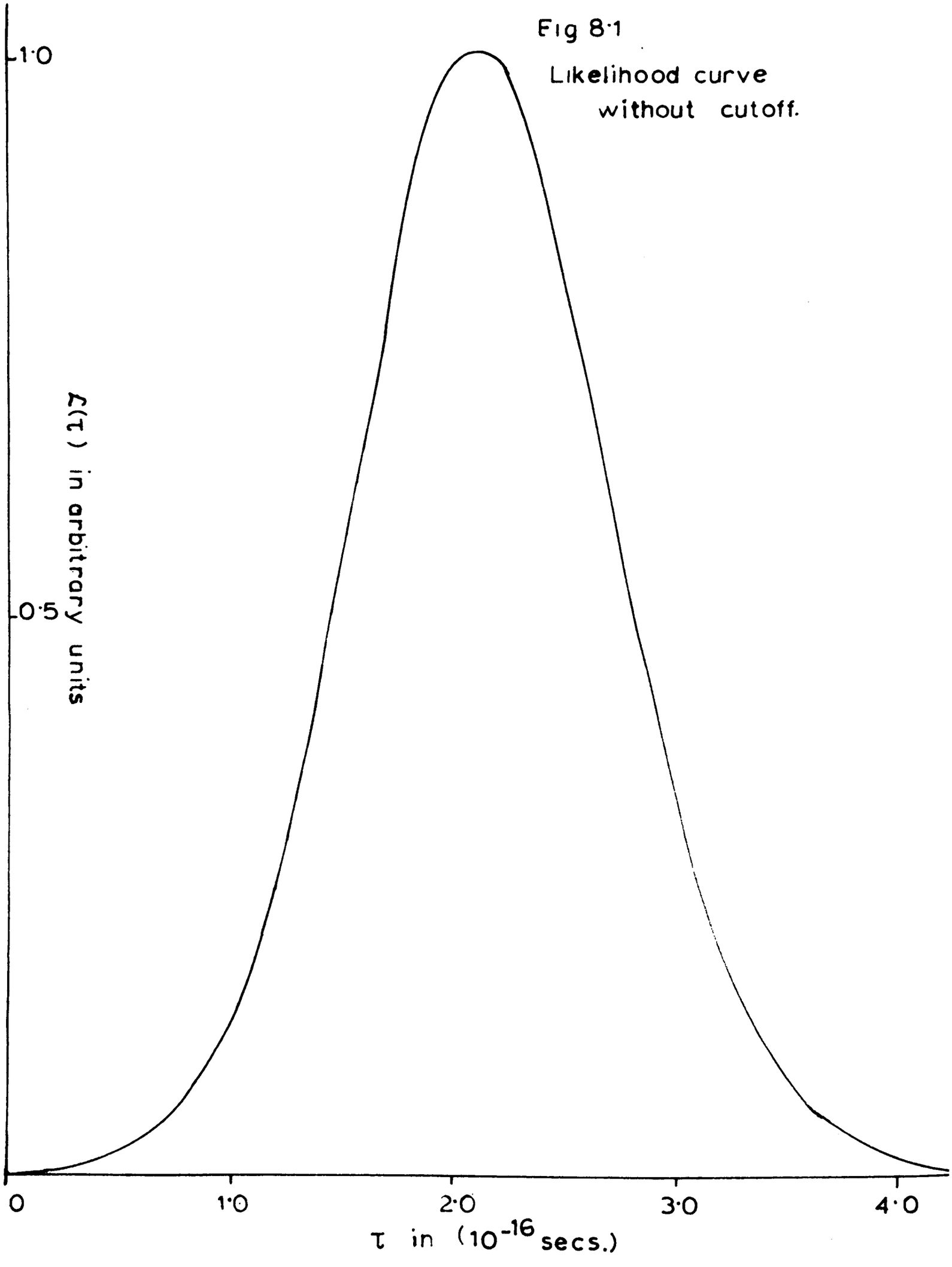
(ii) events where the separate measurements were not consistent,

(iii) very wide angle events (poor geometry),

(iv) steep events,

(v) events with only one electron, giving consistently "wrong" flight distances.

There were 4 events of type (i); 4 of (ii); 1 of each of (iii),(iv) and (v).


Fig 8·1
Likelihood curve
without cutoff.
1·0
0·5
ℒ(τ) in arbitrary units
0
1·0
2·0
3·0
4·0
τ in (10⁻¹⁶ secs.)

For the events in class (i), the mean flight distance for the event was re-calculated excluding the "faulty" electron. A new set of four measurements was made for the events in class (ii). The events in classes (iii) and (iv) were rejected, the event in class (v) was merely allowed to stay in the sample.

The eight new values for the events in classes (i) and (ii) together with the results from the seven events not previously included in the calculation (see section 8.1) and the one event in class (v) were included with the 47 events which survived the 2.5σ cutoff to give a final sample of 63 events. It is the distributions of x_i and σ_i in this sample which are shown in figs. 7.9 and 7.10, and the table of these values which is given on page 81.

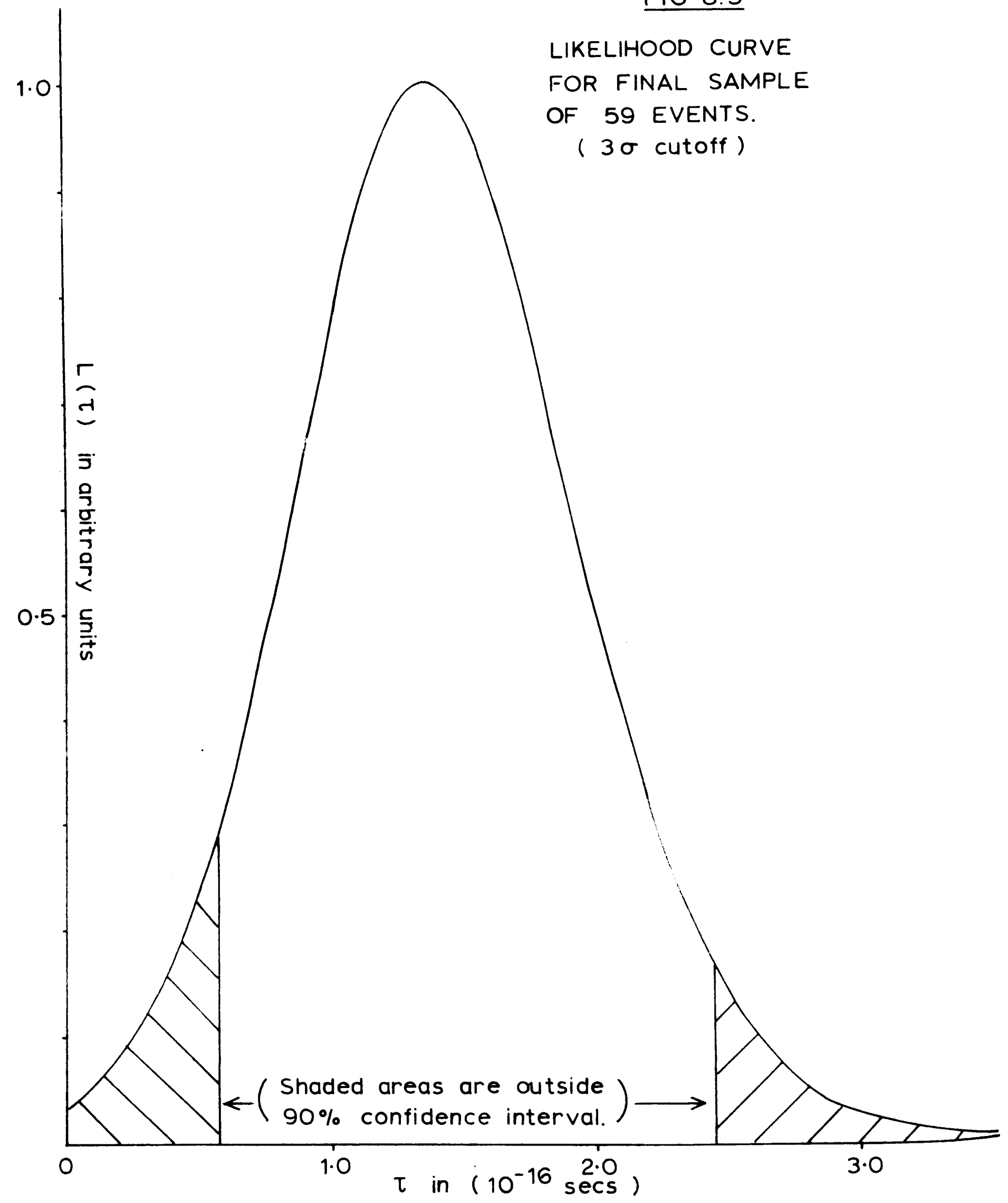
The results obtained are as follows:-

cutoff	τ_{ml}	no. of events	no. of iter'ns	τ_{wm}	no. of events	no. of iter'ns
none	2.10	63	-	1.04	63	-
3 σ	1.36	59	2	1.17	59	1
2.5σ	1.54	57	3	1.37	58	1
2 σ	1.33	52	1	1.61	52	1

It is seen that with the rejection of only four events by the 3σ criterion, the two estimates become consistent. The slight variations in the estimates for the other cutoff factor is within the error of about 0.5 attributed earlier to the estimates. Some estimation of the error from the

FIG 8.5

LIKELIHOOD CURVE FOR FINAL SAMPLE OF 59 EVENTS. (3σ cutoff)



likelihood curve is required, this is described in the next section.

The likelihood curve obtained from the whole of the 63 events is shown in figure 8.1; that for the 59 events remaining after the 3σ cutoff is shown in fig. 8.5. In both cases the values of $L(\tau)$ are normalised so that the maximum value is $L = 1$. The likelihood curve has dropped to $L = 0.04$ for $\tau = 0$ in the case of the 59 events. Some form of confidence interval is needed to express the result of the experiment more clearly.

8.9 Confidence interval

The estimation of confidence intervals or of errors, from likelihood functions is to a large extent empirical. It can be shown that the likelihood function approximates to a Gaussian curve when the number of events increases greatly. The curves obtained in this experiment bear a superficial resemblance to the Gaussian curve. Using this assumption various formulae may be derived. The simplest of these is obtained by noting that if:-

$$L(x) = Ae^{-(\mu-x)^2/2\sigma^2}$$

$$\text{and} \quad w(x) = \log_e(L)$$

$$\text{then} \quad d^2w/dx^2 = \sigma$$

Thus, for a curve approximating to a Gaussianm the associated error is taken to be the mean value of w'' over the range of x. This definition suffers from the disadvantage that it does not deal with skew functions. It can be seem that the function

FIG 8.3

S (τ) for concocted samples

⊙ weighted mean value.

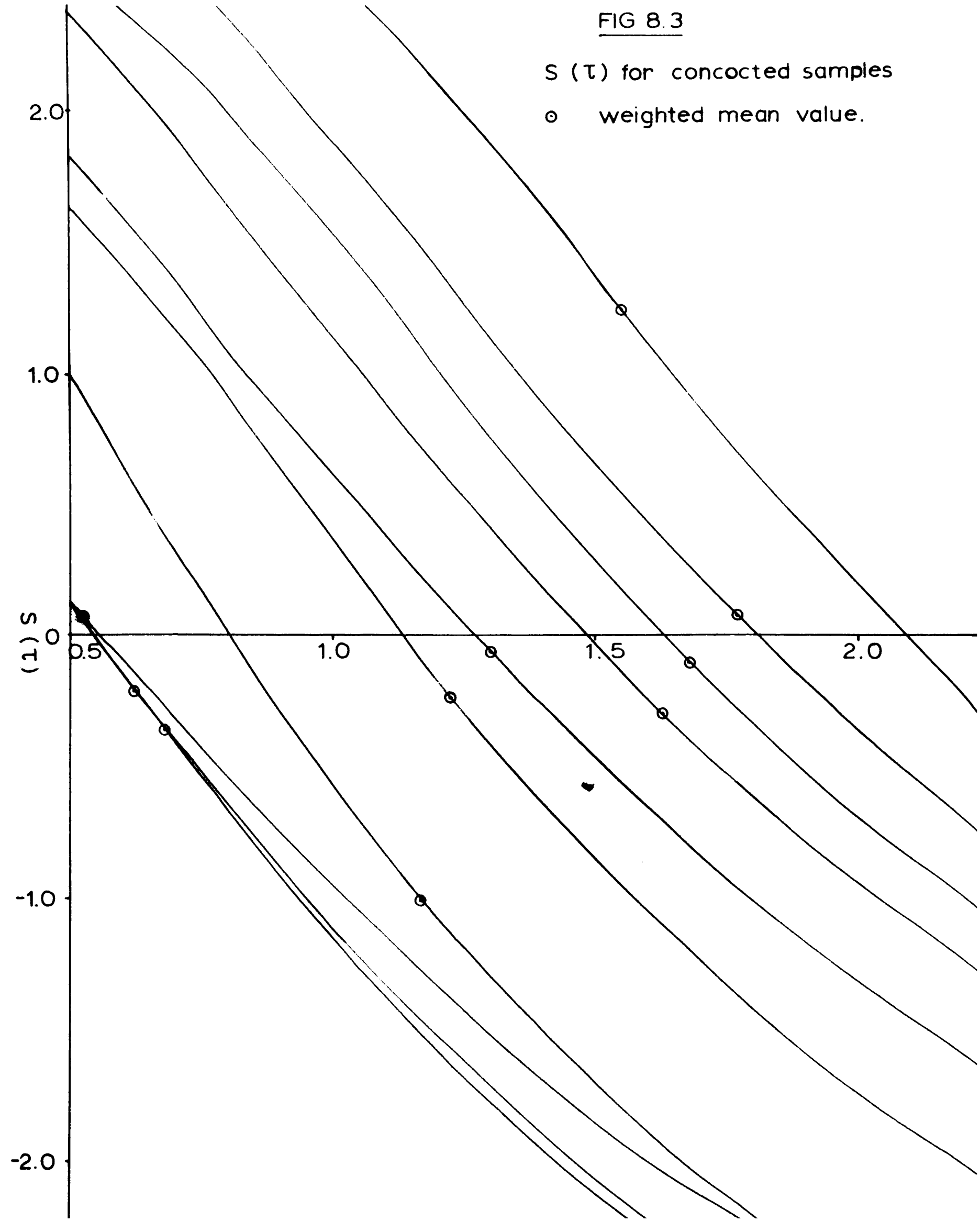
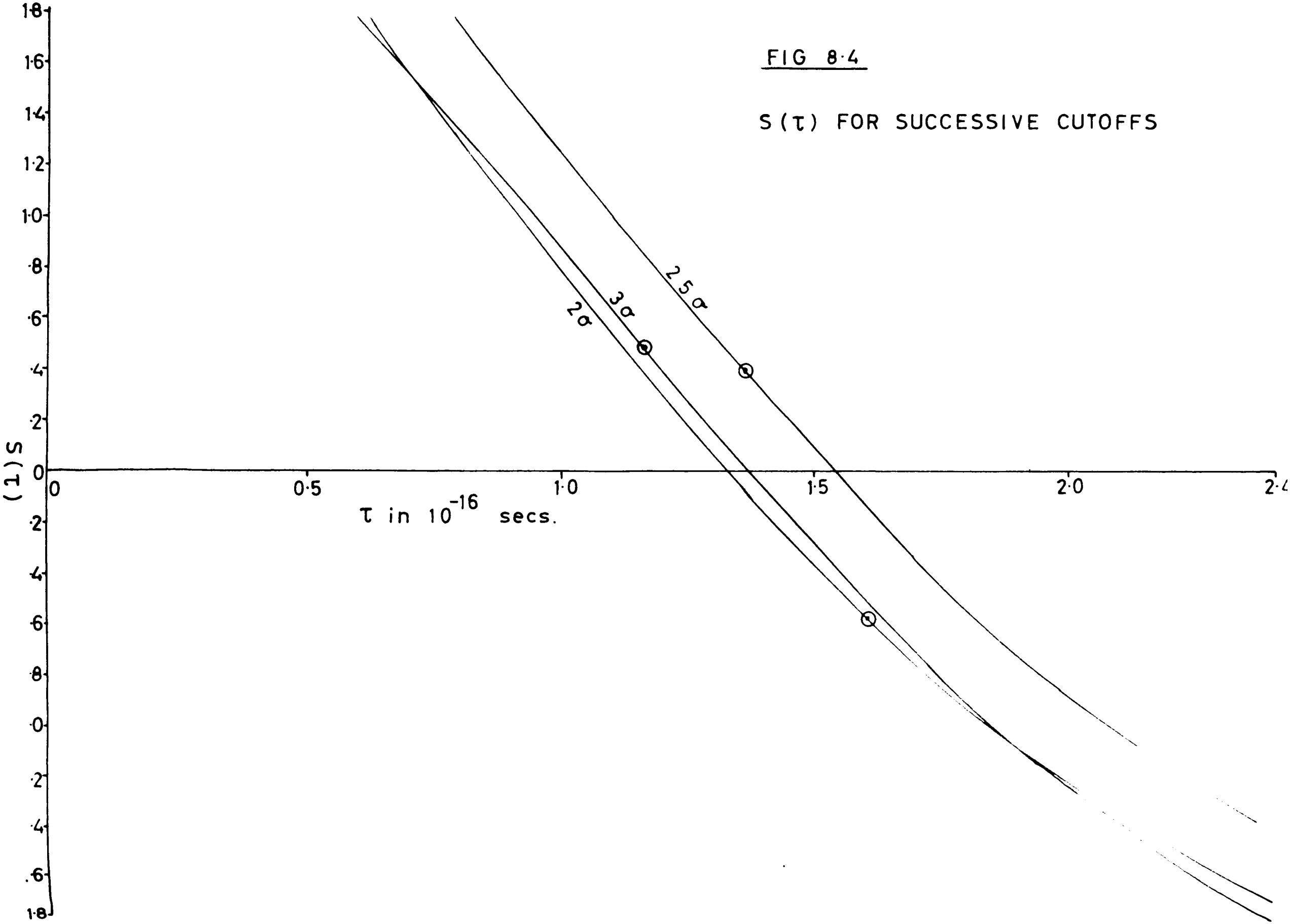


FIG 8·4

S(τ) FOR SUCCESSIVE CUTOFFS



obtained in this experiment is slightly skew, showing more of a "tail" to higher values of τ.

A method which can deal with skew distributions is quoted by Orear [24]) and is attributed to Bartlett [25]). A function $S(\tau)$ is defined by the following relations:-

$$S(\tau) = \frac{1}{C}\frac{dw}{d\tau} \quad \text{where} \quad C^2 = -\int_{\tau min}^{\tau max} L(\tau).\frac{d^2w}{d\tau^2}\, d\tau \; ; \; w = \log_e L$$

For a Gaussian form of $L(\tau)$, $S(\tau)$ is a straight line which intersects the τ axis at the maximum likelihood estimate of τ, while solution of the equations $S(\tau) = \pm 1$ gives the "one standard deviation" points about the maximum likelihood estimate. Solution of $S(\tau)$ for any other number gives that number of standard deviations about the τ_{ml}. A non-Gaussian $L(\tau)$ will give an S function which deviates from a straight line; $S(\tau) = 0$ will still give the value of τ_{ml} and the solutions of $S(\tau) = \pm n$ are taken to be the "n-standard deviation points".

This calculation, the details of which are given in the appendix, was performed for all the maximum likelihood determinations made. Fig. 8.3 shows the curves obtained for the concocted samples; the encircled points represent the weighted mean values of τ.

A 90% confidence interval may be deduced by solving $S(\tau) = \pm 1.65$. (For a gaussian, the 90% interval lies between the 1.65σ points.) This applied to the 59 event results yields:-

$$\underline{(0.58 \leq \tau_{ml} \leq 2.44) \times 10^{-16} \text{ secs.}}$$

A similar interval may be obtained from the weighted mean calculation. The value of the weighted mean for the 59 events was:-

$$\tau_{wm} = (1.17 \pm 0.53) \times 10^{-16} \text{ secs.}$$

Hence, calculating the 1.65σ points the following interval is obtained:-

$$\underline{(0.30 < \tau_{wm} < 2.04) \times 10^{-16} \text{ secs.}}$$

8.10 Correction for contamination events

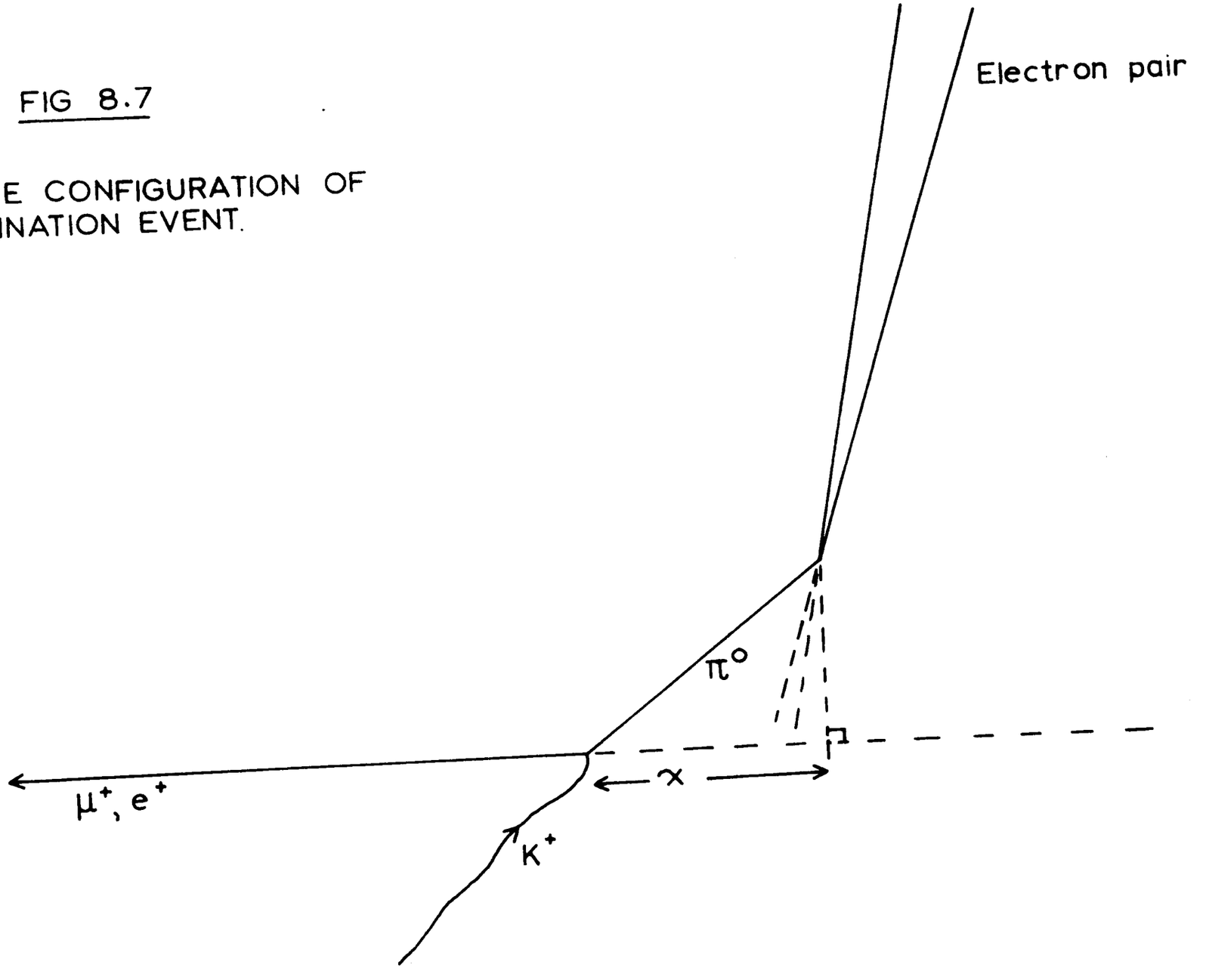
In section 3.4 it was shown that the presence of the contaminating events due to $K_{\mu 3}$ and K_{e3} decays would be expected to alter the experimental value of lifetime by a constant factor. It was also indicated that the factor was expected to be less than 1.3. The evaluation of this factor will now be carried out more precisely.

For the sake of the argument we will at first consider events to fall into two classes: "true" events (i.e. $K_{\pi 2}$ decays) and "false" events ($K_{\mu 3}$ and K_{e3} decays). We also consider a non-distributed lifetime for the π^o, τ_π.

Measurements on a pure population of true events will yield τ_π for the lifetime. Measurements upon purely $K_{\mu 3}$ or K_{e3} false events treated as two-body $K_{\pi 2}$ events will yield false lifetimes of $\tau_{f\mu}$ and τ_{fe}. These lifetimes can be considered to be approximately those obtained by applying the kinematics of the $K_{\pi 2}$ decay to the mean projection of the π^o flight distance on to the line of flight of the charged particle. This is

FIG 8.7

POSSIBLE CONFIGURATION OF CONTAMINATION EVENT.



illustrated in fig. 8.7. This shows a possible configuration for a contamination event. It is seen that the projection of the π^o flight distance on to the line of the charged secondary is not exactly the same distance as would be obtained in the calculations described in section 7.1. However, the calculation is simplified if the projection is considered; for good geometry events which contribute most information to the experiment the approximation is quite good.

We assume that the spectrum in momentum of the π^o is:-

$$f(p, \Theta)dp\ \sin\Theta d\Theta d\emptyset$$

where p is the momentum of the π, Θ the angle between the π and the charged secondary (μ^+ or e^+) and $\emptyset$ is the azimuth angle about the charged secondary trajectory as axis.

We have the following relations:-

$p = m\beta\gamma$; $x = \beta\gamma c\tau_\pi = pc\tau_\pi/m$; where x is the true flight distance, m is the mass of the π^o.

The mean projected length is then:-

$$\bar{x} = \frac{c\tau_\pi}{m} \int_0^{p_{max}} dp \int_{-\pi}^{\pi} d\Theta \int_0^{2\pi} d\emptyset . p . f(p,\Theta)\cos\Theta\sin\Theta$$

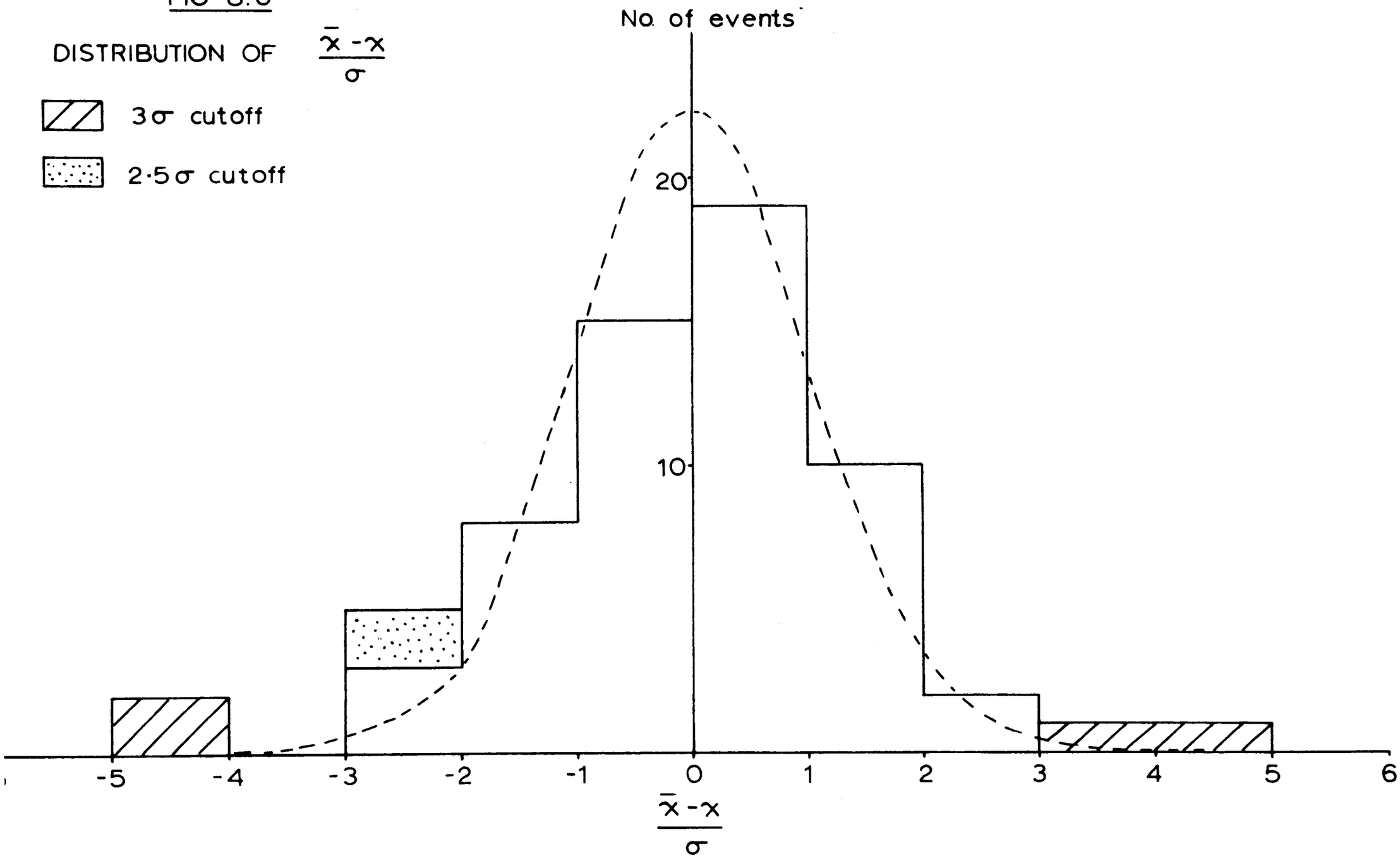
Finally the "false" lifetime τ_f is given by:-

$\bar{x} = (\beta\gamma)_{\pi 2} . c\tau_f$ where $(\beta\gamma)_{\pi 2}$ is the value appropriate for the π^o in $K_{\pi 2}$

These calculations were made taking the momentum spectrum from phase-space considerations. An allowance was made for

FIG 8.6

DISTRIBUTION OF $\frac{\bar{x}-x}{\sigma}$



the $K_{\mu 3}$ decays which had been eliminated as a result of the grain density measurements. The results obtained were:-

$$\tau_{f\mu} = 0.50\tau_{\pi} \quad ; \quad \tau_{fe} = 0.39\tau_{\pi}$$

From the branching ratios the following ratios of different events is expected:-

$$K_{\pi 2},\ 0.77 \quad ; \quad K_{\mu 3}\ \ 0.09 \quad ; \quad K_{e3}\ \ 0.14.$$

Thus we have:-

$$\tau_{exp} = (0.77 \times 1 + 0.14 \times 0.39 + 0.09 \times 0.50)\tau_{\pi}$$

$$= 0.87\ \tau_{\pi}$$

Whence $$\underline{\tau_{\pi} = 1.15\ \tau_{exp}}$$

This factor will not alter the width of the confidence interval but is applied to the estimate of the lifetime. Applying the factor to the maximum likelihood and weighted mean determinations gives the following results:-

	Max. likelihood	Weighted mean
Lifetime	1.56	1.34
90% confidence interval	0.78 - 2.64	0.47 - 2.21

(units of 10^{-16} secs.)

The distribution in fig 8.6, (where $\bar{x}$ is the flight distance for τ_{ml}) would be expected to be approximately normal with zero mean and unit standard deviation if the error calculations have been reasonable. The dotted line indicates the trend for unit standard deviation and it is seen that the distribution is not inconsistent with this.

CHAPTER IX

DISCUSSION OF EXPERIMENT

9.1 General remarks

This chapter will fall into two parts. The first deals with a brief discussion of the method in retrospect. The magnitudes of some small sources of error are estimated to demonstrate the reason for neglecting them in the main experiment. An analysis of the main sources of error is attempted. In the second part, other attempts to measure the π^o lifetime are briefly described and a measure of comparison is attempted. Finally, the place of the lifetime in theoretical problems is indicated.

9.2 Synopsis of the experiment

In this experiment, nuclear emulsions have been used in an unconventional manner. In normal usage, measurements of length are made directly and the distances involved are much greater than the grain size; the emulsion is used as a gauge to determine the energies, momenta and identity of particles as well as the geometry of their flight. In this sort of use corrections for the finite resolution of the emulsion are small. In this experiment it has been demonstrated that the emulsion is being used to the limit of its resolution. The distance corresponding to the lifetime measured is of the order of 0.05μ while the developed grain diameter of the emulsion is about 0.3μ.

It has also been shown that the measurement error in any event cannot be less than 0.14μ, nearly three times the distance being measured. This figure of 0.14μ was also seen to be due to the granular nature of the silver image. This very large error makes the experiment statistical in nature; a large number of individual events have to contribute before any meaningful conclusions may be drawn. In view of this statistical nature, it was considered essential that the nature and the magnitudes of the errors involved in the determination should be thoroughly investigated. Chapter VII has dealt with the large sources of error, but for the sake of completeness the other and as will be seen very much smaller errors will be considered.

9.3 Miscellaneous errors

In this category are placed those errors which are not du e to the actual measurement of events or to the nature of the emulsion. As indicated above, all these errors should be considered with reference to the main sources of error.
The factors to be discussed in this section are:-

(a) Shrinkage factor of emulsion,

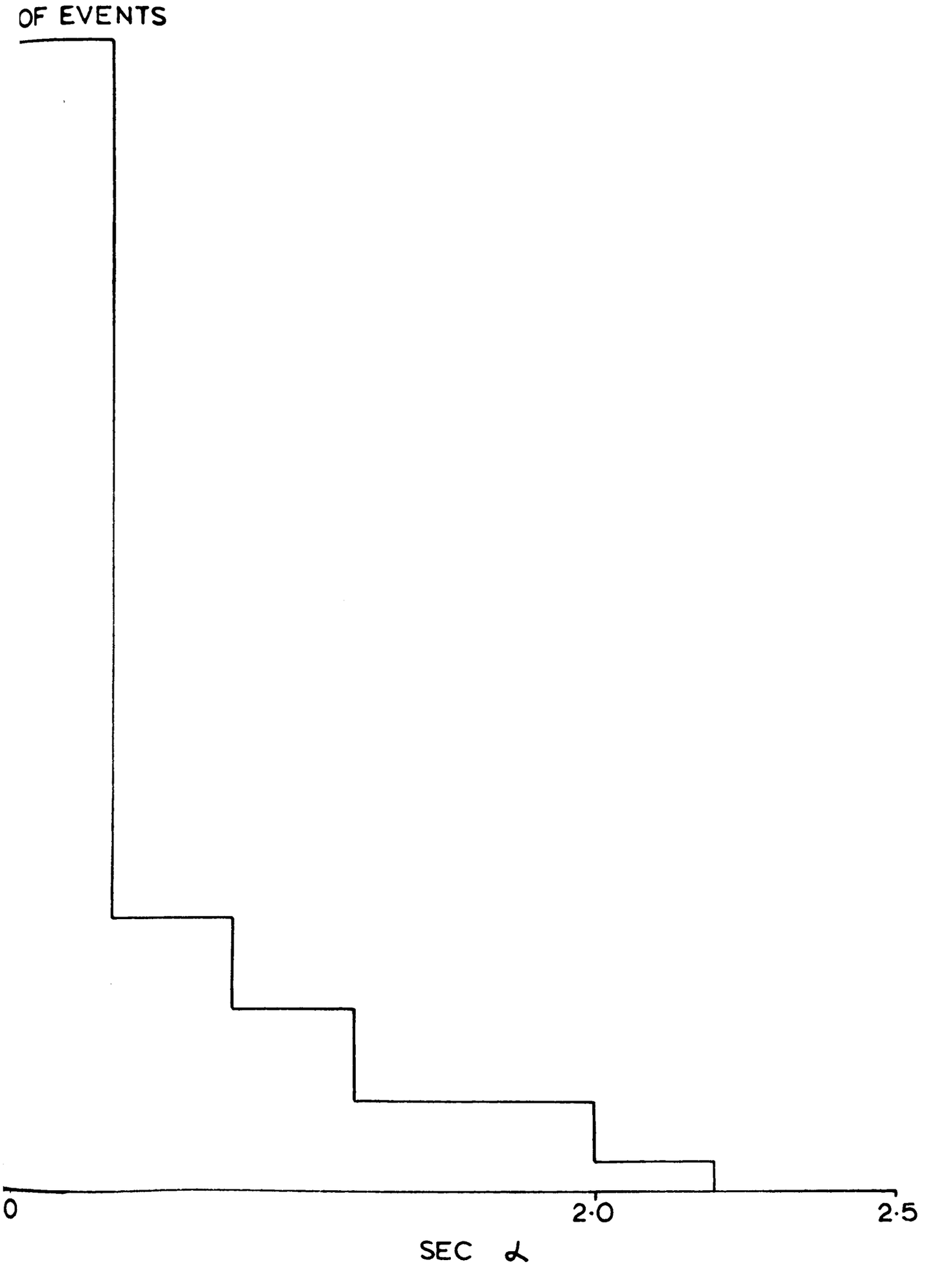
(b) Determination of dip of π^+ track,

(c) Lateral distortion of the emulsion ("C" shaped),

The following remarks are intended as a justification that the measurements of the above quantities were not performed with the greatest possible accuracy.

FIG 9·1

DISTRIBUTION OF SEC α



(a) The fractional error in sec α caused by an error in shrinkage factor δs is given by:-

$$\frac{\delta(\sec \alpha)}{\sec \alpha} = \sin^2\alpha . \frac{\delta s}{s}$$

The variation in thickness of the shrunk emulsion is about $\pm 10\mu$, giving a fractional error in s of 5%.

The distribution of sec α for the events measured is shown in fig. 9.1. It is clear that the greatest weight in the final result comes from "flat" events, i.e. those with small sec α. Over half of the events have sec α less than 1.2. This weighting is further translerred to flat events since the steeper events are given larger errors (due to sec α factor) and are consequently weighted less. Taking sec $\alpha < 1.2$ gives $\sin^2\alpha < 0.2$ so that the fractional error is less than 1%.

(b) The determination of the dip of the π^+ track involves the measurement of two quantities: the projected length of a section of the track and the change in depth along this length. The effect of error in the projected length is given by:-

$$\frac{\delta(\sec \alpha)}{\sec \alpha} = \sin^2\alpha . \frac{\delta L}{L}$$ where L is the projected length.

In most cases, L was of the order of 100μ and δL of the order of 1μ. The considerations discussed in the previous paragraph concerning the effect of the $\sin^2\alpha$ factor apply equally here, so that the maximum expected error is about 0.2% in each event.

The effect of error δh in the depth measurement is given by:-

$$\frac{\delta(\sec \alpha)}{\sec \alpha} = \sin\alpha . \cos\alpha . s \frac{\delta h}{L}$$

We then have that $\delta h \sim 1\mu$, $L \sim 100\mu$ and $s \sim 2$. Consideration of the distribution in dip gives $\sin\alpha\cos\alpha < 0.45$. Combination of the contributions in error from δL and δh gives a total error in flight distance of about 1% for each event.

When it is considered that the measurement error for each event cannot be less than 300% it is clear that the error arising from these sources is negligible.

(c) Lateral distortion of the emulsion changes straight lines of tracks into curve and alters the angles between the tracks.

Any deviation of the tracks from straight lines is immediately detected in the line fitting programme and such tracks or events rejected. This was not found to happen in any of the events measured.

If the distortion were to alter the angles but preserve the rectilinearity of the tracks the effect may be considered as a linear transformation of the geometry of the event. The intersections of the tracks would be unaltered while the change in linear dimensions can be at most a few per cent; consequently this form of distortion is negligible.

9.4 Main sources of error

The assumed nature and the determination of the sizes of the various large sources of error has been described in detail in earlier sections. It will now be attempted to consider together these sources in relation to the present experiment.

It has been assumed that the errors present are of two types:-

(i) those due to imprecise measurement technique,

(ii) those due to the finite resolution of the emulsion.

These errors are not necessarily independent. For example, the measurement of a single grain to obtain information about the trajectory or position of decay of a particle is subject to both these errors. Any measurement technique is subject to some random error so that the position of the grain is uncertain to this extent; the centre of the grain does not lie upon the trajectory of the particle or does not lie at the point of decay.

The first of these errors has been considered in section 5.5 where repeated measurements upon grain positions yielded a standard deviation of 0.05μ in the determination of the postion of the centre of the grains. This figure is dependent upon several factors:-

(a) the size of the "digit" of digitisation,

(b) the design of the cross-wires,

(c) the shape and size of the grains,

(d) the personal error of the observer.

It has been shown that the effect of (a) was negligible. The type of cross-wire used where the grain is effectively "boxed in" for a measurement was that best suited for this type of measurement. The system has a larger uncertainty if

the grain is not circular and in these cases personal judgement plays a greater part than with circular grains. This was the difficulty experienced with the location of the end of the K^+ track. The separate grains in the tracks were rarely mis-shapen and little difficulty was encountered.

Personal error was not explicitly accounted for: if it be random, it is included in the calculated errors since these were all obtained from measurements by the same person; if it be systematic, all grain measurements are shifted and hance the event as a whole is shifted and there is no effect upon the intersections of the tracks.

The errors in grain positions in an event have the following effects:-

(a) uncertainty in fitting the straight lines to the tracks which in turn gives the error in determining the decay point of the π^o, this error has been denoted by $\sigma_{\pi e}$,

(b) class (i) error in K^+ end grain position, denoted by σ_{k1},

(c) class (ii) error in K^+ decay position, denoted by σ_{k2}.

A theory for (a) is described in section 7.12 and in the appendix. This error depends upon the spread of the measured positions of the grains about a straight line and so accounts for both classes of error with out separating them.

The treatment of (b) and (c) has been described in sect. 7.5 et seq. where a satisfactory separation of the two classes of error was obtained. It is further noted that class (ii) is the dominant effect while the estimate for (b) agrees with the measurement error on a grain quoted in a previous paragraph. It should here be noted that the division of the error into these two classes expresses explicitly the different effects of repeated measurements of the same event and of measurements on a large number of independent events. Were only class (i) error present, it should be possible to determine the flight distance for that event to any desired degree of accuracy merely by making repeated measurements. This is clearly not so, examination of the actual measured flight distances for the same event shows in a number of cases consistent values which are clearly absurd when considered alone (e.g. negative values). However, the introduction of class (ii) error places a lower limit on the error in any single event. Further accuracy may only be achieved by measuring a larger sample of events.

The magnitude of class (ii) error is directly related to the grain size. It was in anticipation of this effect that L4 emulsion was expected to give a better result than the G5 used by Harris et al. [15]. At present, however, L4 is the finest grained emulsion available from Ilford. It is of interest to consider the possible effects of using a finer-grained emulsion with (say) a developed grain diameter of 0.1μ.

The immediate effect is that the class (ii) error should be reduced by a factor of three, i.e. $\sigma_{k2} \sim 0.05\mu$. However, the smaller grain size does not necessarily decrease the setting error, in fact the greater difficulty in observing the grains may even increase this error. More advantage would now be gained from repeated measurements on the same event. The situation may also be improved by employing a higher magnification. This, however, would introduce fresh problems, among them: a reduced field of view and hence fewer grains in each track (a hypersensitised emulsion would help here); the actual problem of producing the increased magnification by a factor of three, the best place to introduce it would be between the cross-wires and the eye.

9.5 Future experiments

The preceding remarks indicate that it is the emulsion itself which limits the accuracy. Nevertheless, measurement of a greater sample of events would yield a better result. It is hoped that this will be done in the near future.

If a finer grained emulsion becomes widely available it would be of interest to repeat the experiment using the new material.

9.6 Cause of "wild" events

Four events were rejected from the final sample of events as they yielded flight distances inconsistent with the results from the main body of the events. In addition to these, four

events had one electron rejected which gave consistently "odd" results. The flight distances and errors for the four rejected events are:-

x	σ
-0.75	0.17
-1.28	0.33
1.10	0.24
0.84	0.25

Two possible reasons for these results may be considered:-

(a) the first grain of one of the secondary tracks was formed so close to the K^+ ending as to be indistinguishable from the true end of the track,

(b) the electron suffers a single scatter near the K^+ ending, if this took place before a grain was formed it would not be detected.

Of these two possibilities, the first does not seem tenable when the magnitude of the above flight distances is considered. They are too large to be considered due to an extra grain diameter even allowing for the effect of dip; in the above cases the greatest dip has $\sec \alpha = 1.6$.

The second possibility seems more likely especially when the other rejected electrons are considered.

9.10 Other π^o lifetime determinations

In the subsequent sections will be discussed the experiments performed since that of Harris et al. It will be most convenient to consider first those experiments employing the $K_{\pi 2}$ decay in a similar manner to the present one.

Three experiments using the original method of Harris have been made:-

(i) Glasser et al. [16])

(ii) Tietge et al. [17])

(iii) Koller et al. [18])

For convenience these will be referred to as G, T and K respectively. They will each be briefly described in the following paragraphs.

G. The events were measured using an unorthodox form of bifilar eyepiece comprising two independent translatable cross-wires one of which was rotatable. Both filars were aligned by eye along the π^+ and one electron track respectively. The subsequent displacement required in the filar passing through the electron track to then pass through the K^+ ending is related to the flight distance. A three-fold likelihood calculation was then performed with parameters: τ the lifetime; δ, the rms. deviation of grain positions from the straight trajectory; α the standard deviation of the measurements on the K^+ ending. The results gave: $\tau = 1.8 \times 10^{-16}$ secs.; $\delta = 0.048\mu$; $\alpha = 0.051\mu$. After correction for contamination

the final result given is:-

$$\underline{\tau = (1.9 \pm 0.5) \times 10^{-16} \text{ secs.}}$$

T. The positions of the grains forming the event were measured using a bifilar eyepiece which gave the (x, y) co-ordinates. However, unlike the present experiment, the differences in co-ordinates between adjacent grains were measured in an attempt to combat thermal drift. Line fitting was done using a procedure explicitly taking into account multiple scattering and the deviation of the grains from the true trajectories as well as the measurement error. No account is given of the calculation of the errors for individual events although it is noted that the length of the perpendicular from the K^+ measured ending on to the π^+ track is taken as an estimate of the error in determining the K^+ decay point. A maximum likelihood estimate similar to that used in the present experiment is used although no cutoff procedure is applied. The final result given is:-

$$\underline{\tau = (2.3 \,^{+\ 1.1}_{-\ 1.0}) \times 10^{-16} \text{ secs.}}$$

K. Drawings of the $K_{\pi 2}$ events were made using a camera lucida; "best fit" lines were drawn by eye through the tracks and the flight distance measured on the drawing. The error for each event was assumed to be of the form:-

$$\sigma_i^2 = (A^2 + B^2 \cot^2 \theta_i) \sec^2 \alpha_i$$

Where θ_i is the angle between the π^+ track and the electron

track, α_i is the dip angle of the π^+, and A and B are constants to be determined. A and B are estimated from τ decays measured in the same way as the main events, the values quoted are: A = 0.23μ and B =~0.15μ. A maximum likelihood estimate of the lifetime was obtained, no cutoff being applied. The result given is:-

$$\tau = (2.8 \pm 0.9) \times 10^{-16} \text{ secs.}$$

An experiment using emulsions as the recording mediumm has been performed by Shwe et al.[19]) using a new approach. The π^o is produced in an interaction between an incident π^- of 3.5GeV energy and a nucleus in the emulsion. The π^- were from a beam of the stated energy to which the stack of emulsions was exposed. The π^o is produced in such a reaction as:-

$$\pi^- + p \rightarrow \pi^o + n$$

The neutral pions are produced with high energies. By this means it was hoped to take advantage of the time dilation factor and have longer flight distances of the order of 1μ. 2,000 interactions were measured in a similar was to the events in the present experiment. If a π^o decaying in the Dalitz mode were present, two of the tracks intersected at a point significantly different from the centre of the star defined by the intersection of the other tracks. 61 such stars were found. The momentum distribution of the π^o's was assumed to be the same as for the charged π's. A chi-squared treatment

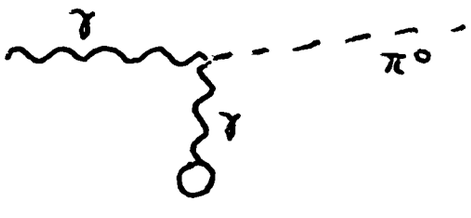
of the data yielded a value of:-

$$\tau = (1.9 \,^{+\ 1.3}_{-\ 0.8}) \times 10^{-16} \text{ secs.}$$

An entirely different approach to the problem has been made by von Dardel et al.[20]) in an experiment using counter technique. High energy π^o's were produced in platinum foils of various thicknesses from 3μ to 60μ exposed to the 18 GeV internal proton beam of the CERN proton synchrotron. The production of positrons due to the materialisation of the π^o decay γ's was measured. The probability of this materialisation is a function of the flight distance of the π^o and of the thickness of the foil. The expression for the probability also involves two unknown parameters A and B. The three unknowns are determined by measurements with three foils of different thicknesses. In fact four foils were used as an internal consistency check. The final result obtained was:-

$$\tau = (1.05 \pm 0.18) \times 10^{-16} \text{ secs.}$$

All the above determinations depend upon measurements made on decaying π^o's and depend upon a determination, direct or indirect, of the flight distance. It was pointed out by Primakoff [26]) that a study of the inverse process, the photoproduction of pions, would yield information on the lifetime. This process may be represented by the following diagram:-



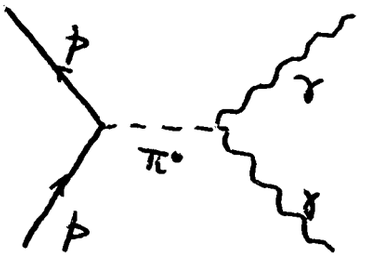
One of the photons in the process is a virtual one provided by the coulomb field of a heavy nucleus. Glaser and Fenell [27] assuming a direct interaction between the π^o and the electromagnetic field have shown that the contribution to the photoproduction cross-section due to this effect may be separated from purely nuclear background production by considering the differential cross-section at small angles where the effect has a large peak. An experiment was performed by Tollestrup et al. [21] and a result of $(1.7 \pm 1.4) \times 10^{-16}$ secs. was obtained.

9.11 Theoretical aspects of the π^o lifetime

Before the existence of the π^o had been demonstrated, Steinberger [28] calculated using perturbation theory the rates of decay of scalar, pseudoscalar, vector and pseudovector neutral mesons. The pseudoscalar case is appropriate to the π^o and a value of 5×10^{-17} secs. was obtained. A later attempt by Goldberger and Treiman [29] using dispersion relation treatment obtained a very similar figure although the final expression for the decay rate was very different from the perturbation treatment.

The connection between the decay rate of the π^o and proton Compton scattering was investigated by Jacob and Mathews [30]. The effect of the inclusion of the term due to the following diagram with the normal theory was compared with the available

data on low energy γ-p scattering.



The fit of the data gave limits of:-

$$10^{-16} > \tau > 5 \times 10^{-19} \text{secs.}$$

The method of Goldberger and Treiman which was a modification of their more successful treatment of the decay of the charged pion, has been developed and investigated by various workers. The improved technique has been applied by Bose [32]) to yield an expression for the decay amplitude in terms of the electric charge, the pion-nucleon coupling constant and the anomalous magnetic moment of the proton. The value of lifetime obtained is 1.4×10^{-16} secs.

The situation with regard to the thoery of the lifetime is still ambiguous. With the exception of the last estimate quoted, all the approaches indicate a lifetime shorter by an order of magnitude than that indicated by all the experiments listed in section 9.11 (and including the present experiment). The decay rate of the π^o occurs as a parameter in other problems. The decay rate of $\omega \rightarrow \pi^+ + \pi^- + \pi^o$ has been related to that of the π^o by Gellman et al. [32]) and Geffen [32]).

9.12 Comparison of Emulsion experiments

The experiments of Glasser et al., Tietge et al., Koller

et al. and the present experiment allow direct comparisons to be made of the experimental methods. An exhaustive survey will not be made but the following points are worthy of note.

The experiment is of a statistical nature and consequently, as has previously been mentioned, the evaluation of the errors involved is important. The dominant effect is the error in determining the point of decay of the K^+. An estimate of this is made using τ decays by K and the present experiment (denoted in the following discussion by E); by consideration of the deviation of the K^+ end from the π^+ trajectory in T, and by a likelihood method applied to the $K_{\pi 2}$ events themselves in G.

Equivalent values of the constants A and B used by K have been calculated for the present experiment. The following table indicates the results for the two experiments:-

	A	B
Koller	0.23μ	0.15μ
Evans	0.15μ	0.03μ

The figures were obtained by assuming the form of error described in section 7.5 with the values of σ_{k1} and σ_{k2} obtained from τ measurements together with the form of the intersection error derived in the appendix (equation 3.5 with $\sigma_\pi = \sigma_e = 0.05\mu$). K employed G5 emulsion which has an unprocessed grain diameter of 0.27μ while the L4 used by E has a figure of 0.15μ for this

dimension. This is reflected in the magnitude of the parameter A; when this constant was estimated from the present data it was clear that the dominant contribution to it was from σ_{k2}, the error parameter which expresses the effect of grain size. The contribution to B is entirely from the error parameters σ_π or σ_e (see appendix section 3) which express the effect of measurement errors and grain noise combined. Here, there is a significant improvement with the present experiment, the accuracy being improved by a factor of five. Some of this is again due to the finer grain size and the consequent smaller grain noise but also the higher accuracy of co-ordinate measurement is demonstrated.

A crude analysis comparing the expected distribution of the "residual K length" mentioned in section 7.41 with the expected distribution of the perpendiculars from the K^+ end on to the π tracks indicated that they should be similar and examination of the distributions for the τ decays measured confirmed this. Thus the use of the perpendiculars to estimate the K^+ error, by T is equivalent to the use of the crude estimate obtained by considering the "residual K length" distribution. No figures are quoted by T so that quantitative comparison is not possible.

The parameter quoted as α by G is almost identical to σ_{k2}. G gives $\alpha = 0.051\mu$ while E gives $\sigma_{k2} = 0.137\mu$. The emulsions used were L4 in both cases. However, α was determined

from the $K_{\pi 2}$ events by a maximum likelihood method which would be expected to give self-consistent values of the various parameters. It has been shown in the present work that events are likely to be present in the measured sample which give anomalous values of intercept. Such events may seriously affect the estimates of these parameters.

It has been shown that the so-called "wild" events have a large effect upon the likelihood or weighted mean determinations but that once they have been excluded, the estimates become less sensitive to the rejection of "normal" events. It was indicated in section 8.3 that the "wild" events should always tend to give a larger value for the maximum likelihood estimate than do the normal events alone. The "no-cutoff" value obtained with the first sample of 58 events was 2.3×10^{-16} secs. This compares favourably with the results of G, 1.9; T, 2.3 and K, 2.8 $\times 10^{-16}$ secs. The presence of this effect would reconcile the somewhat high values of the emulsion experiments with the lower value of 1.05×10^{-16} obtained by von Dardel.

The experiment of Shwe et al. does not lend itself to point-for-point comparison. However, the following points may be demonstrated. Although it was hoped to take advantage of a longer flight distance due to the higher energy, this is off-set to some extent by the uncertainty in the energy of the π^{o}. The problems of locating the end-points of the flight

distance are reversed; the point of production is well defined by the intersection of a number of tracks, while the decay point is defined by the intersection of the electron pair tracks. Over half of the events had electron pairs with an opening angle of less than 20°; consequently the error in the position of the point of decay could be large in a number of cases. In addition, a very great amount of "non-informative" measurement was necessary to detect the useful events.

The possibility of improving upon the $K_{\pi 2}$ method has been discussed at some length elsewhere, but for the sake of completemess, the conclusion reached will be repeated here. Although some improvement in measuring technique is possible, it is clear that a significant improvement in the accuracy of the method is possible only by the measurement of a larger number of events and continuing to use L4 emulsion. This is the only way in which the effect of the σ_{k2} error may be reduced, if one does not consider the use of finer grained emulsions.

9.13 Summary of existing data on π^o lifetime

Author	Date	Lifetime (all x 10^{-16} secs.)
Glasser et al.	1961	1.9 ± 0.5
Shwe et al.	1962	$1.9 \begin{smallmatrix}+1.3\\-0.8\end{smallmatrix}$
Tietge et al.	1962	$2.3 \begin{smallmatrix}+1.1\\-1.0\end{smallmatrix}$
Koller et al.	1963	2.8 ± 0.9
von Dardel et al.	1963	1.05 ± 0.18
Present Experiment	1963	$1.6 \begin{smallmatrix}+0.6\\-0.5\end{smallmatrix}$

Weighted mean of above results:-

$$\tau_{\pi^o} = (1.28 \pm 0.15) \times 10^{-16} \text{ secs.}$$

List of references

1) Feynman, "Theory of Fundamental Processes", Lecture Note Series.

2) S.K.Bose, Nuovo Cimento, 23, 408 (1962)

3)Gellman & Rosenfeld. Ann.Rev.Nucl.Sci. 7, 418 (1957)

4) Bjorklund et al. Phys. Rev. 77, 213 (1950)

5) Steinberger et al. Phys. Rev. 78, 802 (1950)

6) Panofsky et al. Phys. Rev. 81, 565 (1951)

7) Chinowsky, Phys. Rev. 93, 586 (1954)

8) Haddock et al. Phys, Rev. Letts. 3, 478 (1959)

9) Kaplon et al. Phys Rev. 85, 900 (1952)

10) Carlson et al. Phil. Mag. 41, 701 (1950)

11) Lord et al. Phys. Rev. 80, 970 (1950)

12) Lord et al. Phys. Rev. 87, 538 (1952)

13) Dalitz, Proc. Phys. Soc. (London) A64, 667 (1951)

14) Anand, Proc. Roy. Soc. A220, 183 (1953)

15) Harris et al. Phys Rev. 106, 327 (1957)

16) Glasser et al. Phys. Rev. 123, 1014 (1961)

17) Tietge et al. Phys. Rev. 127, 1324 (1962)

18) Koller et al. Nuovo Cim. 27, 1405 (1963)

19) Shwe et al. Phys. Rev. 125, 1024 (1962)

20) von Dardel et al. Phys. Letters 4, 51 (1963)

21) Tollestrup et al. Proceedings of 1960 Rochester Conference,p.27

22) Blackie, Oxford B.Sc. thesis "Mean Life of Neutral Pion"

23) Crawford, Proceedings of 1962 Rochester Conference p.838.

24) Orear, Notes on Statistics for Physicists (unpublished)
UCRL-8417

25) Bartlett, Phil. Mag. 44, 249 (1953)

26) Primakoff, Phys. Rev. 81, 899 (1951)

27) Glaser & Fenell, Phys. Rev. 121, 886 (1961)

28) Steinberger, Phys. Rev. 76, 1180 (1949)

29) Goldberger & Treiman, Nuovo Cim. 9, 451 (1958)

30) Jacob & Mathews, Phys. Rev. 117, 854 (1960)

31) Gellman et al. Phys. Rev. 124, 374 (1962)

32) Geffen, Phys. Rev. 128, 374 (1962)

APPENDIX

1. Minimum perpendiculars track fitting

The problem is to fit a straight line $y = mx + c$ to a set of co-ordinates (x_i, y_i) such that:-

$$P^2 = \sum_i (y_i - mx_i - c)/(1 + m^2) \qquad (1.1)$$

is a minimum.

For convenience take new axes with origin at the "centre of gravity" of the (x_i, y_i). It can be proved that the best fit passes through this point. For brevity, the new set of co-ordinate values will also be referred to as (x_i, y_i) as no confusion will arise.

The equation of the line may now be expressed as:-

$$px + qy = 0; \quad \text{where } p^2 + q^2 = 1 \qquad (1.2)$$

With this representation:-

$$P^2 = \sum_i (px_i + qy_i)^2/(p^2+q^2) = \sum_i (px_i + qy_i)^2 \qquad (1.3)$$

We now have that:-

$$d(P^2) = \frac{\partial P^2}{\partial p}\, dp + \frac{\partial P^2}{\partial q}\, dq$$

$$= 0 \quad \text{for max. or min. of } P^2 \qquad (1.4)$$

However, p and q are not independent variables and from (1.2):-

$$2p.dp + 2q.dq = 0 \qquad (1.5)$$

Hence, using the method of Lagrange's undetermined multipliers:-

$$\left(\frac{\partial P^2}{\partial p} - 2\alpha p\right)dp + \left(\frac{\partial P^2}{\partial q} - 2\alpha q\right)dq = 0 \qquad (1.6)$$

giving:-

$$\begin{aligned} p(S_{xx} - \alpha) + q.S_{xy} &= 0 \\ p.S_{xy} + q(S_{yy} - \alpha) &= 0 \end{aligned} \qquad (1.7)$$

where $S_{xx} = \sum_i x_i^2$; $S_{yy} = \sum_i y_i^2$; $S_{xy} = \sum_i x_i y_i$.

For non-zero solutions:-

$$\begin{vmatrix} S_{xx}-\alpha & S_{xy} \\ S_{xy} & S_{yy}-\alpha \end{vmatrix} = 0 \qquad (1.8)$$

which is a quadratic equation for α:-

$$\alpha^2 - (S_{xx} + S_{yy})\alpha + S_{xx}S_{yy} - S_{xy}^2 = 0 \qquad (1.9)$$

but, from (1.3) $P^2 = p^2S_{xx} + 2pq.S_{xy} + q^2S_{yy}$

$= \alpha$ from (1.7) (1.10)

Since the co-ordinates lie very close to the fitted line, α will be small compared to $(S_{xx} + S_{yy})$. This gives computation difficulties when it is attempted to solve (1.9) in the normal manner. The series approximation for this situation has the first term:-

$$\alpha = \frac{(S_{xx}S_{yy} - S_{xy}^2)}{S_{xx} + S_{yy}} \qquad (1.11)$$

It should here be noted that the x and y co-ordinates are treated symmetrically.

In the actual computation the second term is also used as a small carrection. Expression (1.11) gives the required smaller root of (1.9). p and q are then calculated using

equations (1.7) and hence the gradient $m = -p/q$ is obtained. The co-ordinates are restored to the original axes to give c. These two parameters are stored for each track for use in the geometrical section of the programme.

1a. Cutoff routine

The δ_{rms} for the calculated track is given by:-

$$\delta_{rms} = (\alpha/N)^{\frac{1}{2}} \quad \text{where N is the number of grains in the track.} \qquad (1.12)$$

The cutoff procedure referred to in section 7.11 uses δ as a criterion to reject grains from the track. If $\delta > 0.08\mu$ the programme enters a routine which calculates the individual perpendicular distances:-

$$p_i = (y_i - mx_i - c)/(1 + m^2)^{\frac{1}{2}} \qquad (1.13)$$

detects the grain with the greatest p_i, rejects it and repeats the line fitting procedure. Further grains are rejected if necessary until $\delta < 0.08\mu$. The process is halted if some fault in the co-ordinates causes all but two grains to be rejected. If the faulty track is the π^+ or first electron, the measurement is rejected, if it is the second electron, the event is rescued by limiting the subsequent calculations to the two remaining tracks.

When all the tracks are suitably fitted, the calculation proceeds to the geometrical section.

2. Geometrical reconstruction of the event

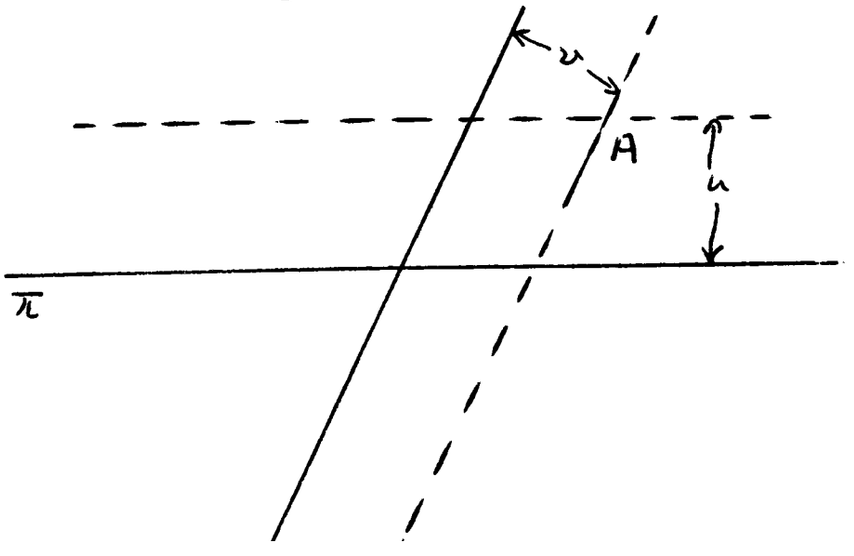
If two electron tracks are present, this section of the calculations is repeated,, each track being taken in turn with the π^+.

The equations of the two tracks concerned are available in the simple form y=mx+c. Fig. 7.2 has shown the quantities to be calculated, these are obtained by straightforward methods of analytical geometry and will not be discussed.

3. Intersection error theory

It is assumed that the fitted lines must pass through the "centre of gravity" of the measured co-ordinates but that, due to the scatter of the co-ordinates, the calculated gradient of the line has an error δm.

The following sketch represents the two intersecting tracks with the dotted lines representing possible displacements in each caused by their respective δm's, these are denoted by u and v. The centres of gravity of the two tracks are sufficiently distant for the dotted lines to be considered parallel to the centre positions.



It is now assumed that u and v are normally distributed about the central positions with standard deviations σ_π and σ_e respectively. Taking these central positions as oblique axes, a point such as A may be assigned co-ordinates (u, v) as indicated. We then have that the probability that the point of intersection lies in an element (dudv) about A is:-

$$p(u,v)dudv = \text{const. } e^{-\frac{1}{2}(u^2/\sigma_\pi^2 + v^2/\sigma_e^2)}dudv \qquad (3.1)$$

where the constant is such that p(u,v) is normalised.

Rectangular axes are now taken with the same origin and with the x axis along the π track. The transformation relations are:-

$$u = y \quad ; \quad v = \frac{\alpha x - y}{1 + \alpha^2} \qquad \text{where} \quad \alpha = \tan \theta_{\pi e} \qquad (3.2)$$

Using these relations we obtain the probability distribution (3.1) referred to the new axes:-

$$p'(x,y)dxdy = p(u,v) \frac{\alpha}{(1 + \alpha^2)^{\frac{1}{2}}} dxdy \qquad (3.3)$$

where the extra factor is the Jacobian of the transformation.

The marginal probability distribution of x, i.e. the probability that the intersection lies between x and x+dx regardless of the value of y, is given by integrating p'(x,y) from $y = -\infty$ to $y = \infty$ along a strip of width dx, at x. The resulting distribution turns out to be a normalised gaussian with zero mean and variance:-

$$\sigma^2 = \frac{\sigma_\pi^2 + (1 + \alpha^2)\sigma_e^2}{\alpha^2}$$

$$\sigma^2 = \sigma_\pi{}^2 \cot^2\theta_{\pi E} + \sigma_e{}^2 \operatorname{cosec}^2\theta_{\pi e}$$

$$= (\sigma_\pi{}^2 + \sigma_e{}^2)\operatorname{cosec}^2\theta_{\pi e} - \sigma_\pi{}^2 \qquad (3.5)$$

This σ is taken to be the error in the flight distance.

σ_π and σ_e are calculated from:-

$$\sigma_\pi = r_\pi \delta m_\pi \quad ; \quad \sigma_e = r_e \delta m_e \qquad (3.6)$$

For the normal type of least squares fit (which assumes no error in the x co-ordinate) δm is given by:-

$$(\delta m)^2 = \frac{S_{xx}S_{yy} - S_{xy}{}^2}{(N-2)S_{xx}} \qquad (3.7)$$

where S_{xx} etc, have the same meanings as before and N is the number of co-ordinates (grains) in the track.

The minimum perpendiculars fit becomes identical to the usual type if the gradient of the fitted line is zero. The given co-ordinates are transformed to axes in which the new x axis is the calculated line. Hence δm is calculated.

4. Lifetime likelihood calculation

The probability distribution of the measured flight distance x for an event with measurement error σ is given by:-

$$p(x)dx = \frac{1}{x_0\sigma\sqrt{2\pi}} \int_0^\infty \exp\left\{-\frac{x'}{x_0} - \frac{(x'-x_i)^2}{2\sigma^2}\right\} dx'\,dx \qquad (4.1)$$

where $x_0 = \beta\gamma c\tau$

Hence the likelihood function for a set of N events with given x_i and σ_i is:-

$$L(\tau) = \prod_i^N p(x_i) \qquad (4.2)$$

It is convenient to work in terms of $w = \log_e L$ so that,

$$w(\tau) = \sum_{i}^{N} \log_e p(x_i) \qquad (4.3)$$

Equation (4.1) is not convenient for numerical evaluation due to the infinite range of integration. Completing the square of the exponent in the integrand gives:-

$$p(x)dx = \frac{1}{x_0} e^{\frac{1}{2}\left(\frac{\sigma}{x_0} - \frac{x}{\sigma}\right)^2} \cdot e^{-\frac{x^2}{2\sigma^2}} \cdot \frac{1}{\sqrt{2\pi}} \int_{\frac{\sigma}{x_0} - \frac{x}{\sigma}}^{\infty} e^{-\frac{1}{2}u^2} du \qquad (4.4)$$

The final factor is the well-known function:-

$$\operatorname{erfc}(\varepsilon) = (2\pi)^{-\frac{1}{2}} \int_{\varepsilon}^{\infty} e^{-\frac{1}{2}u^2} du \qquad (4.5)$$

We therefore have:-

$$\log p = -\log x_0 + \tfrac{1}{2}\varepsilon^2 - x^2/2\sigma^2 + \log \operatorname{erfc}(\varepsilon) \qquad (4.6)$$

$$\text{where} \quad \varepsilon = \sigma/x_0 - x/\sigma$$

For large ε, $\log \operatorname{erfc}(\varepsilon)$ is large and negative while $\frac{1}{2}\varepsilon^2$ is large and positive. The resulting sum is thus subject to large error in a mumerical calculation.

The asymptotic series for $\operatorname{erfc}(\varepsilon)$ is useful:-

$$\operatorname{erfc}(\varepsilon) \sim \frac{1}{\sqrt{2\pi}} \varepsilon^{-1}(1 - \varepsilon^{-2} + 1.3\varepsilon^{-4} - 1.3.5\varepsilon^{-6} + \ldots.)e^{-\frac{1}{2}\varepsilon^2} \qquad (4.7)$$

The explicit dependence upon $e^{-\frac{1}{2}\varepsilon^2}$ can be used to cancel out the $e^{+\frac{1}{2}\varepsilon^2}$ before numerical work begins. Series (4.7) cannot be used for small values of ε and as it is an asymptotic series, care must be taken over the number of terms used. It was found that a maximum of seven terms gave sufficient accuracy.

The function

$$\phi(\alpha) = \frac{2}{\sqrt{\pi}} \int_0^{\alpha} e^{-u^2} du \qquad (4.8)$$

has a rational function approximation which is useful for digital computing.

$$\phi(\alpha) \sim 1 - \left(\sum_{n=0}^{6} a_n \alpha^n\right)^{-16} \qquad (4.9)$$

where

$a_0 = 1$

$a_1 = 0.070\ 523\ 078\ 4$

$a_2 = 0.042\ 282\ 012\ 3$

$a_3 = 0.009\ 270\ 527\ 2$

$a_4 = 0.000\ 152\ 014\ 3$

$a_5 = 0.000\ 276\ 567\ 2$

$a_6 = 0.000\ 043\ 063\ 8$

$\phi(\alpha)$ is related to erfc(ε), giving the following expression:-

$$\text{erfc}(\varepsilon) \sim \tfrac{1}{2}\left(\sum_{n=0}^{6} a_n \alpha^n / 2^{\frac{1}{2}n}\right)^{-16} \qquad (4.10)$$

The expression is not valid for all positive ε. The polynomial part of (4.9) represents a small departure from $\phi = 1$, for large α, while it represents the whole of the value of erfc(ε).

A comparison was made between the rational function and the asymptotic expansion. It was found that a suitable transition point was at $\varepsilon = 3.7$, the rational function being used below this, and the expansion above.

Use was made of symmetry to calculate erfc(ε) for negative ε.

$$\text{erfc}(\varepsilon) = 1 - \text{erfc}(-\varepsilon) \qquad (4.11)$$

The rational function was used to calculate erfc($-\varepsilon$) for the whole negative range of ε.

The values of $L(\tau)$ and $w(\tau)$ were calculated for a set of

equally spaced values of τ. They are normalised so that the maximum tabulated value of $L(\tau)$ is unity.

Note on distribution function

The mean and variance of the distribution function of the flight distances (4.1) can be calculated.

$$\bar{x} = \int_{-\infty}^{\infty} x\, p(x)dx$$

$$= (x_o \sigma\sqrt{2\pi})^{-1} \int_{-\infty}^{\infty} dx \int_{0}^{\infty} dx' \quad x \exp(-x'/x_o - (x'-x)^2/2\sigma^2)$$

which gives on exchanging the order of integration:-

$$\bar{x} = x_o^{-1} \int_{0}^{\infty} e^{-x'/x_o}\, dx' \;.\; (\sigma\, 2\pi)^{-1} \int_{-\infty}^{\infty} x \exp(-(x'-x^2)/2\sigma^2)dx$$

$$= x_o^{-1} \int_{o}^{\infty} x'\; e^{-x'/x_o}\, dx'$$

$$= x_o \quad \text{i.e. the flight distance corresponding}$$

to the mean lifetime

A similar calculation for the variance gives:-

$$\sigma_o^2 = x_o^2 + \sigma^2$$

It is interesting to note that as the variances of the two distributions exponential and normal, are respectively x_o^2 and σ^2, the total error for the compound distribution is the same as the elementary combination of errors.

Note on weighted mean procedure for individual measurements of the same event

The set of x_i and σ_i for the events measured were obtained by taking the weighted means for the flight distances obtained from independent measurements of the same event. A more logical method would have been to treat these basic results in an extended likelihood calculation. It can be shown, however,

that this procedure is identical to the one actually carried out. This may be appreciated qualitatively since the exponential distribution does not affect measurements of the same event. These measurements are assumed to be normally distributed and hence the weighted mean is the correct estimate to use.

5. Bartlett S function and confidence interval estimation

The function $S(\tau)$ is defined:-

$$S(\tau) = \frac{1}{C}\frac{dw}{d\tau}; \quad C^2 = -\int_{\tau_{min}}^{\tau_{max}} (d^2w/d\tau^2).L(\tau)d\tau \; ; \quad w = \log_e L \qquad (5.1)$$

and $L(\tau)$ is normalised $\int_{\tau_{min}}^{\tau_{max}} L(\tau)d\tau = 1$

The table of values of $L(\tau)$ and $w(\tau)$ at equally spaced values of argument, calculated as described in section 4., is suitable to the numerical differentiation and integration required in (5.1). However, evaluation of second derivatives numerically is not a reliable process and the expression for C^2 may be modified by integrating by parts:-

$$C^2 = \int_{\tau_{min}}^{\tau_{max}} (dw/d\tau)^2.L(\tau)d\tau \quad - \left[\frac{dL}{d\tau}\right]_{\tau_{min}}^{\tau_{max}} \qquad (5.2)$$

The numerical differentiation formula used is:-

$$Dw_{\frac{1}{2}} = \delta w_{\frac{1}{2}} + \frac{1}{24}\delta^3 w_{\frac{1}{2}} \qquad \text{where} \quad D \equiv d/d\tau \qquad (5.3)$$

The δ's are the usual finite difference operators and the standard notation $w_{\frac{1}{2}} = w(\tau+\frac{1}{2}h)$ is used. (h is the increment in τ between tabulated values.)

(5.3) yields the derivatives at points midway between the tabulated points. An interpolation formula is used to calculate the corresponding values of w:-

$$w_{\frac{1}{2}} = \frac{1}{16}(-w_{-1} + 9w_o + 9w_1 - w_{w2})$$

The necessary integrations are performed using Simpson's rule.

The equations:-

$$S = \pm 1 \quad ; \quad \mathbf{S} = 0$$

are solved from the calculated $S(\tau)$ by simple inverse linear interpolation. The solution for $S = 0$ is the maximum likelihood estimate of τ which is used in the cutoff procedure described in section 8.6. The 90% confidence interval was obtained by a graphical solution of $S(\tau) = \pm 1.65$.

6. Data concocting programme

For an exponential distribution:-

$$p(t)dt = \tau^{-1} e^{-t/\tau} dt \qquad (6.1)$$

we obtain the probability that t is less than t':?-

$$P(t') = p(t \quad t') = \int_0^{t'} p(t)dt = 1 - e^{-t'/\tau} \qquad (6.2)$$

P(t') takes values between 0 and 1. If x is one of a set of random numbers in this range, then the corresponding solution of $P(t') = x$ represents a random sample from a population with (6.1) as distribution function. A precisely similar argument may be applied for the normal distribution function.

A value of τ is assumed. The choice of one random number generates a possible "lifetime" t' and hance true flight distance $x' = \beta\gamma ct'$. This x' is then taken as the mean of a normal

distribution with a given variance σ_i^2. The choice of a second random number gives a possible value of measured flight distance x_i. The values of σ_i used are those taken from the experimental results.

```
TITLE
DIGITISED* INPUT - 3 TRACKS     EVANS.

CHAPTER1
A→10
B→4
C→30
D→30
U→10
£→10
G→10
X→60
Y→60
Z→3
V→10
W→30
E→14

1)HALT

2)READ(A)
JUMP1,0>A
READ(B)
READ(0)
PRINT(A)2,3
PRINT(B)2,4
PRINT(0)1,0
NEWLINE
JUMP19,0=2
JUMP20,0=3
D=0.149
JUMP21
19)D=0.165
JUMP21
20)D=0.250
21)P=0
Q=0
R=0

3)600,32
005,32
135,1
080(3)
600,32
005,32
135,5
080(99)
600,32
001,32
011(T)
```

reads event code number

reads date of measurmment

reads objective code number

prints the identification codes

sets calibration factor depending upon objective

searches tape for "1" beginning each punched set of co-ordinates

test for "(" symbol preceding the co-ordinates

reads track code number set by control on equipment - puts number in location "T"

```
4)II5,0
300,-2
400,3I.58
410,38
I06,4
600,39+
016,38
440,38
I26,5
I76,24
085,4
417,3I.54
385,I
600,38
006,38
I76,6
080(98)
600,32
006,32
080(3)
JUMPI2,T>4
X=X-I6384
Y=Y-I6384
X=DX
Y=DY
JUMP5,T≠3
G*9=X
GI0=Y
JUMP3

5)JUMP7,T=2
JUMP6,T=I
P=P+I
XP=X
YP=Y
JUMP3

6)Q=Q+I
X(**Q+20)=X
Y(Q+20)=Y
JUMP3

7)R=6>+I
X(R+40)=X
Y(R+40)=Y
JUMP3
```

reads in co-ordinates in binary form from the tape and transfers them to locations "X","Y","Z"

tests for ")" symbol closing the co-ordinate sets

tests for "erase" symbol - if present, the next set of co-ordinates is read in, over-writing the faulty set

tests for "dummy" co-ordinates to initiate (calculations

restores co-ordinates to true zero from "machine" zero

converts co-ordinates to μm.

records co-ordinates of K^+ ending

sorts co-ordinate sets into "tracks" according to track code number "T"

```
12)T=0
PRINT(P)2,0
PRINT(Q)2,0
PRINT(R)2,0
NEWLINE
13)K=3T
JUMP22,T=1
JUMP23,T=2
N=P
JUMP25

22)N=Q
JUMP25

23)N=R
JUMP24,R=0
***
25)I=1(1)N
J=N+1
L=20T+1
CI=XL
CJ=YL
REPEAT

14)AK=0
A(K+1)=0
I=1(1)N
J****=N+1
AK=AK+CI
A(K+1)=A(K+1)+CJ
REPEAT

AK=AK/N
A(K+1)=A(K+1)/N
B1=0
B2=0
B3=0
GK=CN
G(K+1)=C1
G(K+2)=C(N+1)
I=1(1)N
J=N+1
CI=CI-AK
CJ=CJ-A(K+1)
B1=B1+CICI
B2=B2+CJCJ
B3=B3+CICJ
REPEAT
```

prints initial number of grains measured in each (track

each track now fitted in turn, order π^+, e_1, e_2

sets number of grains in track being fitted

if no e_2 track present, fitting routine applied twice only

calculates "centroid" of co-ordinates in track

shifts to new axes through centroid and calculates S_{xx}, S_{yy} and S_{xy}

```
£1=B1+B2
£3=£1£1£1
£2=B1B2-B3B3
£1=£2/£1+6£2£2/£3
£2=£1-B1
£2=B3/£2
£3=£2AK+A(K+1)
£1=£1/N
JUMP9,£1>0
JUMP8,£1>-0.00001
NEWLINE
620,27
620,15
620,21
620,20
K=K+3
JUMP6,8>K
JUMP2

8)£1v0
9)£1=XSQRT(£1)
UK=-£2
U(K+1)=£3
JUMP10,0.08>£1
1=1(1)N
J=N+1
```

calculates α, m, c; solution of quadratic equation by suitable approximation

£1 = δ_{rms} (r.m.s. deviation of grains from calculated (track))
UK = m_K
U(K+1) = c_K
tests for $\delta > 0.08$ μm.

spurious grain rejection routine

```
DI=UKC1-CJ
DI=DIDI
REPEAT
M=XMAX(D0,1,N)
NEWLINE
620,31
PRINT(1000K+M)4,0
N=N-1
JUMP26,N=2
I=1(1)N
JUMP15,I>M
CI=CI+AK
JUMP16
15)CI=C(I+1)+AK
16)REPEAT
I=1(1)N
J=N+1
*JUMP17,I>M
CJ=C(J+1)+A(K+1)
JUMP18
17)CJ=C(J+2)+A(K+1)
18)REPEAT
JUMP14

10)EK=£1
JUMP11,K>7
```

finds the grain lying furthest from the calculated track

prints an identifying number for the rejected grain

rejects spurious co-ordinate and restores the remaining co-ordinates to the original axes

```
DOWN:/2
11)T=T+1
JUMP13,T≠3
24)ACROSS2/2

26)JUMP2,2>T
R=0
620,27
620,14
620,15                    prints "NO E2" if all grains in second
620,0                     elctron track rejected
620,14
620,27
620,5
620,0
620,2
NEWLINE
JUMP24

99)NEWLINE
620,5
JUMP3
NEWLINE                   records lack of "(" or ")" in read-in routine

98)NEWLINE
620,6
JUMP3
NEWLINE
XSQRT
CLOSE

CHAPTER2
VARIABLES1
1)£0=UKUK+1               error parameter calculation for each track
£0=XSQRT(1/£0)
B1=0
B2=0
B3=0
I=1(1)N
J=N+1
W1=C1£0+CJUK£0            rotates to new axes with track as new X axis.
WJ=CJ£0%-C1UK£0
B1=B1+W1W1
B2=B2+WJWJ
B3=B3+W1WJ
REPEAT
A2=A0£0+UKA1£0            calculates  δm for each track
£1=B3B3/B1
B0=B2-£1
S=N-2
```

```
A=Bo/S
VK=A/BI                    VK = δm_K
£2=A/N+AA2A2/BI
V(K+I)=£2/£o               V(K+1) = δc_K   (not used in present error cal-
                                            (culation
UP
2)K=3(3)6
£o=Uo-UK
£I=U(K+I*)-UI
X=£I/£o                    calculates cosec^2 θ_πe and magnitude and
Y=U(K+I)+XUK               sign of flight distance x
£3=I+UKUo
£3=£3/£o
E(K+I)=£3£3+I
£I=G9+UoGIo-UoUI
£2=UoUo+I
£I=£I/£2
£3=Uo£I+UI
W=£I-GI
£I=X-£I
£3=Y-£3
W=W£I
£I=£I£I+£3£3
£I=XSQRT(£I)
£Io=XSIGN(W)
E(K+2)=£I£Io
£I=XRADIUS(Ao-X,A*I-Y)
£2=XRADIUS(AK-X,A(K+I)-Y)
A=£I£IVo                   calculation of error in x
B=£2£2VK
£5=AE(K+I)+BE(K+I)-A
E(K+6)=XSQRT(£5)
E(K+8)=I/£5
£I=GIo-UoG*9-UI            calculates length of perpendicular from K+ end
£2=XSQRT(UoUo+I)           on to π+ track
£I=-£I/£2
E(K+7)=£I
JUMP3,R=o                  does not repeat calculation if no e2 track present.
REPEAT
3)ACROSSI/3
XSQRT
XSIGN
CLOSE

CHAPTER3
VARIABLESI                 print-out of relevant quantities
I)NEWLINE
K=3(3)6
PRINT(E(K+2))2,4           x
```

```
NEWLINE
PRINT(E(K+6))2,4  ——        σ
PRINT(E(K+1))2,4  ——        cosec²θπe
%NEWLINE
PRINT(E(K+8))4,2  ——        1/σ²
PRINT(E(K+2)E(K+8))4,4 —— x/σ²
NEWLINE
PRINT(Eo)1,4      ———       δπ+
PRINT(EK)1,4      ———       δe
NEWLINE
PRINT(E(K+7))2,4  ———       p
NEWLINE
NEWLINE
NEWLINE
JUMP2,R=o
REPEAT
2)ACROSS2/1   ————————      proceeds to new measurement
CLOSE

CHAPTERo
ACROSS1/1
CLOSE
→
**********************************
```